Midwestern Journal of Undergraduate Sciences

ARMORING THE IMMUNE SYSTEM
MOBILIZING CAR T CELLS FOR COMBAT

Vol. 4 Iss. 1
Summer 2025
https://journals.ku.edu/MJUSc

To The Reader,

I am pleased to introduce the latest edition of the Midwestern Journal of Undergraduate Sciences, an annual publication dedicated to showcasing the research, insight, and creativity of undergraduate scientists. Our mission remains focused: to provide a platform for high-quality student work that might not otherwise find a path to publication — especially work that stands independently of larger, faculty-led research projects.

This year, our Topics in Biotechnology course — which sets the thematic focus for each issue — explored the development and promise of CAR T cell therapies. From their early design in the 1990s to today's armored constructs capable of navigating the tumor microenvironment, CAR T cells represent one of the most exciting advances in immunotherapy. For the first time, this year's class was accompanied by a student-facing podcast, Reprogrammed: The Biotechnology Podcast, which followed the weekly reading of primary literature and offered a parallel track for discussion and engagement. Several of the review articles included in this issue were shaped by ideas first voiced on the podcast.

As always, our journal includes a range of article types: original research papers from undergraduate-led projects, mini-reviews that synthesize key developments in the journal's theme. In addition, we are featuring the reading list that from the topics class that sets the theme. This year, we are pleased to welcome an article presenting a classroom-based activity exploring evolutionary research performed in a classroom.

We are proud of the work our students have produced and hope that this journal continues to offer both recognition and opportunity for emerging scientists. For submission guidelines, article categories, and formatting expectations, please consult our author's guide.

-JF Treml

Contributors

This journal is supported by the University of Kansas Libraries and Marianne Reed

Cover Art
Created by AI assistance
via OpenAI, adapted by
J.F. Treml, 2025.

Table of Contents

Table of Contents (continued)

Armored T Cells striking out to fight against tumor cells

NABT 2025 ST LOUIS OCT 30-NOV 2, 2025

PROJECT IGELS

Come see Project IGELS at the 2025 Annual NABT Conference

Undergraduate instructors of non-majors biology courses are invited to this workshop to learn more about implementing activities and resources developed by the IGELS (Interactions in General Education Life Science) project. IGELS "Catalysts" will be introduced to the suite of IGELS resources and frameworks, including the LifeSkills guide, the Intentional Pedagogy Framework, and new models of Scientific Literacy and the Undergraduate Science Education Ecosystem.

This workshop will provide the Catalysts an opportunity to reflect on their personal teaching philosophies and course curricula and develop an action plan for using the IGELS frameworks.

Interested participants will have additional opportunities to participate in the IGELS research project with mentoring and financial support.

Lunch and registration to the NABT conference will be provided.
Space is limited.

Armoring the Immune System:
Undergraduate Perspectives on the Evolution of CAR T Cell Therapy

By J.F. Treml*†

Chimeric Antigen Receptor (CAR) T cells represent one of the most powerful tools in modern medicine's arsenal against cancer—and, increasingly, autoimmune disease. Each year, the Topics in Biotechnology course at the University of Kansas Edwards Campus selects a timely and transformative area of research to anchor student investigation. For Spring 2025, the course explored the rise of T cell-based immunotherapies, tracing the trajectory from early adoptive transfer experiments to the development of armored, logic-gated, and multifunctional CAR platforms. The student-authored review articles featured here represent the best examples of how undergraduates can critically engage with the primary literature and contribute meaningfully to scientific conversation.

This was also the first year the course was accompanied by a podcast: Reprogrammed: The Biotechnology Podcast, created by the instructor to introduce and contextualize the key concepts in each week's reading. Each episode offered a short, structured conversation—between a human and an AI cohost—designed to scaffold students' understanding while inviting a broader audience into the unfolding story of CAR T cell research. Transcripts and show notes are available at https://downhousesoftware.wordpress.com, and the podcast is available through Apple Podcasts.

The student reviews in this issue reflect both the conceptual depth and technical diversity of the field. Benji Orth explores tandem CARs capable of targeting glioblastoma's heterogeneous antigens. Carson Gray and Yenny Feng each examine structural refinements to the scFv domain—Gray focusing on expression and antigen affinity, Feng expanding the concept into macrophage-based CARs (CAR-M) as a complementary cell therapy. Arianna Theleman reviews the integration of IL-36γ as an immune-enhancing cytokine, while Soham Kawade discusses IL-24-armored CARs targeting cancer stem cells. Yusef Elghzali considers how nanobody-based CARs, paired with dendritic/tumor fusion vaccines, may improve outcomes in solid tumors.

Two reviews extend the potential of CAR technology beyond oncology. Isabella Press and Samia Chergui examine the application of anti-CD19 CAR T cells in systemic lupus erythematosus (SLE), highlighting the therapeutic promise of fully human constructs that minimize cytokine toxicity while retaining efficacy against autoreactive B cells.

These papers represent the culmination of a semester-long exploration not only into the mechanics of CAR T cell design and function, but also into the power of scientific storytelling. We hope these reviews inspire further reading, reflection, and engagement with the exciting frontiers of cell-based immunotherapy. If you are interested in having your class participate by using this course's reading list in the future—enabling your students to submit News and Views-style articles for upcoming issues of the journal—please visit us online at the downhouse software site (see above) and at the Journal's home at: https://journals.ku.edu/MJUSc/index, where future reading lists will be posted. Or feel free to contact me directly to collaborate in generating new ones.

Reviews on other topics are also welcome, but a short format is preferable.

*University of Kansas, Edwards Campus, Biotechnology

†Corresponding Author jtreml@ku.edu

A Double Strike Against Tumor Resistance: IL-24 Enhances CAR-T Therapy by Disarming Cancer Stem Cells

By Soham Kawade [b]

Despite the transformative success of chimeric antigen receptor (CAR)-T cell therapy in hematologic malignancies, its efficacy against solid tumors remains disappointing. One increasingly recognized obstacle is the persistence of cancer stem cells (CSCs), which are resistant to conventional therapies and capable of repopulating tumors.[1] A 2024 study published in the British Journal of Cancer by Zhang et al., addresses this challenge by engineering CAR-T cells to co-express interleukin-24 (IL-24), a cytokine with known tumor-suppressive functions.[2] This strategy not only augments T cell activation and persistence but also directly suppresses cancer stem cells (CSCs) through apoptosis and stemness inhibition. This dual-targeting approach reframes our understanding of CAR-T limitations and introduces a promising new direction for overcoming therapeutic resistance in solid tumors.

Numerous factors contribute to the failure of CAR-T cells in solid tumors—including poor infiltration, immunosuppressive microenvironments, antigen heterogeneity, and T cell exhaustion.[3,4] A recurring theme in recent literature was the crucial but underappreciated role of CSCs in therapy resistance and tumor relapse. These rare, self-renewing tumor-initiating cells exhibit enhanced plasticity, resist immune-mediated killing, and regenerate tumor bulk following treatment.

Zhang et al. introduce CAR-T cells engineered to express IL-24, a cytokine previously characterized for its tumor-suppressive and immunomodulatory roles. By pairing antigen targeting with IL-24 secretion, the authors demonstrate improved tumor control through both T cell enhancement and direct CSC eradication.

The study opens by confirming the limited effectiveness of standard CAR-T cells in killing CSCs. Using NKG2D and Her2-targeting CARs in lung and esophageal cancer models, they observed that while CAR-T cells effectively lysed bulk tumor cells, a population of residual cells remained. These surviving cells exhibited expression of CSC markers (e.g., CD133, SOX2, PROM1) and characteristics (e.g., greater sphere-forming capacity and increased tumor-initiating potential in vivo). Importantly, antigen loss was ruled out as a cause of escape, confirming that CSCs resist CAR-T killing despite maintaining antigen expression.

This finding echoes the insights from prior work including Prager et al., which highlight CSCs as central architects of tumor heterogeneity and resilience and reinforces the notion that therapies failing to eliminate CSCs merely prune the tumor mass, allowing regrowth from the root.[5]

IL-24, a member of the IL-10 cytokine family, has been studied for its ability to selectively induce apoptosis in tumor cells without harming normal tissue. Beyond its direct cytotoxicity, IL-24 is known to modulate the tumor immune microenvironment and sensitize tumors to other therapies.[2,6] Zhang et al. build on this legacy by exploring IL-24's effects in the CAR-T context.

First, they show that exogenous IL-24 suppresses CSC viability, reduces sphere formation, and downregulates stemness-associated genes. These effects are partially mediated through inhibition of the Wnt/β-catenin pathway, a key regulator of CSC maintenance. Western blot data revealed that IL-24 treatment decreased active β-catenin and increased cleaved caspase-3, indicating apoptosis validating previous reports that IL-24 suppresses tumor growth by targeting CSCs.[7]

Second, Zhang et al. demonstrate that IL-24 boosts T cell function. In vitro, IL-24-treated T cells showed elevated expression of activation markers (CD69, CD28), increased central memory differentiation (CCR7+ CD45RO+), and enhanced proliferation. Interestingly, IL-24 did not increase apoptosis of tumor cells directly, suggesting that its effects are mediated by T cells rather than them being directly toxic to tumor cells.

To integrate these dual benefits, the authors generated CAR-T cells that co-express IL-24 using a lentiviral construct. These CAR.IL-24-T cells exhibited superior cytotoxicity against tumor cells compared to conventional CAR-Ts and produced more IL-2 and IFN-γ in co-culture. In sphere-formation assays, residual tumor cells from IL-24-CAR-T co-cultures had dramatically reduced stemness, suggesting effective CSC elimination.

In mouse xenograft models of lung and esophageal cancer, CAR.IL-24-T cells

The University of Kansas Edwards Campus Biotechnology Program is made possible by the generous support from the

Johnson County Research and Education Triangle

demonstrated improved tumor control, higher T cell infiltration, reduced PD-1 expression (indicative of lower exhaustion), and longer survival. Strikingly, in late-stage tumors, only CAR.IL-24-T cells prevented relapse and conferred durable responses. These in vivo results strongly support the idea that CSCs are central to recurrence and that targeting them is key to long-term remission.

Zhang et al.'s work aligns with a growing appreciation that immune therapies must address not only the bulk tumor and microenvironment but also the intrinsic plasticity of tumor cells. CSCs represent a resilient population capable of adapting to selective pressure and reigniting disease. As seen in this study, IL-24 is a promising agent that simultaneously disarms CSCs and fortifies CAR-T cells (**Figure 1)**.

This dual-function strategy may prove particularly useful in combination with other next-generation CAR-T innovations, such as checkpoint inhibition, chemokine receptor engineering,[8] or metabolic modulation.[9] Moreover, IL-24's synergy with existing chemotherapeutics suggests that it may serve as a broadly useful adjuvant, both within and beyond CAR-T platforms.[10]

However, several questions remain. The precise mechanisms by which IL-24 regulates T cell memory and exhaustion warrant further study. Additionally, the lack of a patient-derived xenograft (PDX) model limits its direct clinical translation. Finally, while IL-24 appears safe in preclinical models, its effects on human immune homeostasis in vivo remain to be tested. A Phase I clinical trial involving IL-24 CAR-Ts is reportedly underway, which may address these concerns.

Zhang et al. (2024) have delivered a pivotal contribution to the field of cancer immunotherapy. By incorporating IL-24 into CAR-T cells, they achieve a rare and valuable synergy: improving T cell fitness while directly targeting the elusive CSC population. This study reframes how we think about cytokine engineering—not just as immune adjuvants, but as molecular tools that reshape tumor biology at its core. As the field moves forward, such multi-targeted designs may become the new blueprint for overcoming therapeutic resistance in solid tumors.

References

1. D'Accardo, C. et al. Cancer cell targeting by CAR-T cells: A matter of stemness. Front. Mol. Med. 2, (2022).
2. Zhang, K. et al. IL-24 improves efficacy of CAR-T cell therapy by targeting stemness of tumor cells. Br. J. Cancer 130, 1337–1347 (2024).
3. Chen, T., Wang, M., Chen, Y. & Liu, Y. Current challenges and therapeutic advances of CAR-T cell therapy for solid tumors. Cancer Cell Int. 24, 133 (2024).
4. Guzman, G., Reed, M. R., Bielamowicz, K., Koss, B. & Rodriguez, A. CAR-T Therapies in Solid Tumors: Opportunities and Challenges. Curr. Oncol. Rep. 25, 479–489 (2023).
5. Prager, B. C., Xie, Q., Bao, S. & Rich, J. N. Cancer Stem Cells: The Architects of the Tumor Ecosystem. Cell Stem Cell 24, 41–53 (2019).
6. Modi, J. et al. Insights into the Mechanisms of Action of MDA-7/IL-24: A Ubiquitous Cancer-Suppressing Protein. Int. J. Mol. Sci. 23, 72 (2022).
7. Targeting breast cancer-initiating/stem cells with melanoma differentiation-associated gene-7/interleukin2-4 - Bhutia - 2013 - International Journal of Cancer - Wiley Online Library. https://onlinelibrary.wiley.com/doi/10.1002/ijc.28289.
8. Craddock, J. A. et al. Enhanced tumor trafficking of GD2 chimeric antigen receptor T cells by expression of the chemokine receptor CCR2b. J. Immunother. Hagerstown Md 1997 33, 780–788 (2010).
9. Fultang, L. et al. Metabolic engineering against the arginine microenvironment enhances CAR-T cell proliferation and therapeutic activity. Blood 136, 1155–1160 (2020).
10. McKenzie, T. et al. Combination therapy of Ad-mda7 and trastuzumab increases cell death in Her-2/neu–overexpressing breast cancer cells. Surgery 136, 437–442 (2004).

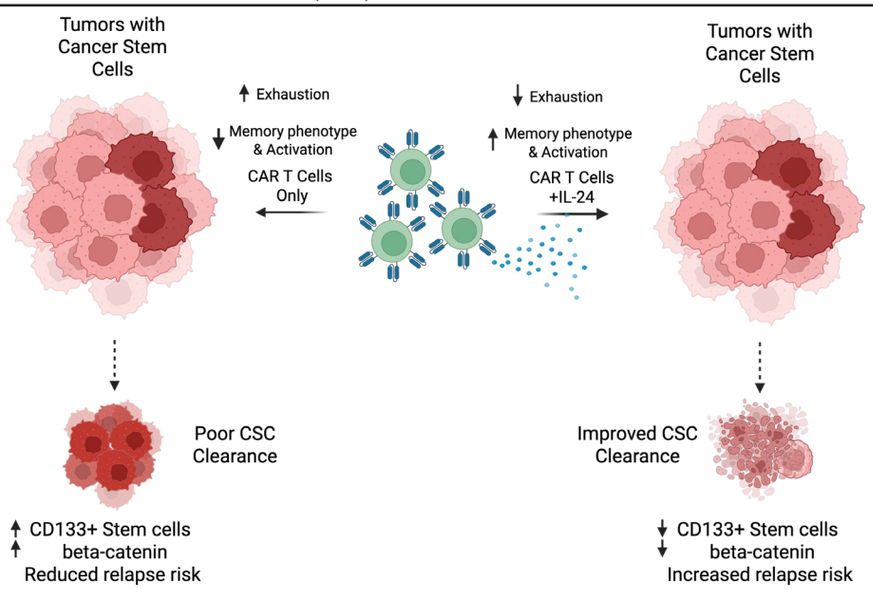

Figure 1 | IL-24-armed CAR-T cells overcome cancer stem cell (CSC)-mediated resistance in solid tumors. (Left) Conventional CAR-T cells (lacking IL-24) effectively target bulk tumor cells but fail to eliminate CD133+ CSCs due to persistent Wnt/β-catenin signaling, which maintains stemness and survival. Residual CSCs drive tumor relapse. CAR-T cells exhibit limited activation (low CD69+/CD28+) and increased exhaustion. (Right) IL-24-expressing CAR-T cells dual-target bulk tumor cells and CSCs. IL-24 disrupts CSC resistance by: (i) suppressing Wnt/β-catenin activity, reducing CD133+ stemness; (ii) inducing apoptosis; and (iii) enhancing CAR-T cell fitness (elevated activation markers, memory differentiation, and reduced exhaustion). This combined action improves tumor clearance and reduces relapse risk.

A Humanizing Rewrite for CAR T Cells in Autoimmune Disease: A Step Toward Repeatable, Durable Therapy

By Samia Chergui

Can the immunogenicity challenges of traditional CD19 CAR T cells be solved by replacing the murine antibody component with a human analog? In their 2024 Molecular Therapy – Methods & Clinical Development study, Peng et al. present CABA-201, a fully human anti-CD19 CAR T therapy aimed at treating autoimmune disease with greater persistence and safety.[1]

Autoimmune diseases affect more than 4% of the global population and often require chronic treatments that carry serious side effects.[2] Conditions such as systemic lupus erythematosus (SLE), multiple sclerosis (MS), and pemphigus vulgaris (PV) involve aberrant B cell activity and the production of self-reactive antibodies.[3] While anti-CD20 monoclonal therapies like rituximab have provided clinical relief, they fall short in fully eliminating tissue-resident B cells and often necessitate repeated dosing.[4,5] These limitations have driven interest in the use of chimeric antigen receptor (CAR) T cell therapies targeting CD19, a B cell marker, to achieve deeper, more durable immunomodulation.[6,7,8]

Recent clinical reports suggest that CD19 CAR T cells may induce long-lasting remission in SLE and other autoimmune disorders.[7,8] Yet most CD19 CAR constructs in use today contain murine-derived antigen-binding regions, which can trigger immune responses that compromise therapeutic persistence and limit the feasibility of retreatment.[9,10] This raises a key question: Can a fully human anti-CD19 CAR T cell preserve therapeutic efficacy while reducing immunogenicity, particularly in patients who may need repeated dosing?

A schematic of this therapeutic strategy is presented in **Figure 1** to illustrate the proposed mechanism of B cell depletion in autoimmune disease. The authors evaluate CABA-201 across a series of preclinical models using both healthy donors and patients with autoimmune diseases, comparing it to the widely used murine-based FMC63 CAR T cell.

Both CABA-201 and FMC63 CARs demonstrated robust surface expression and equivalent CD4/CD8 T cell subset composition after *ex vivo* manufacturing. In cytotoxicity assays, CAR T cells from both constructs showed >70% killing efficiency against $CD19^+$ leukemia cells across a range of effector-to-target ratios. Cytokine profiling revealed high levels of IFN-γ, TNF-α, IL-2, and GM-CSF, with CABA-201 eliciting slightly higher output in some conditions.[1] These results align with previous work showing that fully human CAR constructs can elicit potent cytotoxic and cytokine responses *in vitro*.[11,12]

In vivo, both CAR T products induced strong tumor clearance in NSG mice bearing CD19+ leukemia xenografts. Bioluminescent imaging and flow cytometry confirmed CAR T cell trafficking to lymphoid organs and prolonged persistence, especially in the spleen. Importantly, CABA-201 did not bind or lyse CD19-negative epithelial cells in co-culture assays, indicating minimal off-target toxicity.[1]

To extend relevance to autoimmune disease, Peng *et al.* tested CABA-201 using T cells from patients with SLE, RA, MS, PV, scleroderma, and inflammatory myopathy. In all cases, CAR T cells maintained high surface expression, displayed antigen-specific activation markers (CD25, CD69), and eliminated autologous $CD19^+$ B cells without affecting healthy epithelial cells.[1] These findings support the versatility of CABA-201 across disease settings and patient backgrounds.

By eliminating the murine antibody domain, CABA-201 may offer a path toward more durable treatments without eliciting immune responses against the construct, which would allow for future retreatments that are critical in attenuating autoimmunity[1,11,12] While Peng *et al.* convincingly demonstrate the preclinical efficacy and selectivity of this platform, questions remain about how these effects will translate in human autoimmune settings. Disease heterogeneity, antigen escape, and T cell exhaustion may complicate long-term outcomes. Nonetheless, CABA-201 represents a significant step forward in humanizing CAR T cell platforms for safer and more sustainable use in chronic immune disorders.

References

1. Peng, B. J. et al. Preclinical specificity & activity of a fully human 4-1BB-expressing anti-CD19 CAR therapy for treatment-resistant autoimmune disease. Mol. Ther. Methods Clin. Dev. 32, 140–151 (2024).
2. Hayter, S. M. & Cook, M. C. Updated assessment of the prevalence, spectrum and case definition of autoimmune disease. Autoimmun. Rev. 11, 754–765 (2012).
3. Davidson, A. & Diamond, B. Autoimmune diseases. N. Engl. J. Med. 345, 340–350 (2001).
4. Merrill, J. T. et al. Efficacy and safety of rituximab in moderately-to-severely active systemic lupus erythematosus: the randomized, double-blind, phase II/III systemic lupus erythematosus evaluation of rituximab trial. Arthritis Rheum. 62, 222–233 (2010).
5. Roll, P. et al. Regeneration of B cell subsets after rituximab treatment in patients with rheumatoid arthritis. Arthritis Rheum. 58, 598–604 (2008).
6. Gill, S. & June, C. H. Going viral: chimeric antigen receptor T-cell therapy for hematologic malignancies. Immunol. Rev. 263, 68–89 (2015).
7. Mackensen, A. et al. Anti-CD19 CAR T cell therapy for refractory systemic lupus erythematosus. N. Engl. J. Med. 387, 2030–2038 (2022).
8. Mougiakakos, D. et al. CD19-targeted CAR T cells in autoimmune disease. Nat. Med. 29, 115–123 (2023).

University of Kansas
Corresponding Author jtreml@@ku.edu

9. Maus, M. V., Grupp, S. A., Porter, D. L. & June, C. H. Antibody-modified T cells: CARs take the front seat for hematologic malignancies. Blood 123, 2625–2635 (2014).
10. Brudno, J. N. & Kochenderfer, J. N. Chimeric antigen receptor T-cell therapies for lymphoma. Nat. Rev. Clin. Oncol. 15, 31–46 (2018).
11. Hale, M. et al. Engineering CAR-T cells with a fully human scFv to reduce immunogenicity in cancer and autoimmune disease. Mol. Ther. 30, 1341–1353 (2022).
12. Sommermeyer, D. et al. Fully human anti-CD19 CAR T cells for the treatment of B cell malignancies and autoimmune disease. Blood 127, 2081–2090 (2016).
12. Sommermeyer, D. et al. Fully human anti-CD19 CAR T cells for the treatment of B cell malignancies and autoimmune disease. Blood 127, 2081–2090 (2016).

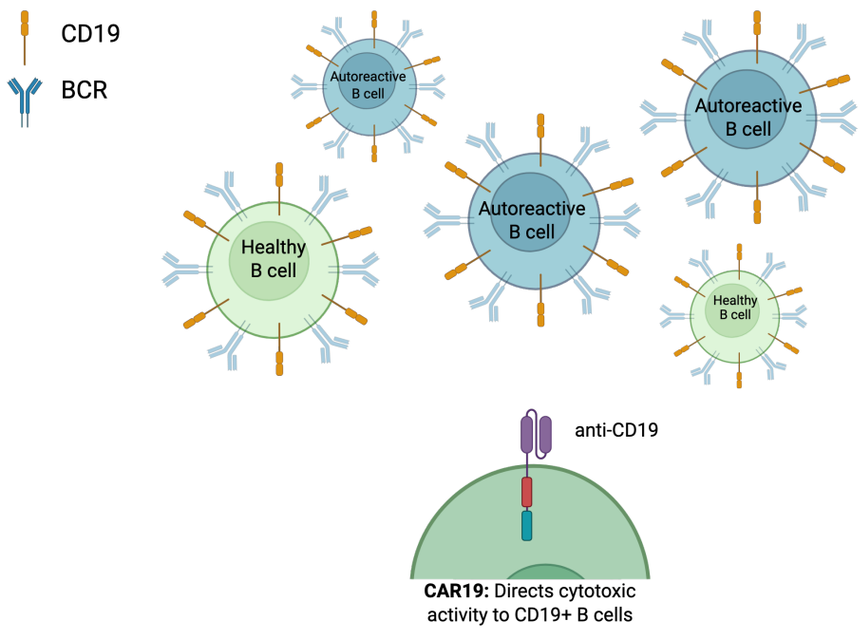

Figure 1 | Anti-CD19 CAR T Cells improve antibody-mediated autoimmune disorders | CABA-201 CAR T cell therapy utilizes fully human anti-CD19 CAR (IC78 scFv with 4-1BB), to target and eliminate over-represented autoreactive $CD19^{+}$ B cells, helping restore immune balance.

Armored CARs rooting out cancer cells in a hostile tumor microenvironment

FCs and CAR Ts:

Teamwork Makes the Dream work

By Yusef Elghzali

Chimeric Antigen Receptor (CAR) T-cell therapy uses genetically engineered receptors to redirect T cells toward tumor-associated antigens (TAAs). These synthetic receptors typically include a single-chain variable fragment (sFv) linked to a CD3ζ signaling domain, enabling precise recognition and killing of cancer cells.

Gross and Eshhar first demonstrated immunoglobulin-based chimeric molecules as functional receptors for T cells in 1989[1]; since then, CAR T-cell therapy has rapidly developed, resulting in seven FDA-approved therapies to date which target B-cell antigens such as CD19 or BCMA.[2,*] In a 2023 Cancer Immunology and Immunotherapy article, Sun et al., investigated whether combining a dendritic cell/tumor fusion cell (FC) vaccine with EGFRvIII-specific nanobody-based CAR T cells could enhance anti-tumor efficacy against solid glioblastoma tumors.[14-16]

Without any modifications, these early CARs (now referred to as 'first-generation') bearing only CD3ζ signaling regions were limited by poor persistence, as T-cell activation requires both a primary and a co-stimulatory signal for intracellular signaling. Successive generations of receptors implemented revisions and additions to address activation, persistence, and efficacy of these cells.

- First-generation CARs: CD3ζ only; limited persistence
- Second-generation: CD3ζ + CD28 or 4-1BB; improved persistence and activation[3]
- Third-generation: CD3ζ + two costimulatory domains (CD28 + 4-1BB)[4]
- Next-gen modifications: IL-12 secretion, armored CARs, etc., aim to overcome tumor microenvironment suppression.[5]

The clinical efficacy of CAR T cells was demonstrated in 2013, when Brentjens and colleagues showed remission in adults with B-cell tumors after second generation CAR T-cell treatment.[6] Since then, many studies have shown clinical efficacy of CAR T cells when treating cancer.

Despite their success, CAR T cells are still limited in their ability to treat solid tumors. This is likely due to poor infiltration and persistence within the complex tumor microenvironment. Solid tumors are characterized by complex tumor microenvironments that include conditions like high oxidative stress, acidic pH, hypoxia and presence of suppressive immune cells/cytokines.[7]

Nanobody-based CAR T cells (Nb-CAR T Cells) offer a promising solution. Nanobodies, derived from camelid heavy-chain antibodies are smaller and have less steric hindrance than traditional sFv domains, increasing the CAR's ability to access hidden epitopes, thereby enhancing tumor recognition. Because of the inherent simplicity of their structure, Nb-CAR T Cells are less likely to aggregate due to their single-domain structure, nanobodies eliminate the need for heavy/light chain pairing, reducing misfolding and aggregation risk.

Lastly, due to their camelid origin, they are more stable in the complex tumor microenvironment leading to decreased T cell exhaustion.[8] Overall, nanobody-based CAR T cells have demonstrated improved tumor regression compared to traditional sFv-based CARs. [9-12] (and Mustafa *et al*.)

Researchers generated three CAR T-cell types:

- EGFRvIII-specific Nb-CAR T Cells
- Irrelevant-CAR T Cells (expressing a non-specific Nb-CAR)
- Mock CAR T cells (expressing no CAR).

EGFRvIII-specific Nb-CAR T cells showed enhanced proliferation, increased expression of activation markers (CD25, CD69), and elevated cytokine production (TNF-α, IL-2, IFN-γ), outperforming irrelevant and mock CAR T cells. Cytotoxicity assays revealed higher lysis of $EGFRvIII^+$ tumor cells by EGFRvIII Nb-CAR T Cells, with minimal activity against EGFRvIII-negative cells, demonstrating antigen-specific cytotoxicity.

In vivo, tumor-bearing mice treated with EGFRvIII Nb-CAR Ts exhibited increased survival and reduced tumor growth compared to controls. No significant systemic side effects were observed. Flow cytometry showed higher $CD3^+$ T-cell infiltration in tumors and spleens, and greater CAR T-cell persistence in blood.

To create the fusion vaccine, dendritic cells were fused with EGFRvIII-positive tumor cells using polyethylene glycol. The study then compared four groups: anti-EGFRvIII Nb-CAR T Cells alone, with live, non-fused dendritic cells, and with live FCs (dendritic cells fused with tumor cells), and FC alone. The -CAR T + FC group demonstrated the highest proliferation, activation marker expression, and central memory phenotype ($CD62L^+CD45RA^-$). Increased expression of LAG-3 and TIM-3 suggested early T-cell exhaustion, likely due to heightened activation. Additional cytotoxicity assays and in vivo experiments confirmed that the Nb-CAR T Cell + FC group had the greatest tumor cell lysis, persistence, longest survival, and lowest tumor burden.

While the study did not explicitly investigate bidirectional signaling between CAR T cells and FCs, it raises an interesting possibility: that cytokine secretion from CAR T cells—particularly IFN-γ—may counteract FC-induced regulatory T-cell differentiation, which may decrease potency of the vaccine in vivo. This hypothesis warrants further investigation.[17]

Pairing EGFRvIII-specific nanobody-based CAR T cells with a dendritic/tumor fusion vaccine significantly enhances T-cell activation, cytotoxicity, persistence, and anti-tumor efficacy in preclinical models. This combination outperformed CAR T cells alone and CAR T cells with non-fused dendritic cells, representing a promising advancement in CAR T-cell therapy for solid tumors. Overall, this study shows an innovative way to improve cancer treatment.

References

1. Gross G, Eshhar Z. Endowing T cells with antibody specificity using chimeric T cell receptors. Nature. 1989;339(6225):70-72.
2. June CH, Sadelain M. Chimeric Antigen Receptor Therapy. N Engl J Med. 2018;379(1):64-73.
* https://israelihospitals.org.il/car-t-updates-2025-latest-fda-approved-treatments-and-advancements.html
3. Finney HM, Lawson AD, Bebbington CR, Weir AN. Chimeric receptors providing both-

University of Kansas
Corresponding Author jtreml@@ku.edu

primary and costimulatory signaling in T cells from a single gene product. J Immunol.1998;161(6):2791-2797.
4. Imai C, Mihara K, Andreansky M, Nicholson IC, Pui CH, Geiger TL, et al. Chimeric receptors with 4-1BB signaling capacity provoke potent cytotoxicity against acute lymphoblastic leukemia. Leukemia. 2004;18(4):676-684.
5. Chmielewski M, Abken H. CAR T cells releasing IL-12 convert the suppressive tumor microenvironment of pancreatic cancer into a highly inflammatory milieu. Cancer Immunol Immunother. 2012;61(4):653-662.
6. Brentjens RJ, Davila ML, Riviere I, Park J, Wang X, Cowell LG, et al. CD19-targeted T cells rapidly induce molecular remissions in adults with chemotherapy-refractory acute-lymphoblastic leukemia. Sci Transl Med. 2013;5(177):177ra38.
7. Newick K, O'Brien S, Moon E, Albelda SM. CAR T cell therapy for solid tumors. Annu Rev Med. 2017;68:139-152.
8. Bannas P, Hambach J, Koch-Nolte F. Nanobodies and nanobody-based human heavy-chain antibodies as antitumor therapeutics. Front Immunol. 2017;8:1603.
9. Xie, Y. J., Dougan, M., Jailkhani, N., Ingram, J. R., & Ploegh, H. L. (2022). Nanobody-based CAR-T cells for cancer immunotherapy. Signal Transduction and Targeted Therapy, 7(1), 36.
10. Xie YJ, Dougan M, Ingram JR, Pishesha N, Fry TJ, Mahmood U, et al. Improved antitumor efficacy of chimeric antigen receptor T cells derived from camelid single-domain antibodies. Cancer Immunol Res. 2019;7(7):1266-1273.
11. Li T, Qi S, Unger M, Hou Y, Deng Q, Liu J, et al. Suppression of tumor escape by targeting TGF-β signaling in CAR-T cell therapy. Mol Ther. 2020;28(11):2302-2312.
12. Liu X, Jiang S, Fang C, Yang S, Olalere D, Pequignot EC, et al. Affinity-tuned ErbB2 or EGFR chimeric antigen receptor T cells exhibit an increased therapeutic index against tumors in mice. Cancer Res. 2015;75(17):3596-3607.
13. Sun Y, Zhang C, Wang Z, Song J, Wang Y, Wang Z, et al. Dendritic cell/tumor fusion cell vaccine combined with EGFRvIII-specific nanobody CAR T cells enhances antitumor efficacy against glioblastoma. Cancer Immunol Immunother. 2023;72(2):345-359.
14. Heimberger AB, Hlatky R, Suki D, Yang D, Weinberg J, Gilbert M, et al. Prognostic effect of epidermal growth factor receptor and EGFRvIII in glioblastoma multiforme patients. Clin Cancer Res. 2005;11(4):1462-1466.
15. Gan HK, Cvrljevic AN, Johns TG. The epidermal growth factor receptor variant III (EGFRvIII): where wild things are altered. FEBS J. 2013;280(21):5350-5370.
16. Sampson JH, Archer GE, Mitchell DA, Heimberger AB, Bigner DD. Tumor-specific immunotherapy targeting the EGFRvIII mutation in patients with malignant glioma. Semin Immunol. 2008;20(5):267-275.
17. Palucka K, Banchereau J. Dendritic-cell-based therapeutic cancer vaccines. Immunity. 2013;39(1):38-48.

Striking a Balance: scFv affinity modulates expression and activation in CAR T cells

By Carson Gray

Chimeric-antigen receptor (CAR) T cells represent a substantial advance in anti-tumoral therapies due, in large part, to their cell-specific toxicity and minimal off-target effects. These therapeutics are produced by transduction of a CAR construct containing, at least, an extracellular antigen-binding domain and a T cell activation domain in the form of CD3ζ into autologous T Cells from the patient.[1] Most commonly, the CAR will also include costimulatory motifs such as the signaling region of CD28.[2] Together, these allow the cell to bind targets in an antigen-dependent manner and mount a highly specific cytotoxic response. The antigen-binding domain of most CARs is a modified antibody variable fragment (Fv) known as a single-chain variable fragment (sFv).[1] This approach has yielded significant clinical successes, including some complete remissions in patients who otherwise had exhausted their therapeutic options.[3]

Since their inception in the 1980s, improvements have enhanced the durability and efficacy of CAR-based therapies. One area of insight has been in the avidity of CAR constructs. Avidity of a CAR is a combination of two important attributes: surface expression and antigen binding.[4] While it is clear that CARs must have a robust avidity to mount a response, excess signaling can also be problematic. Specifically, excessively potent CAR-mediated activation can result in T cell exhaustion, off-target tissue damage, and cytokine toxicity. An important advancement in this area was the use of CRISPR platforms to target CAR to the endogenous T cell receptor (TCR) promoter.[5] This placed CAR surface expression under the same regulation as the endogenous TCR, which is dynamically expressed in the presence of antigen. This has been beneficial in optimizing surface expression and avidity, but research into modulating antigen-affinity is lacking.

However, paralleling the challenges faced by natural lymphocytes during their development and antigen receptor randomization, basic questions concerning the physical expression, stability, and binding capacity of CAR sFv regions remained unanswered. To address these, Fujiwara et al., in the March 2020 issue of Biochemical and Biophysical Research Communications, examined sFv structural influences on antigen-binding and expression.1 They constructed four anti- Kinase insert Domain Receptor (KDR) CARs from the variable fragments of antibodies with a range of antigen affinities. Four distinct CAR T Cells were made from these constructs, which each included a GFP reporter to ensure equivalent transduction efficiencies. One construct exhibited significantly decreased surface expression efficiency, suggesting that it was intracellularly degraded. Two others had higher-than-expected molecular weights, suggesting post-translational modifications.

Only one construct bound KDR, as evidenced by specific lysis of a KDR-expressing B Cell line, L1.2. Immunofluorescent staining was done to observe the distribution of the CARs in each of the sFv types; it was found that CAR1-L3H was evenly distributed about the cell surface, while CAR2-L3H and CAR4-L3H formed clusters of aggregate. This provides further evidence for post-translational modifications that could be the cause of intermolecular adherence and aggregate formation.

When these L1.2 cells were transduced with the CAR constructs to assess differences in surface expression regulation, each exhibited high surface expression, including CAR3-L3H, which previously exhibited low expression in T cells. This suggests that the chaperone machinery in B cells could be better suited to expression of sFv- containing constructs.

To assess structural influence on sFv surface expression and antigen specificity, Fv order and linker structure was modified. CAR1-L3H, which previously was shown to be highly expressed and have strong affinity for KDR, was unaffected by either Fv order or linker structure, which suggests that these properties do not significantly affect sFv expression or binding. Alternatively, it was found that the framework regions (FRs) of the sFv have a potent influence on membrane stability. FRs and complementary-determining regions (CDRs) are the two components that make up the Fv. CDRs are the component that determine antigen binding affinity, while FRs are the scaffolding that orient the CDRs. CDR grafting is a technique where the CDRs of one antigen-binding region are grafted into the FRs of another (**Figure 1**). This has traditionally been done to reduce the immunogenicity of antibody-based therapies derived from murine antibodies by grafting their CDRs into human immunoglobulin. This allows for retention of antigen specificity while maintaining the properties of the antibody.10 Fujiwara *et al.* utilized this technique in the context of CAR sFv's.

Sequence analysis revealed that CAR3-L3H possesses a high similarity to CAR4-L3H. Thus, to increase surface expression efficiency of CAR3-L3H, the CDRs of CAR3-L3H were grafted into the FRs of CAR4-L3H. Interestingly, this construct, termed CAR5-L3H, exhibited significantly improved surface expression from CAR3-L3H. Another construct using the FRs of CAR1-L3H and CAR3-L3H, termed CAR6-L3H, was not expressed on T cells. While CAR1-L3H originally had high surface expression, it does not have much sequence similarity with CAR3-L3H. These data suggest that the FRs of sFv's is a potent determinant of surface expression, and that CDR grafting is an effective method to express s sFv's of low surface expression efficiency. It also appears that expression of grafted chimeras requires high sequence similarity between the two sFv's .

These findings provide valuable information in the progression of CAR efficacy. While the order of Fv's and linker structure do not appear to significantly affect CAR surface expression or antigen specificity, the FR's seem to have a major influence. Post-translational modifications and intracellular degradation may be important considerations in the avidity of CAR constructs, as evidenced by aggregation or low expression in some sFv's . CDR grafting represents a potential step forward in tuning CAR-mediated T cell activation by conferring variable antigen-specificity to FR's of high membrane stability. B cell proteins involved in the biosynthesis and trafficking of antibodies may also be an important area of further investigation, as it was found that B cells exhibit high surface expression efficiency, even in CAR constructs that previously were found to be minimally expressed in T cells. Further research into the structural influence of sFv's is necessary to achieve optimal clinical outcomes in CAR T cell therapies.

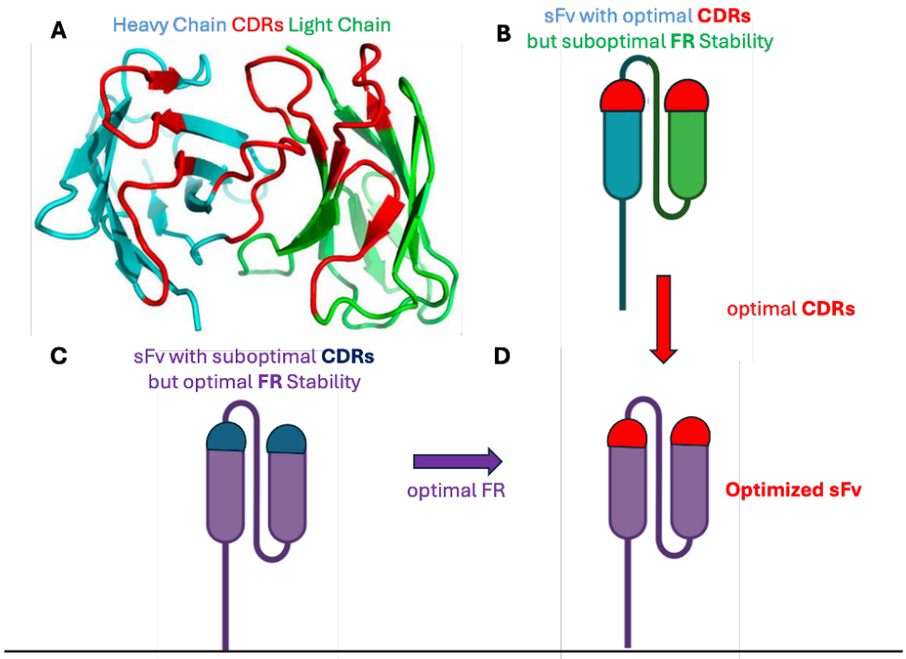

Figure 1 | Grafting of optimal affinity CDRs to FRs generates fine-tuned sFv. A) Ribbon Diagram of sFv with FR and optimal CDR elements highlighted. B) A Cartoon of the same sFv from A with region coloration preserved. C) An sFv with suboptimal CDR, but stable FR region. D) A chimeric sFv with optimal CDR and FR regions.

References

1. Gross, G., Waks, T. & Eshhar, Z. Expression of immunoglobulin–T-cell receptor chimeric molecules as functional receptors with antibody-type specificity. Proc. Natl Acad. Sci. USA 86, 10024–10028 (1989).
2. Maher, J., Brentjens, R., Gunset, G. et al. Human T-lymphocyte cytotoxicity and proliferation directed by a single chimeric TCRζ/CD28 receptor. Nat. Biotechnol. 20, 70–75 (2002).
3. Brentjens, R. J. et al. CD19-targeted T cells rapidly induce molecular remissions in adults with chemotherapy-refractory acute lymphoblastic leukemia. Sci. Transl. Med. 5, 177ra38 (2013).
4. Fujiwara, K., Masutani, M., Tachibana, M. & Okada, N. Impact of scFv structure in chimeric antigen receptor on receptor expression efficiency and antigen recognition properties. Biochem. Biophys. Res. Commun. 527, 350–357 (2020).
5. Eyquem, J. et al. Targeting a CAR to the TRAC locus with CRISPR/Cas9 enhances tumour rejection. Nature 543, 113–117 (2017).

University of Kansas
Corresponding Author jtreml@@ku.edu

Reprogramming the Enemy Within:

Patient-Derived CAR-T Cells Effectively Target Inflammation-Inducing B cells

By Isabella Press

Systemic lupus erythematosus (SLE) is an autoimmune disease characterized by the production of autoantibodies by B cells. Under normal conditions, autoreactive B and T cells are eliminated during maturation. However, in SLE, central tolerance is disrupted, resulting in widespread inflammation and tissue damage.[1] Current therapies include the use of monoclonal antibodies to aid in the depletion of autoreactive cells, although these antibodies may fail to adequately penetrate the affected tissues where cells reside.[2] In contrast to monoclonal antibodies, CAR T cells have been shown to exhibit superior tissue penetration[3] resulting in greater depletion of B cells in SLE patients. Specifically, a second generation[4] anti-CD19 fully human CAR construct that includes a CD28 costimulatory domain,[5] as well as a CD8α hinge and transmembrane domain and a CD3ζ activation domain,[6] was developed using a CAR vector Hu19-CD828Z provided by Kyverna Therapeutics. In their 2024 paper, Dingfelder *et al*. denote the potential of autologous, fully human CAR T cells in treating SLE patients.[7]

The authors first sought to determine whether CAR T cells could be generated from cryopreserved leukapheresis material obtained from SLE patients who had undergone immunosuppressive therapies. To do this they transduced cryopreserved $CD4^+$ and $CD8^+$ T-cells with a lentiviral vector to express the Hu19-CD828Z CAR fully human anti-CD19 second generation CAR from five SLE patients and five healthy donors (HD). Both SLE- and HD- transduced T cells exhibited similar expansion rates and CAR expression levels with no significant differences between the two groups. Although the authors observed comparable CAR expression and expansion between SLE-derived and HD-CAR T cells, they noted a more balanced CD4/CD8 T cell ratio in the SLE group. In both SLE and HD samples, central memory T cells (T_{cm}; $CD45RO^+CCR7^+$) predominated. However, SLE-derived CAR T cells exhibited a modest increase in the proportion of effector memory T cells (T_{em}; $CD4^+CD45RO^+CCR7^-$) relative to HD-derived cells. The authors also noted that the exhaustion markers (TIM-3, LAG-3, and PD-1) increased minimally in CD4+ SLE and HD CAR T-cells.

In order verify CD19 dependent proliferation of CAR T-cells, the authors first characterized CD19 expression in B cells enriched from the leukapheresis of both SLE and HDs. B cells enriched from SLE patients were found to have 1.8-fold lower CD19 expression when compared to B cells enriched from HDs. The CD19+ control cell line NALM-6 was found to express significantly higher CD19 expression than primary B cells isolated from SLE patients and HD, while the $CD19^-$ control cell line U937 exhibited no expression at all.

To demonstrate CD19-dependent proliferation, researchers co-cultured both CAR T cells and non-transduced T cells with each of the B Cell lines characterized above. SLE and HD CAR T cells exhibited notably higher proliferation rates than non-transduced T cells when co-cultured with $CD19^+$ autologous B cells and NALM-6 cells. SLE-derived CAR T cells exhibited reduced proliferation in response to autologous B cells relative to HD-derived CAR T cells, consistent with lower CD19 expression levels in SLE B cells. However, both SLE and HD CAR T cells exhibited similar proliferation when cultured with $CD19^+$ NALM-6 cells indicating that CD19 expression has a direct effect on the proliferation of the T Cells. Minimal proliferation was seen when co-cultured with $CD19^-$ U937 cells confirming CD19-dependent proliferation of Hu19-CD828Z CAR T cells.

In addition to characterizing CD19-dependent proliferation, the authors tested the in vitro cytotoxic activity of SLE- and HD-CAR T cells. SLE CAR T cells demonstrated CAR-mediated cytolytic activity against $CD19^+$ autologous B cells as well as NALM-6 cells. Once again confirming the CD19-specific targeting of the Hu19-CD828Z CAR T cells.

Finally, the authors characterized the in vitro functionality of the SLE CAR T cells. SLE CAR T cells co-cultured with autologous B cells exhibited elevated production of IFN-γ and TNF-α relative to non-transduced controls, while IL-2, IL-6, and IL-1β remained at comparably low levels. When co-cultured with the $CD19^+$ NALM-6 cells however SLE CAR T cells produced significant amounts of IFN-γ, TNF-α, IL-2, IL-6 and IL-1B over control cells, however HD CAR T cells notably produced significantly more of these cytokines. The authors noted that the lower cytokine release seen in SLE CAR T cells may be attributed to the low dose steroid treatments SLE patients received at the point of apheresis. Importantly, SLE CAR T cells still exhibited therapeutic efficacy despite reduced cytokine production.

These findings support the feasibility of generating autologous CAR T cells from cryopreserved leukapheresis material of SLE patients, even after immunosuppressive treatment. The resulting T cells demonstrate CD19-specific cytotoxic activity with reduced proinflammatory cytokine release, highlighting their potential as a therapeutic option for B cell depletion in autoimmune disease.

University of Kansas
Corresponding Author jtreml@@ku.edu

References

1. Tsokos, G. C. Systemic Lupus Erythematosus. N. Engl. J. Med. 365, 2110–2121 (2011).
2. Tabrizi, M., Bornstein, G. G. & Suria, H. Biodistribution Mechanisms of Therapeutic Monoclonal Antibodies in Health and Disease. AAPS J. 12, 33–43 (2009).
3. Szöőr, Á. et al. Trastuzumab derived HER2-specific CARs for the treatment of trastuzumab-resistant breast cancer: CAR T cells penetrate and eradicate tumors that are not accessible to antibodies. Cancer Lett. 484, 1–8 (2020).
4. Maher, J., Brentjens, R. J., Gunset, G., Rivière, I. & Sadelain, M. Human T-lymphocyte cytotoxicity and proliferation directed by a single chimeric TCRζ /CD28 receptor. Nat. Biotechnol. 20, 70–75 (2002).
5. Cappell, K. M. & Kochenderfer, J. N. A comparison of chimeric antigen receptors containing CD28 versus 4-1BB costimulatory domains. Nat. Rev. Clin. Oncol. 18, 715–727 (2021).
6. Zhang, C., Liu, J., Zhong, J. F. & Zhang, X. Engineering CAR-T cells. Biomark. Res. 5, 22 (2017).
7. Dingfelder, J. et al. Fully Human Anti-CD19 CAR T Cells Derived from Systemic Lupus Erythematosus Patients Exhibit Cytotoxicity with Reduced Inflammatory Cytokine Production. Transplant. Cell. Ther. Off. Publ. Am. Soc. Transplant. Cell. Ther. 30, 582.e1-582.e10 (2024).

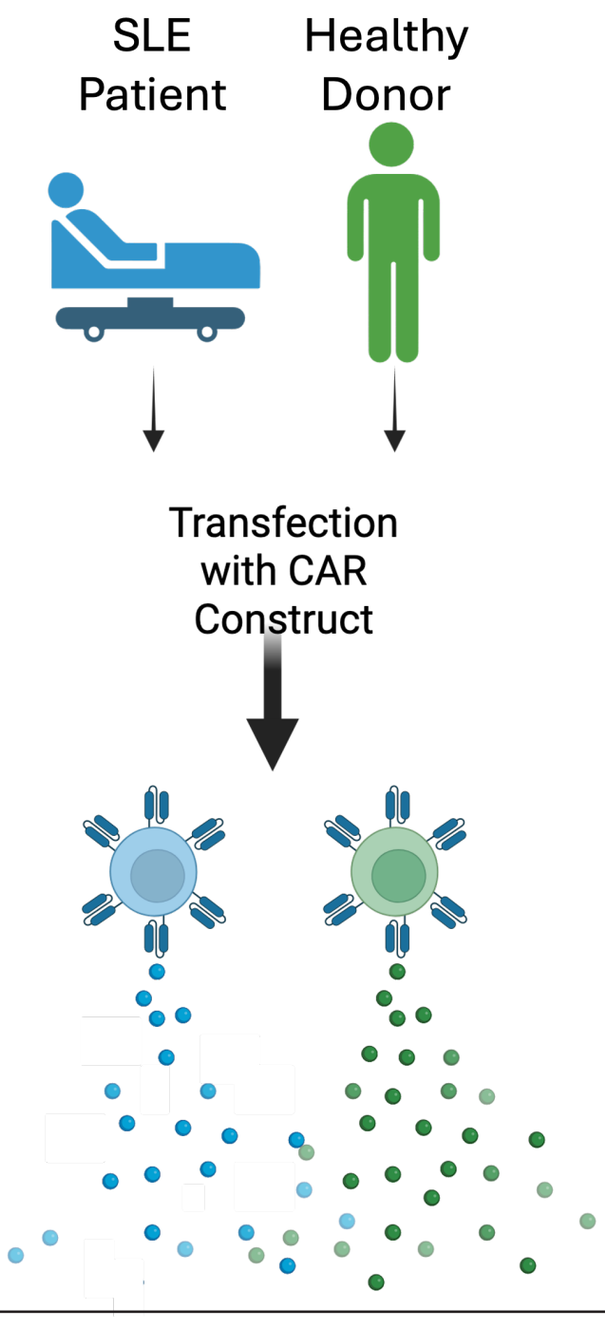

Figure 1| SLE Patient-Derived Cells produce Effective CAR T Cells. Patient-derived cells proliferated similarly to those derived from healthy donors and also produced similar, but lower, amounts of pro-inflammatory cytokines.

A Brand New CAR:
Moving CAR Constructs into Macrophages

By Yenny Feng

Chimeric antigen receptor (CAR) T cells have revolutionized cancer therapy, yet the challenges of off-target effects and excessive cytokine release persist.[1] The single-chain variable fragment (sFv) plays a critical role for receptor expression and antigen recognition, with framework regions, complementarity-determining regions, gene locus, and construct type all significantly influencing CAR T cell performance.[2] In their 2020 Nature Biotechnology article, Klichinsky *et al*. explore strategies to optimize CAR T cells for enhanced efficacy and precision by applying sFv optimization to CAR macrophages (CAR-M), for improved tumor infiltration and phagocytosis of solid tumors.[3]

Klichinsky *et al.* developed CAR-Ms by engineering human macrophages with CARs targeting Human Epidermal Growth Factor Receptor 2 (HER2), using an sFv linked to a CD3ζ signaling domain. The sFv was optimized for stability, affinity, and to ensure robust expression and specific antigen binding. *In vitro*, CAR-Ms exhibited enhanced phagocytosis of HER2-positive tumor cells compared to un-transduced macrophages. *In vivo*, mouse models of ovarian and lung cancer demonstrated significant tumor reduction and prolonged survival after a single CAR-M infusion. Optimized sFv affinity reduced off-target effects and excessive immune activation, addressing key CAR T cell limitations.[1] By leveraging macrophages' ability to infiltrate solid tumors, CAR-Ms offer a novel platform for sFv-based immunotherapy.[4]

CAR T cell therapy has undergone continuous enhancement across multiple generations, as extensively reviewed by Tomasik *et al.*[5] First-generation CARs, which included only the CD3ζ signaling domain, demonstrated limited persistence and clinical efficacy.[6] Second-generation CARs improved outcomes in hematologic malignancies by incorporating a costimulatory domain—such as CD28, 4-1BB, or OX40—to enhance T cell activation and survival.[7,8] Despite these advances, their effectiveness remained largely confined to hematologic, or "liquid," tumors. These cancers produce abundant circulating malignant cells but do not form dense, solid tumor masses, which are often protected by immunosuppressive barriers within the tumor microenvironment (TME).[4]

Third-generation CARs addressed this by combining multiple costimulatory domains (*e.g.*, CD3ζ-CD28-OX40 or CD3ζ-CD28-4-1BB), resulting in enhanced T cell proliferation and persistence.[9] Fourth-generation CARs, known as TRUCKs (T cells Redirected for Universal Cytokine Killing), further advanced the technology by delivering cytokines like IL-12 to modulate the TME and improve antitumor activity.[1] Armored CARs added yet another layer by including a second receptor to disrupt inhibitory pathways in T cells, such as those mediated by CTLA-4 or PD-1. Finally, fifth-generation CARs integrated these elements with the chemokine receptor CCR2b, enhancing cellular migration and achieving improved tumor control over fourth-generation constructs. Despite these innovations, challenges such as tumor heterogeneity and immunosuppressive TMEs continue to impede success in solid tumors.[4]

Klichinsky *et al.* introduced CAR-Ms (chimeric antigen receptor macrophages) as a complementary approach to traditional CAR T cell therapies, incorporating sFv optimization to improve tumor targeting and control. Unlike T cells, macrophages are naturally adept at infiltrating solid tumors, helping to overcome one of the major limitations of early anti-CD19 CARs.[4,10] CAR-Ms were generated using chimeric Ad5f35 adenoviral vectors to transduce primary human macrophages with CAR constructs. This strategy enhances innate immune responses, and the scalability of the vector system suggests potential for both autologous and allogeneic applications—though the complexity of production introduces regulatory challenges.

Further, CAR-Ms uniquely cross-present tumor antigens to $CD4^+$ and $CD8^+$ T cells, a capability not shared by CAR T cells, which primarily mediate cytotoxicity.[4] As antigen-presenting cells, macrophages phagocytize tumor antigens and present them via both MHC class I or II.[10] Klichinsky *et al.* showed that CAR-Ms traffic to tumor sites, upregulate MHC genes in other antigen presenting cells, and recruit T cells in humanized mouse models, enhancing tumor control. This cooperative mechanism amplifies adaptive immunity, potentially leading to sustained anti-tumor responses. This feature positions CAR-M as a bridge between innate and adaptive immunity, critical for solid tumor therapies.[4]

The efficacy of CAR-Ms arises from multiple mechanisms. Direct phagocytosis of HER2-positive tumor cells, as demonstrated in vitro with SKOV3 cells, is a primary mechanism for removal of target cells. Antigen presentation and cross-presentation to $CD4^+$ and $CD8^+$ T cells, respectively, drives secondary T cell activation, boosting adaptive immunity. CAR-Ms also secrete pro-inflammatory cytokines, shifting M2 macrophages to pro-inflammatory M1 macrophages. The role of B cell activation or antibody-dependent cellular phagocytosis (ADCP) was not directly assessed, but plausible. Future studies in lymphocyte-depleted mouse models could clarify the specific cells involved in anti-tumor immunity. Klichinsky *et al.*'s innovation lies in using CD3ζ signaling, which is inherently T cell-specific, to activate macrophages. The CD3ζ domain's homology to the FcγR ITAM on macrophages enables phagocytosis, showing that a CD3ζ domain can drive innate immunity on these cells. This approach suggests CAR constructs could be adapted for a variety of innate cells, such as dendritic cells, NK cells, and others, expanding the potential for CAR-based cell therapy's reach.

The CAR-M strategy expands the potential of CAR-based therapies to include solid tumors, where TME barriers have historically limited CAR T cell efficacy.[4] However, the development of CAR-Ms does not resolve key challenges such as high production costs and regulatory complexity—especially when using healthy donor-derived monocytes for allogeneic applications. Optimizing scFv affinity remains essential for minimizing off-target effects and improving safety.[4] Like all cell-based therapies, CAR-Ms will require careful monitoring for adverse events, including cytokine release. Looking ahead, future strategies may combine CAR-Ms with advanced CAR T

University of Kansas,
Corresponding Author jtreml@ku.edu

cells or CAR-NK cells to enhance antitumor responses.[4,9] Integration with mutation-specific T cell therapies could also support the development of highly personalized treatments.[11] Continued refinement of sFv design will be critical to increasing therapeutic precision and clinical impact.[4]

CAR-Ms interact with tumors directly through phagocytosis or indirectly by presenting and cross-presenting antigens to CD4+ and CD8+ T cells (See **Figure 1**). Direct phagocytosis offers rapid tumor clearance, while CD8+ T cell activation via cross-presentation drives robust cytotoxicity, while CD4+ T cell engagement enhances sustained immunity. Combining all interactions could maximize tumor control in vivo, engaging both native and CAR T cell types for long-term efficacy.

Klichinsky *et al*.'s sFv-optimized CAR-Ms advance immunotherapy for solid tumors, overcoming important T cell limitations. Enhanced phagocytosis, cross-presentation, and adaptive immunity distinguish CAR-Ms. Combining CAR-M with CAR T cells, CAR-T cells, or mutation-specific therapies could yield precise treatments. The novel CD3ζ signaling of these constructs in macrophages bridges innate and adaptive immunity, contributing to a new era of immunotherapy.

References

1. Chang, P. S., Lee, J. C., Koneru, M. & Brentjens, R. J. 408. CD19-Targeted CAR T Cells "Armored" To Secrete IL-12 Demonstrate Superior Efficacy Against B Cell Acute Lymphoblastic Leukemia and Resist Treg Immunosuppression. Mol. Ther. 23, S161 (2015).
2. Eyquem, J. et al. Targeting a CAR to the TRAC locus with CRISPR/Cas9 enhances tumour rejection. Nature 543, 113–117 (2017).
3. Klichinsky, M. et al. Human chimeric antigen receptor macrophages for cancer immunotherapy. Nat. Biotechnol. 38, 947–953 (2020).
4. Tokarew, N., Ogonek, J., Endres, S., von Bergwelt-Baildon, M. & Kobold, S. Teaching an old dog new tricks: next-generation CAR T cells. Br. J. Cancer 120, 26–37 (2019).
5. Tomasik, J., Jasiński, M. & Basak, G. W. Next generations of CAR-T cells - new therapeutic opportunities in hematology? Front. Immunol. 13, (2022).
6. Gross, G., Waks, T. & Eshhar, Z. Expression of immunoglobulin-T-cell receptor chimeric molecules as functional receptors with antibody-type specificity. Proc. Natl. Acad. Sci. 86, 10024–10028 (1989).
7. Krause, A. et al. Antigen-dependent CD28 signaling selectively enhances survival and proliferation in genetically modified activated human primary T lymphocytes. J. Exp. Med. 188, 619–626 (1998).
8. Maher, J., Brentjens, R. J., Gunset, G., Rivière, I. & Sadelain, M. Human T-lymphocyte cytotoxicity and proliferation directed by a single chimeric TCRzeta /CD28 receptor. Nat. Biotechnol. 20, 70–75 (2002).
9. Roselli, E. et al. 4-1BB and optimized CD28 co-stimulation enhances function of human mono-specific and bi-specific third-generation CAR T cells. J. Immunother. Cancer 9, e003354 (2021).
10. Penn, I. Occurrence of cancer in immune deficiencies. Cancer 34, 858–866 (1974).
11. Tran, E. et al. Cancer immunotherapy

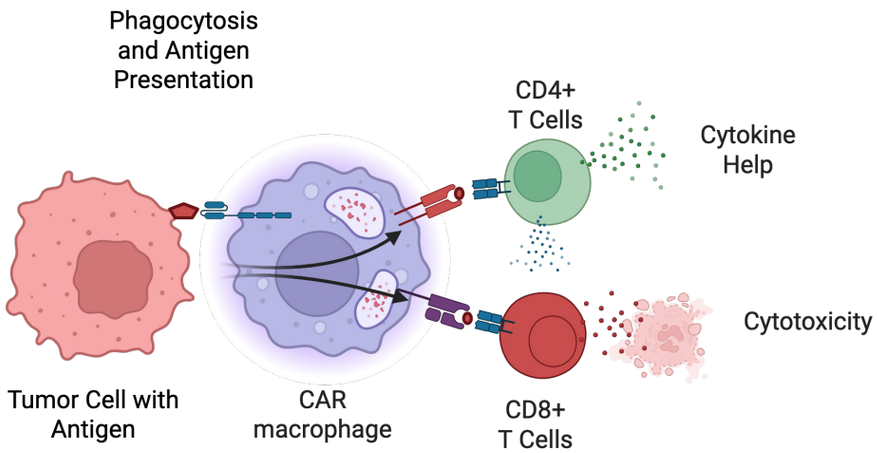

Figure 1 | CAR-M interactions with tumors and T cell activation lead to enhanced tumor control. CAR-M engages tumors directly via the sFv to mediate phagocytosis and subsequent presentation to CD4+ T and CD8+ T cells.

Disparate Biosocial Risk of Malaria and Sickle Cell Disease in The United State

By Sloane M. Murphy

Human malaria is caused by parasites in the genus *Plasmodium*, which are vectored by female *Anopheles* mosquitoes. Malaria disproportionately affects the Sub-Saharan African region, whose population has had historically limited access to fair and equivalent healthcare as compared to Western regions.[1] Sickle cell disease (SCD), a known population scale consequence of malarious countries,[2] is a condition wherein abnormally shaped red blood cells inhibit mosquito feeding, therefore providing protection against *Plasmodium* infection and subsequent development of malaria.[3] The presence of SCD in the United States can be traced to global imperialism that led to the forced movement of peoples from African malarious countries for purposes of enslavement in growing colonies.[4] Current patterns demonstrate a disproportionate burden of SCD in Black and African Americans, further emphasizing the medical and biosocial isolation experienced by this subpopulation in the United States.

Malaria is endemic throughout Africa, due in part to optimal climate and habitat availability for Anopheline mosquitoes.[5] The disease presentation of malaria in humans is categorized as either uncomplicated or severe. Uncomplicated malaria presents with flu-like symptoms, such as fever, chills, nausea, and vomiting.[5] Severe malaria can present as a variety of conditions such as acute respiratory distress, low blood pressure, abnormal behavior, seizures, or acute kidney injury.[5] A diagnosis of malaria usually requires a blood sample from patients to either detect the parasite itself or related antigens. Accurate diagnoses can be hindered in resource poor regions where laboratory facilities and trained personnel may not be available, as well as different species of malaria parasite present which accumulate at varying rates in the blood, present differing antigens, and initiate various immunological responses.[6] Delayed diagnosis delays appropriate treatment, which severely inhibits positive patient outcomes and has been identified as the primary cause of malaria-related death in many countries of Sub-Saharan Africa.[5,6]

American Burden of SCD

There are an estimated 100,000 Americans with sickle cell disease, and more than 3,000,000 who are heterozygous carriers of the HbS allele that causes the disease.[3,6] Originally, this genetic mutation offered protection to those who had diagnosable SCD, but also to those known as sickle-cell trait (SCT) carriers, people who possessed a heterozygous combination of one recessive SCD gene and one functional hemoglobin gene.[7] In fact, SCT carriers had up to 60% protection from malaria, even without presenting SCD traits.[7,8] Both homozygous recessive and heterozygous presentations of the HbS allele created protection for those living in malarious regions, but this benefit has disappeared as those carrying the sickle-cell trait have migrated to malaria-free regions. Sickle cell has continued to persist despite the negation of these protective advantages, leaving individuals in areas such as the U.S. solely with the socio-physical complications presented by the disease.

From the 1500s to the mid-1800s, at least 10 million African people were forcibly displaced by African slavers, an event known commonly as the Trans-Atlantic Slave Trade.[9,10] When comparing maps of malarious countries and where displaced African populations originated, there are observable patterns in which the majority of the population originated in malaria endemic regions, where the evolutionary pressure of malaria contributed to the long-term development of SCD in the population.[11] In the Americas, much of the contemporary SCD prevalence is directly due to the Trans-Atlantic Slave Trade.[12] Although the risk of contracting malaria is low in the USA,[12] the prevalence of SCD is high, particularly in the Black and African American communities.[7,13] This relationship draws attention to the unidentified cause of the persistence of SCD in this community and the potential for relieving burden.

The conferred advantage granted from SCD to malaria leads to logical and observable patterns of areas with high malaria prevalence coinciding with areas of high SCD prevalence (see, for example, references 14 and 15). With mass underreporting in Africa, it is hard to determine the true historical and modern burden of SCD in malarious countries.[16] Although data shows deaths attributable to SCD in Africa have increased 26% since 2000, this number may be even higher.[17] The direct connection between malaria endemic regions presenting higher prevalence of sickle cell anemia decreases in more recent decades as data sampling has increased in validity and become more representative.[16] More specifically, prevalence of SCD in non-malarious regions has been seen to decrease recently due to consistent early intervention in sickle cell patients.[17] *In-utero* diagnosis of SCD is possible by sampling amniotic fluid of the mother's womb, and infants can be tested at birth before symptoms appear.[18] When early diagnosis procedures are in place, rapid treatments are possible, which can dramatically increase the life expectancy, quality of life, and overall health of those who suffer from SCD. In some cases, there is record of the disappearance of sickled cells in patients who receive stem-cell transplants early in life.[19] However, many health clinics in malarious regions lack technology, services, and funding to be able to provide ample quality care. In 2020 alone, 95% of the 627,000 deaths occurred in the WHO's Africa region, an under-resourced region that disproportionately carries the burden of SCD due to vector prevalence and inadequate access to care.[3,15] While the overall SCD burden is expected to be greater in Africa and other malaria endemic regions due to malaria frequency, differences in access to economic and technological means for treatment has historically interfered with improvement of prevalence and manifestation globally.[1,3,20]

Sickle cell disease was not formally discovered in Western medicine until 1910, although tribes across Africa historically had many records of the disease.[7,21] Sixty-two years after the initial American discovery of SCD, the United States Congress passed the National Sickle Cell Anemia Control Act of 1972, the first federal attempt to educate America and create mass-screening programs across the country.[21,22] The first available treatments, such as blood

transfusions, gained popularity in 1984 and were followed by a series of new therapies like stem cell transplants, genotype modification, targeting of hemoglobin S polymerization, targeting vaso-occlusion, and targeting inflammation.[5,23] Privately insured SCD patients in the United States may spend up to $1.7M USD on direct medical costs associated with the disease before the age of 64,[24] even though the life expectancy of SCD patients in the USA is between 43 years to 55 years.[24,25] These incurred costs consist of the necessities such as comprehensive care for the duration of one's life including regular medical visits, prophylactic treatment, and any costs incurred during acute attacks. SCD, in itself, is taxing in both cost and physical effect. With the amount of money spent on care, attention should be called to cost reduction attempts and research for better methods and cures.

Disparities & Social Determinants of Health in the United States

Social determinants of health are defined as the environmental factors that play significant roles in defining the differences in health and quality-of-life for all groups of people.[14] These determinants are highlighted in the statistical difference in life expectancy at birth for non-Hispanic Black Americans, 70.8 years, versus the expectancy for non-Hispanic Whites, 76.4.[26] Additionally, Black Americans face higher percentages of comorbidities such as diabetes, hypertension, depression, solid cancers, among others and also experience more severe outcomes (*e.g.*, sickle cell crisis, hemochromatosis, stroke, and death) than white Americans.[13,15] These health disparities have been attributed to social differences between Whites and Blacks in the United States, such as decreased pediatric care, poor housing conditions, poor genetic health, and more.[7,27]

Understanding the biological and geographical implications of the existence of malaria in specific populations is important, however, social determinants of American healthcare ultimately create the specific disproportionalities discussed in relation to the virus and sickle cell disease. While social determinants can educate on who may be more susceptible to malaria infection and sickle cell disease naturally, the consequences of these natural inequalities are heightened by the formatted economic and racial systems that disproportionately effect those who suffer higher transmission rates and higher mortality rates than other populations.[7,26–28]

The racial gap in health, along with these social disparities, can be largely attributed to the systematic oppression of Black Americans throughout history, which contributed largely to the persistence of SCD over time. Stigmatization and prejudice based on race have become intertwined with SCD, leaving discrimination as the inferred reason for the delayed progress in sickle cell innovation. In the United States specifically, studies have shown that those with SCD have a long history of inadequate care, which has led patients to only visit doctors when their pain is excruciating due to distrust in care providers.[29–31] Those who have SCD also experience higher rates of substance abuse[29] and depression,[32] two conditions that may also severely affect physical health and general well-being. The disease itself is often falsely described as a "Black disease", a belief held by many Americans even though a wide range of races and ethnicities may have the disease.[33] This sentiment was even echoed by the then American President Richard Nixon, who stated "this disease is especially pernicious because it strikes only Blacks and no one else" in his statement when signing the National Sickle Cell Anemia Control Act of 1972.[34] Despite the fact that this act was meant to prevent stigmatization and discrimination based on SCD, this prejudice continued throughout the 1970s.[7] Modern prejudice is less explicit, but lack of cultural competency in academia and healthcare allows SCD to frequently and incorrectly be regarded as a disease of only Blacks or African Americans. Academia holds part of the blame, as only 9% (~189,000) of Bachelor's degrees awarded in a STEM field were to Black Americans in 2020,[35] even though Black and African Americans represented 12.4% (41.1 million) the country's population at the time.[36] Large groups of non-Black students completing STEM degrees may never meet a person suffering from SCD, and therefore never experiencing the severity of this problem first-hand. This, along with lack of funding, contributes largely to the lack of initiative for epidemiological research that could help improve the manifestation of SCD in the United States.[7,21] An ideal solution to improving cultural competency in rising healthcare workers is closing the race gap in graduating college students and prioritizing diversity and inequality initiatives in education. Though it may take many years to see the impact of a national educational intervention strategy such as this, the stated primary goals to reduce inequalities in SCD research and improve cultural competency should be pillars of academic and social advances.

Conclusion

With the negated benefit of protection from malaria, it is difficult to rationalize the perpetuated burden of sickle cell disease in Black Americans. Epidemiological patterns of disease prevalence in the United States demonstrate the undeniable relationship between these patterns and trends of biosocial isolation and health disparities.[3,13,37] It is by identifying and analyzing these influential factors that there is potential to reduce burden of the disease in America. Unfortunately, the translation of the growing knowledge about the disease translates very slowly into real solutions.[23,38] Many epidemiological researchers and specialists of health disparities are calling out this disproportionally slow innovation process, claiming it as another aspect of why SCD burden continues to be a prominent issue.[38] Without repairing systemic discrimination, we will always see disparities in the treatment of minority groups. In order to diminish the morbidity and mortality caused by SCD, equal research funding and continued widespread education present the best opportunities for continued improvement.

Acknowledgements

This article began as a class paper in 2022. The authors would like to thank Robert Housler and four anonymous student peer-reviewers for their feedback on previous versions of this work.

University of Florida, Department of Geography, Gainesville, FL
Corresponding Author
ghamerlinck@ufl.edu

References

1. World Health Organization. Malaria fact sheet. http://www.who.int/mediacentre/factsheets/fs094/en/ (2023).
2. Rees, D. C., Williams, T. N. & Gladwin, M. T. Sickle-cell disease. Lancet 376, 2018–2031 (2010).
3. Luzzatto, L. Sickle cell anaemia and malaria. Mediterr. J. Hematol. Infect. Dis. 4, (2012).
4. Berghs, M., Ebenso, B. & Ola, B. Social determinants of severity in sickle cell disease. in Sickle Cell Disease in Sub-Saharan Africa (Routledge, 2024).
5. Varo, R., Chaccour, C. & Bassat, Q. Update on malaria. Med. Clínica Engl. Ed. 155, 395–402 (2020).
6. Tangpukdee, N., Duangdee, C., Wilairatana, P. & Krudsood, S. Malaria diagnosis: A brief review. Korean J. Parasitol. 47, 93–102 (2009).
7. Dyson, S. Sickle Cell and the Social Sciences: Health, Racism and Disablement. (Routledge, London, 2019). doi:10.4324/9781315098685.
8. Aidoo, M. et al. Protective effects of the sickle cell gene against malaria morbidity and mortality. Lancet 359, 1311–1312 (2002).
9. Inikori, J. E. Measuring the Atlantic slave trade: An assessment of Curtin and Anstey. J. Afr. Hist. 17, 197–223 (1976).
10. Burnard, T. The Atlantic slave trade. in The Routledge History of Slavery (Routledge, 2010).
11. Kwiatkowski, D. P. How malaria has affected the human genome and what human genetics can teach us about malaria. Am. J. Hum. Genet. 77, 171–192 (2005).
12. Mungai, M., Tegtmeier, G., Chamberland, M. & Parise, M. Transfusion-transmitted malaria in the United States from 1963 through 1999. N. Engl. J. Med. 344, 1973–1978 (2001).
13. Pokhrel, A., Olayemi, A., Ogbonda, S., Nair, K. & Wang, J. C. Racial and ethnic differences in sickle cell disease within the United States: From demographics to outcomes. Eur. J. Haematol. 110, 554–563 (2023).
14. Esoh, K. & Wonkam, A. Evolutionary history of sickle-cell mutation: Implications for global genetic medicine. Hum. Mol. Genet. 30, R119–R128 (2021).
15. Thomson, A. M. et al. Global, regional, and national prevalence and mortality burden of sickle cell disease, 2000–2021: A systematic analysis from the Global Burden of Disease Study 2021. Lancet Haematol. 10, e585–e599 (2023).
16. Makani, J., Williams, T. N. & Marsh, K. Sickle cell disease in Africa: Burden and research priorities. Ann. Trop. Med. Parasitol. 101, 3–14 (2007).
17. World Health Organization. African health ministers launch drive to curb sickle cell disease toll. WHO | Regional Office for Africa https://www.afro.who.int/news/african-health-ministers-launch-drive-curb-sickle-cell-disease-toll (2023).
18. Tebbi, C. K. Sickle cell disease, a review. Hemato 3, 341–366 (2022).
19. Kavanagh, P. L., Fasipe, T. A. & Wun, T. Sickle cell disease: A review. JAMA 328, 57–68 (2022).
20. Monroe, A., Williams, N. A., Ogoma, S., Karema, C. & Okumu, F. Reflections on the 2021 World Malaria Report and the future of malaria control. Malar. J. 21, 154 (2022).
21. Prabhakar, H., Haywood Jr., C. & Molokie, R. Sickle cell disease in the United States: Looking back and forward at 100 years of progress in management and survival. Am. J. Hematol. 85, 346–353 (2010).
22. Manley, A. F. Legislation and funding for sickle cell services, 1972-1982. Am. J. Pediatr. Hematol. Oncol. 6, 67–71 (1984).
23. Salinas Cisneros, G. & Thein, S. L. Recent advances in the treatment of sickle cell disease. Front. Physiol. 11, 435 (2020).
24. Johnson, K. M. et al. Lifetime medical costs attributable to sickle cell disease among nonelderly individuals with commercial insurance. Blood Adv. 7, 365–374 (2023).
25. Payne, A. B. et al. Trends in sickle cell disease–related mortality in the United States, 1979 to 2017. Ann. Emerg. Med. 76, S28–S36 (2020).
26. US Department of Health & Human Services, Office of Minority Health. Black/African American Health. https://minorityhealth.hhs.gov/blackafrican-american-health.
27. Williams, D. R. & Sternthal, M. Understanding racial/ethnic disparities in health: Sociological contributions. J. Health Soc. Behav. 51, S15–S27 (2010).
28. Dankwa-Mullan, I., Pérez-Stable, E. J., Garnder, K. L., Zhang, X. & Rosario, A. M. The Science of Health Disparities Research. (John Wiley & Sons, Incorporated., 2021).
29. Jenerette, C., Funk, M. & Murdaugh, C. Sickle cell disease: A stigmatizing condition that may lead to depression. Issues Ment. Health Nurs. 26, 1081–1101 (2005).
30. Elander, J., Beach, M. C. & Haywood Jr, C. Respect, trust, and the management of sickle cell disease pain in hospital: Comparative analysis of concern-raising behaviors, preliminary model, and agenda for international collaborative research to inform practice. Ethn. Health 16, 405–421 (2011).
31. Brennan-Cook, J., Bonnabeau, E., Aponte, R., Augustin, C. & Tanabe, P. Barriers to care for persons with sickle cell disease: The case manager's opportunity to improve patient outcomes. Prof. Case Manag. 23, 213 (2018).
32. Hood, A. M. et al. The influence of perceived racial bias and health-related stigma on quality of life among children with sickle cell disease. Ethn. Health 27, 833–846 (2022).
33. Naik, R. P. & Haywood, C. Sickle cell trait diagnosis: clinical and social implications. Hematol. Am. Soc. Hematol. Educ. Program 2015, 160–167 (2015).
34. Nixon, R. Statement on signing the national sickle cell anemia control act.
35. National Center for Science and Engineering Statistics (NCSES). Diversity and STEM: Women, Minorities, and Persons with Disabilities 2023. https://ncses.nsf.gov/wmpd (2023).
36. Jones, N., Marks, R., Ramirez, R. & Rios-Vargas, M. 2020 census illuminates racial and ethnic composition of the country. Census.gov https://www.census.gov/library/stories/2021/08/improved-race-ethnicity-measures-reveal-united-states-population-much-more-multiracial.html (2021).
37. Schroeder, W., A., Munger, E. S. & Powers, D. R. Sickle cell anaemia, genetic variations, and the slave trade to the United States. J. Afr. Hist. 31, 163–180 (1990).
38. Tubman, V. N., Mohandas, N. & Abrams, C. S. New ASH initiatives to improve patient care in the long-overlooked sickle cell disease. Blood 142, 230–234 (2023).

A CAR T Cell Reading List

J.F. Treml*†

Every Spring semester, the Biotechnology program at the University of Kansas' Edwards Campus follows a series of journal articles highlighting milestones in one area of biology. This year's topic was how adoptive T Cell therapy spawned one of the most powerful techniques in modern immunotherapy, CAR T Cells. This year, the course was complemented by the podcast, 'Reprogrammed: The Biotechnology Podcast,' which featured a short discussion covering the main contribution each week's articles make to our understanding of how these CAR T Cells survive, proliferate, home to, and kill their tumor targets. Transcripts and notes for each podcast were also published on the website: https://downhousesoftware.wordpress.com/.

Admittedly, I am not much of a podcaster and it was a challenge to approximate an engaging dialog with an AI cohost, but it was nevertheless enjoyable to explore how a podcast could add to a class of this kind. Below, you will find a copy of the reading list for this course and the QR code to navigate to the podcast's home at Apple Podcasts. I encourage educators to consider this strategy to see whether it suits their courses, if for no other reason but to learn something new.

I am lucky enough to have access to a copy of Adobe Audition for recording and assembling my audio into a presentable form. Other tools I used are referenced in Table 1. I was willing to invest in some services that made my job a bit easier, which I recognize may not be readily accessible by everyone, so I encourage you to be creative in seeking out solutions that work for you.

Format

The main article that will be presented by students is highlighted in **bold**, while any additional recommended readings are unbolded. There is also a short introductory podcast available for each week at https://podcasts.apple.com/us/podcast/special-topics-in-biotech/id1781583786.

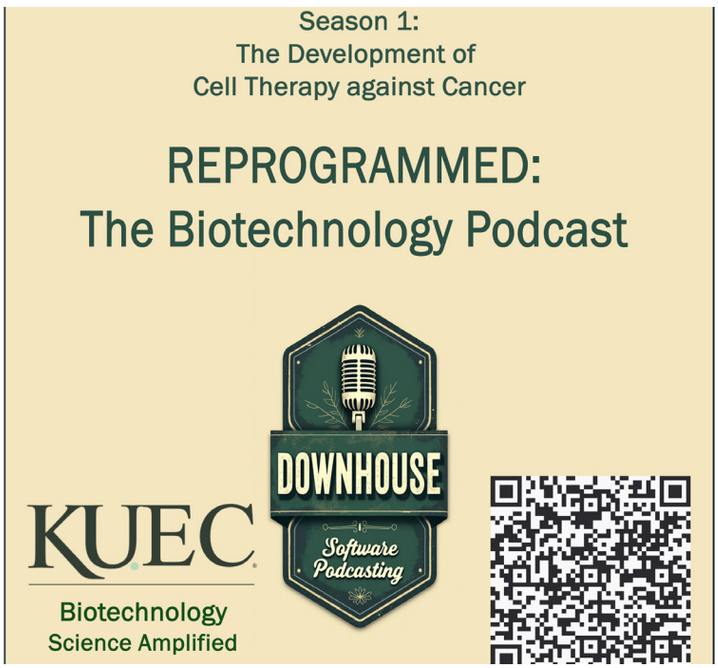

Reading List:

Week 1 (Episode 2): The Immune System and Cancer

In the first week of class, we will read a paper by Israel Penn from 1974 that highlights the importance of the immune system in regulating the initiation and spread of cancer. The instructor will present this paper and some figures from the Hegde et al. paper as a demonstration of the expectations for student presentations throughout the course.

*University of Kansas, Edwards Campus, Biotechnology

†Corresponding Author jtreml@ku.edu

1. **Israel Penn MD. Occurrence of cancer in immune deficiencies.** First published: September 1974. https://doi.org/10.1002/1097-0142(197409)34:3+<858::AID-CNCR2820340712>3.0.CO;2-1
Immunodeficient humans and other animals increases the occurrence of tumors. This demonstrates the importance of the immune system in preventing their occurrence.
2. Hegde S, Krisnawan VE, Herzog BH, Zuo C, Breden MA, Knolhoff BL, Hogg GD, Tang JP, Baer JM, Mpoy C, Lee KB, Alexander KA, Rogers BE, Murphy KM, Hawkins WG, Fields RC, DeSelm CJ, Schwarz JK, DeNardo DG. Dendritic Cell Paucity Leads to Dysfunctional Immune Surveillance in Pancreatic Cancer. Cancer Cell. 2020 Mar 16;37(3):289-307.e9. doi: 10.1016/j.ccell.2020.02.008. PMID: 32183949; PMCID: PMC7181337.
3. Robert D. Schreiber et al., Cancer Immunoediting: Integrating Immunity's Roles in Cancer Suppression and Promotion. Science 331,1565-1570(2011). DOI:10.1126/science.1203486

Week 2 (Episode 3): Adoptive T Cell Therapy, Proof of Concept
Shu et al., present data demonstrating the capacity for isolating T Cells from lymph nodes of immunized animals for ex vivo expansion and use in Adoptive T Cell Therapy in mice. Yee et al., then show a pioneering study on the use of antigen-specific CD8+ T cell clones for treating metastatic melanoma in humans. They demonstrated that these T cells could persist and migrate effectively in vivo, providing early evidence of the potential for adoptive T-cell therapy to achieve significant antitumor effects.

1. Shu SY, Chou T, Sakai K. Lymphocytes generated by in vivo priming and in vitro sensitization demonstrate therapeutic efficacy against a murine tumor that lacks apparent immunogenicity. J Immunol. 1989;143:740–8.

2. **Yee, C., Thompson, J. A., Byrd, D. R., Riddell, S. R., Roche, P. C., Celis, E., … & Greenberg, P. D. (2002). Adoptive t cell therapy using antigen-specific cd8+ T cell clones for the treatment of patients with metastatic melanoma: in vivo persistence, migration, and antitumor effect of transferred t cells.** Proceedings of the National Academy of Sciences, 99(25), 16168-16173. https://doi.org/10.1073/pnas.242600099.

Week 3 (Episode 4): First Generation CAR T Cells: sfv targeting + CD3 signaling domain
3. **Gideon Gross, Tova Waks, and Zelig Eshhar. Expression of immunoglobulin-T-cell receptor chimeric molecules as functional receptors with antibody-type specificity.** Proc. Natl. Acad. Sci. USA. Vol. 86, pp. 10024-10028, December 1989. Immunology. First attempt at making a chimeric antigen receptor on cytotoxic T Cells.

4. Dabas P, Danda A. Revolutionizing cancer treatment: a comprehensive review of CAR-T cell therapy. Med Oncol. 2023 Aug 22;40(9):275. doi: 10.1007/s12032-023-02146-y. PMID: 37608202.

Generational view of CAR T Cell Treatments, from the Dabas Review (**Figure 1**)

Week 4 (Episode 5): Second Generation CAR T Cells (Part 1): sfv targeting of phosphorylcholine plus alpha and beta subunits of the TCR and CD28 Costimulatory domain (or 4-1BB or OX-40)

5. **Krause A, Guo HF, Latouche JB, Tan C, Cheung NK, Sadelain M. Antigen-dependent CD28 signaling selectively enhances survival and proliferation in genetically modified activated human primary T lymphocytes.** J Exp Med. 1998 Aug 17;188(4):619-26. doi: 10.1084/jem.188.4.619. PMID: 9705944; PMCID: PMC2213361.

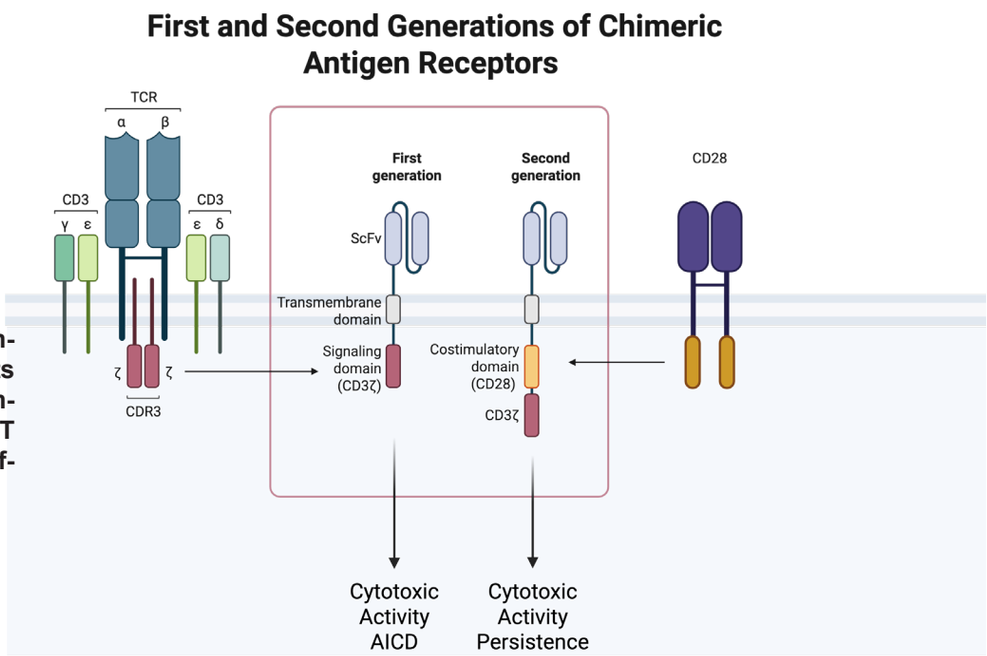

Figure 1 | First and Second-Generation CAR T Cell Constructs show the importance of co-stimulatory signals in activating T Cells for prolonged lives as effectors.

6. Rosenberg SA, Packard BS, Aebersold PM, Solomon D, Topalian SL, Toy ST, Simon P, Lotze MT, Yang JC, Seipp CA, et al. Use of tumor-infiltrating lymphocytes and interleukin-2 in the immunotherapy of patients with metastatic melanoma. A preliminary report. N Engl J Med. 1988 Dec 22;319(25):1676-80. doi: 10.1056/NEJM198812223192527. PMID: 3264384.

Week 4 (Supplemental Episode 5a): T Cell Signaling and Activation
(This Episode does not have a corresponding Special Topics in Biotechnology course)

7. Smith-Garvin JE, Koretzky GA, Jordan MS. T cell activation. Annu Rev Immunol. 2009;27:591-619. doi: 10.1146/annurev.immunol.021908.132706. PMID: 19132916; PMCID: PMC2740335.

8. Lotze, M.T., Olejniczak, S.H. & Skokos, D. CD28 co-stimulation: novel insights and applications in cancer immunotherapy. Nat Rev Immunol 24, 878–895 (2024). https://doi.org/10.1038/s41577-024-01061-1

9. Shah, K., Al-Haidari, A., Sun, J. et al. T cell receptor (TCR) signaling in health and disease. Sig Transduct Target Ther 6, 412 (2021). https://doi.org/10.1038/s41392-021-00823-w

Week 5 (Episode 6): Second Generation CAR T Cells (Part 2)
Second-generation CARs T cells are able to survive, proliferate, and kill prostate cancer cells in the lab, establishing the feasibility of CAR T cell therapy.

10. **Maher, J., Brentjens, R., Gunset, G. et al. Human T-lymphocyte cytotoxicity and proliferation directed by a single chimeric TCRζ / CD28 receptor.** Nat Biotechnol 20, 70–75 (2002). https://doi.org/10.1038/nbt0102-70

11. Imai C, Mihara K, Andreansky M, Nicholson IC, Pui CH, Geiger TL, Campana D. Chimeric receptors with 4-1BB signaling capacity provoke potent cytotoxicity against acute lymphoblastic leukemia. Leukemia. 2004 Apr;18(4):676-84. doi: 10.1038/sj.leu.2403302. PMID: 14961035.

Week 6 (Episode 7): Anti-CD19 CAR T Cells proof of concept
These target uniquely susceptible 'liquid' tumor cells in the mouse.

12. **Brentjens, R., Latouche, JB., Santos, E. et al. Eradication of systemic B-cell tumors by genetically targeted human T lymphocytes co-stimulated by CD80 and interleukin-15.** Nat Med 9, 279–286 (2003). https://doi.org/10.1038/nm827

13. Claudia M. Kowolik, Max S. Topp, Sergio Gonzalez, Timothy Pfeiffer, Simon Olivares, Nancy Gonzalez, David D. Smith, Stephen J. Forman, Michael C. Jensen, Laurence J.N. Cooper; CD28 Costimulation Provided through a CD19-Specific Chimeric Antigen Receptor Enhances In vivo Persistence and Antitumor Efficacy of Adoptively Transferred T Cells. Cancer Res 15 November 2006; 66 (22): 10995–11004. https://doi.org/10.1158/0008-5472.CAN-06-0160

Week 7 (Episode 8): Anti-CD19 CAR T Cell clinical response
This paper examines the clinical response in patients given CAR T Cells.

14. **Renier J. Brentjens et al., CD19-Targeted T Cells Rapidly Induce Molecular Remissions in Adults with Chemotherapy-Refractory Acute Lymphoblastic Leukemia.**Sci. Transl. Med.5,177ra38-177ra38(2013). DOI:10.1126/scitranslmed.3005930

15. Hollyman D, Stefanski J, Przybylowski M, Bartido S, Borquez-Ojeda O, Taylor C, Yeh R, Capacio V, Olszewska M, Hosey J, Sadelain M, Brentjens RJ, Rivière I. Manufacturing validation of biologically functional T cells targeted to CD19 antigen for autologous adoptive cell therapy. J Immunother. 2009 Feb-Mar;32(2):169-80. doi: 10.1097/CJI.0b013e318194a6e8. PMID: 19238016; PMCID: PMC2683970.

Week 8 (Episode 9): CRISPR-targeted CARs
Eyquem et al., examine how intentionally integrating the CAR construct into the T Cell Receptor locus improves the regulation and efficacy of these cells.

16. **Eyquem, J., Mansilla-Soto, J., Giavridis, T. et al. Targeting a CAR to the TRAC locus with CRISPR/Cas9 enhances tumour rejection.** Nature 543, 113–117 (2017). https://doi.org/10.1038/nature21405

Week 9 (Episode 10): Mutation-specific T cells
Shifting focus from engineered CAR T cells to the body's natural immune capabilities, Tran *et al.*, highlight how mutation-specific CD4+ T cells derived from a patient with metastatic cholangiocarcinoma were isolated, expanded, and infused back to achieve significant tumor regression.

17. **Tran E, Turcotte S, Gros A, Robbins PF, Lu YC, Dudley ME, Wunderlich JR, Somerville RP, Hogan K, Hinrichs CS, Parkhurst MR, Yang JC, Rosenberg SA. Cancer immunotherapy based on mutation-specific CD4+ T cells in a patient with epithelial cancer.** Science. 2014 May 9;344(6184):641-5. doi: 10.1126/science.1251102. PMID: 24812403; PMCID: PMC6686185.

18. Lang F, Schrörs B, Löwer M, Türeci Ö, Sahin U. Identification of neoantigens for individualized therapeutic cancer vaccines. Nat Rev Drug Discov. 2022 Apr;21(4):261-282. doi: 10.1038/s41573-021-00387-y. Epub 2022 Feb 1. Erratum in: Nat Rev Drug Discov. 2024 Feb;23(2):156. doi: 10.1038/s41573-023-00873-5. PMID: 35105974; PMCID: PMC7612664.

Week 10 (Episode 11): Third Generation CAR T Cells: 4-1BB and CD28 (CD3ζ-CD28-OX40, CD3ζ-CD28-41BB, CD3ζ-ICOS-4-1BB, and CD3ζ-TLR2-CD28)
Roselli et al.1, explore a critical frontier in CAR T cell engineering: how to build T cells that don't just kill tumors effectively, but also survive, persist, and adapt in the complex and hostile environments characteristic of solid tumors and relapsing hematologic malignancies.

19. **Roselli E, Boucher JC, Li G, Kotani H, Spitler K, Reid K, Cervantes EV, Bulliard Y, Tu N, Lee SB, et al. 4-1BB and optimized CD28 co-stimulation enhances function of human mono-specific and bi-specific third-generation CAR T cells.** J Immunother Cancer. 2021;9:e003354. doi: 10.1136/jitc-2021-SITC2021.105.
20. Sadelain M, Brentjens R, Rivière I. The basic principles of chimeric antigen receptor design. Cancer Discov. 2013 Apr;3(4):388-98. doi: 10.1158/2159-8290.CD-12-0548. Epub 2013 Apr 2. PMID: 23550147; PMCID: PMC3667586.

Week 11 (Episode omitted): Fourth Generation CAR T Cells, also known as T-cell redirected for universal cytokine-mediated killing (TRUCK), universal CAR (UniCAR-T), or armored CAR-T-cells

21. **Avanzi MP, Yeku O, Li X, Wijewarnasuriya DP, van Leeuwen DG, Cheung K, Park H, Purdon TJ, Daniyan AF, Spitzer MH, Brentjens RJ. Engineered Tumor-Targeted T Cells Mediate Enhanced Anti-Tumor Efficacy Both Directly and through Activation of the Endogenous Immune System.** Cell Rep. 2018 May 15;23(7):2130-2141. doi: 10.1016/j.celrep.2018.04.051. PMID: 29768210; PMCID: PMC5986286.

22. Chang, P. S., Lee, J. C., Koneru, M. & Brentjens, R. J. 408. CD19-Targeted CAR T Cells "Armored" To Secrete IL-12 Demonstrate Superior Efficacy Against B Cell Acute Lymphoblastic Leukemia and Resist Treg Immunosuppression. Molecular Therapy 23, S161 (2015).

23. Pegram HJ, Lee JC, Hayman EG, Imperato GH, Tedder TF, Sadelain M, Brentjens RJ. Tumor-targeted T cells modified to secrete IL-12 eradicate systemic tumors without need for prior conditioning. Blood. 2012 May 3;119(18):4133-41. doi: 10.1182/blood-2011-12-400044. Epub 2012 Feb 21. PMID: 22354001; PMCID: PMC3359735.

24. Chmielewski M, Abken H. TRUCKs: the fourth generation of CARs. Expert Opin Biol Ther. 2015;15(8):1145-54. doi: 10.1517/14712598.2015.1046430. Epub 2015 May 18. PMID: 25985798.

Week 12 (Episode 12): Traffic Signals

Craddock et al., explore how engineering T cells to express the chemokine receptor CCR2b—matching the tumor's secretion of CCL2—can dramatically improve tumor infiltration without sacrificing cytotoxic function.

25. **Craddock JA, Lu A, Bear A, et al. Enhanced tumor trafficking of GD2 chimeric antigen receptor T cells by expression of the chemokine receptor CCR2b.** J Immunother. 2010;33(8):780-788. doi:10.1097/CJI.0b013e3181ee6675.

26. Tokarew N, Ogonek J, Endres S, von Bergwelt-Baildon M, Kobold S. Teaching an old dog new tricks: next-generation CAR T cells. Br J Cancer. 2019 Jan;120(1):26-37. doi: 10.1038/s41416-018-0325-1. Epub 2018 Nov 9. PMID: 30413825; PMCID: PMC6325111.

27. Majumder, A. (2024). Evolving CAR-T-Cell Therapy for Cancer Treatment: From Scientific Discovery to Cures. Cancers, 16(1), 39. https://doi.org/10.3390/cancers16010039

Week 13 (Episode 13): AND Logic Gate CARs

Lanitis et al., developed a trans-signaling CAR strategy, consisting of two independent CAR constructs where activation signal 1 (CD3zeta) is physically dissociated from costimulatory signal 2 (CD28) using two CARs of differing antigen specificity: mesothelin and a-folate receptor (FRa).

28. **Lanitis E, Poussin M, Klattenhoff AW, Song D, Sandaltzopoulos R, June CH, Powell DJ Jr. Chimeric antigen receptor T Cells with dissociated signaling domains exhibit focused antitumor activity with reduced potential for toxicity in vivo.** Cancer Immunol Res. 2013 Jul;1(1):43-53. doi: 10.1158/2326-6066.CIR-13-0008. PMID: 24409448; PMCID: PMC3881605.

Week 14 (Episode 14): OR Logic Gate CARs, bivalent cells targeting two antigens
Qin et al., explore how simultaneous targeting of two independent targets (CD19 and CD22, both expressed on B-ALL cells) may reduce the likelihood of antigen loss and improve sustained remission rates.

29. **Qin H, Ramakrishna S, Nguyen S, Fountaine TJ, Ponduri A, Stetler-Stevenson M, Yuan CM, Haso W, Shern JF, Shah NN, Fry TJ. Preclinical Development of Bivalent Chimeric Antigen Receptors Targeting Both CD19 and CD22.** Mol Ther Oncolytics. 2018 Nov 6;11:127-137. doi: 10.1016/j.omto.2018.10.006. PMID: 30581986; PMCID: PMC6300726 (**Figure 1**).

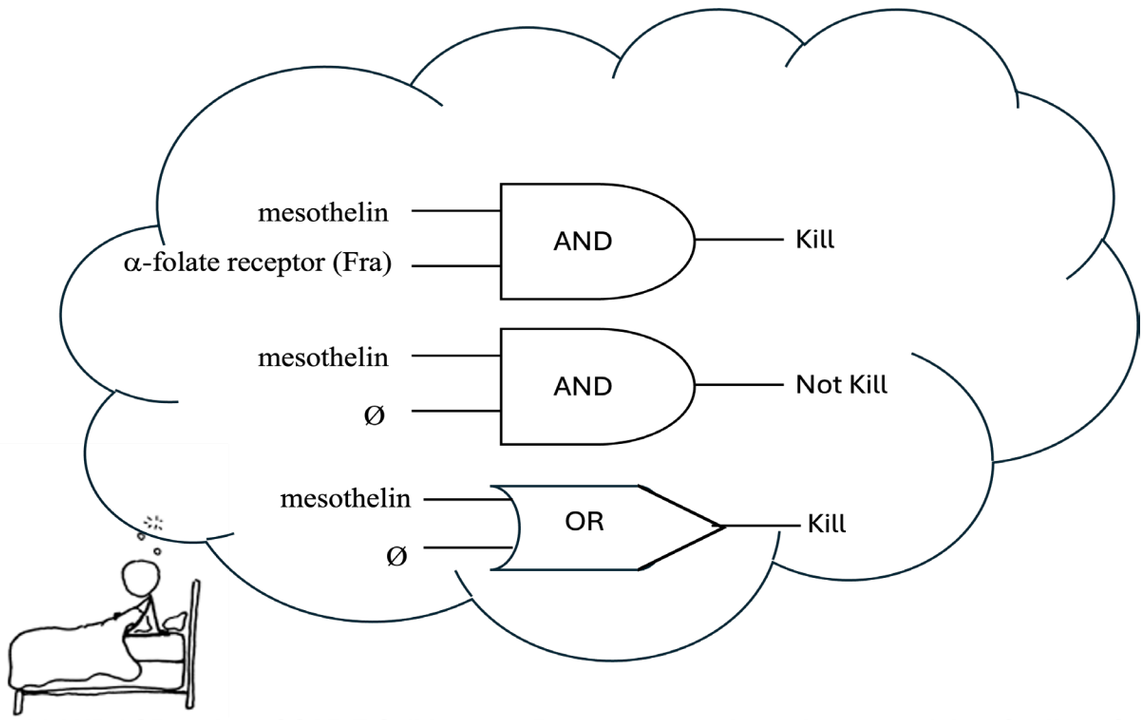

Figure 1 | AND / OR gating of CAR T Cell Immune Responses regulates the cytotoxicity of cells to function under only strictly defined conditions.

Our Journal is Growing

J.F. Treml

The Midwestern Journal of Undergraduate Sciences is growing—and we want to invite you to participate. Last year, we published our first paper from outside of our home (Biotechnology) program, and this year, we're proud to announce that we've officially begun publishing articles from institutions beyond our home University (of Kansas).

As the journal expands, we are actively seeking original research, review articles, and perspective essays authored by undergraduates or recent graduates across all STEM fields. Submissions should demonstrate thoughtful inquiry, sound methodology, and a clear articulation of scientific significance. We particularly welcome work that reflects interdisciplinary thinking, creative approaches to problem-solving, or novel applications of core scientific concepts.

We aim to provide a professional and supportive editorial experience that offers students a taste of formal scientific publishing while preserving the rigor expected in peer-reviewed literature. Submissions undergo a two-stage editorial process that balances mentorship and evaluation, and selected works are copyedited to ensure clarity and coherence.

Whether you are faculty looking to support your students' scholarly communication goals, or a student ready to take the next step in your scientific journey—we invite you to submit your work and join our growing community of undergraduate researchers.

For full submission guidelines, editorial policies, and past issues, visit:
https://journals.ku.edu/MJUSc

In this issue, we are pleased to feature research from Ahmed Elewa of Miami University in Oxford, Ohio, and former students at Augsburg University's Department of Biology in Minneapolis, Minnesota. While this article exceeds our standard length and presents contributions from multiple undergraduates working on facets of a unified project, it powerfully illustrates how undergraduate education can support high-quality research training. In recognition of this, we are introducing this as a second article format option available to authors moving forward.

Lipid Peroxidation as a Biomarker for Heavy Metal Stress in Plants

Soham Kawade*, S. Thomas*, M. Daggett*, B. Mattingly*, and J. F. Treml*†

Heavy metal contamination in soil poses a significant threat to plant health, agriculture, and ecological stability. This study investigates the potential of lipid peroxidation, specifically malondialdehyde (MDA) accumulation, as a biomarker for oxidative stress in plants exposed to heavy metals. Plants were subjected to varying concentrations of Copper Sulfate, and physiological parameters such as root length were recorded to assess growth inhibition. To quantify lipid peroxidation, a thiobarbituric acid reactive substances (TBARS) assay was performed, with a standard curve generated using 1,1,3,3-tetramethoxypropane (TMP) as an MDA equivalent. Results revealed a dose-dependent increase in MDA levels correlating with reduced root growth, indicating enhanced oxidative damage under metal stress. These findings support the use of lipid peroxidation as a reliable indicator of heavy metal toxicity and lay the groundwork for its application in phytoremediation studies and environmental monitoring.

Environmental contamination by heavy metals poses a significant threat to plant health and agricultural productivity. Copper, while essential in trace amounts, becomes toxic at elevated concentrations, leading to the generation of reactive oxygen species (ROS) via redox reactions with the metal. These ROS trigger oxidative stress, damaging cellular components such as proteins, nucleic acids, and lipids.[1]

Lipid peroxidation refers to the oxidative degradation of polyunsaturated fatty acids in cell membranes, a process initiated by ROS. A key byproduct of this reaction is malondialdehyde (MDA), which can be quantitatively measured using a method developed by Janero.[2] The accumulation of MDA thus provides a proxy for assessing oxidative damage in plant tissues.[3]

This study aims to evaluate whether lipid peroxidation, as measured through MDA levels using the thiobarbituric acid reactive substances (TBARS) assay, can serve as a reliable and sensitive biomarker for heavy metal stress in plants. By establishing a correlation between $CuSO_4$ concentrations and MDA accumulation, we seek to validate a cost-effective method for monitoring environmental toxicity.[4]

*University of Kansas, Edwards Campus, Biotechnology

†Corresponding Author jtreml@ku.edu

Materials and Methods

Plant Material and Growth Conditions

Two plant species were selected for this study: *Pisum sativum* (pea) and *Raphanus sativus* (radish). Seeds were surface-sterilized by immersion in 70% ethanol for 1 minute followed by 1% sodium hypochlorite for 10 minutes, then rinsed three times with sterile distilled water to eliminate surface contaminants.[5] Sterilized seeds were germinated in a controlled environment on culture media or soil treated with varying concentrations of copper sulfate ($CuSO_4$).

For the root elongation assay, both pea and radish seeds were germinated on agar-solidified media supplemented with $CuSO_4$ at concentrations of 0 (control), 50, 100, 250, 350, and 500 µM.6 Seeds were spaced evenly in sterile Petri dishes and oriented such that root growth would occur down the length of the plate. Plates were placed at a 45° angle to encourage straight root growth.

For the MDA assay, only radish plants were used. Seeds were sown in soil contained in pots, each amended with six increasing concentrations of $CuSO_4$ (0–400 ppm). Plants were grown for 14 days under ambient light, with daily watering to maintain consistent moisture. One additional radish plant was grown in soil containing 250 ppm $CuSO_4$ for assay validation.

Root Elongation Assay

After 7 days of growth, roots of germinated seedlings were carefully removed from the plates and photographed. For each concentration, two plates containing six seedlings were analyzed. Average root length per treatment was calculated and plotted to evaluate dose-dependent effects of copper toxicity.

MDA Quantification via TBARS Assay

The level of lipid peroxidation in radish tissues was estimated by quantifying malondialdehyde (MDA) using a thiobarbituric acid reactive substances (TBARS) assay, adapted from the protocol described by Dhindsa *et al.*,[3] and followed by Baryla *et al*.[4] Leaf tissues (0.3 g) were harvested from each treatment. Samples were ground in a chilled mortar with 1.25 mL of 0.1% trichloroacetic acid (TCA) containing 1% sodium dodecyl sulfate (SDS) to ensure protein denaturation and lipid solubilization.

The homogenate was centrifuged at 12,000 g for five minutes, after which 300 µL of supernatant was mixed with 1 mL of 20% TCA containing 0.5% thiobarbituric acid (TBA). The mixture was incubated at 95°C for 30 minutes, then cooled rapidly in an ice bath to halt the reaction. Absorbance was measured at 532 nm using a UV-visible spectrophotometer. Non-specific absorbance at 600 nm was subtracted to correct for turbidity.[7]

MDA concentration was calculated using an extinction coefficient of 155 mM^{-1} cm^{-1}.[2] Standard curves were prepared using 1,1,3,3-tetraethoxypropane (TEP) as the MDA standard, allowing for quantitative comparisons. Although the TBARS assay is widely used, it should be noted that it is

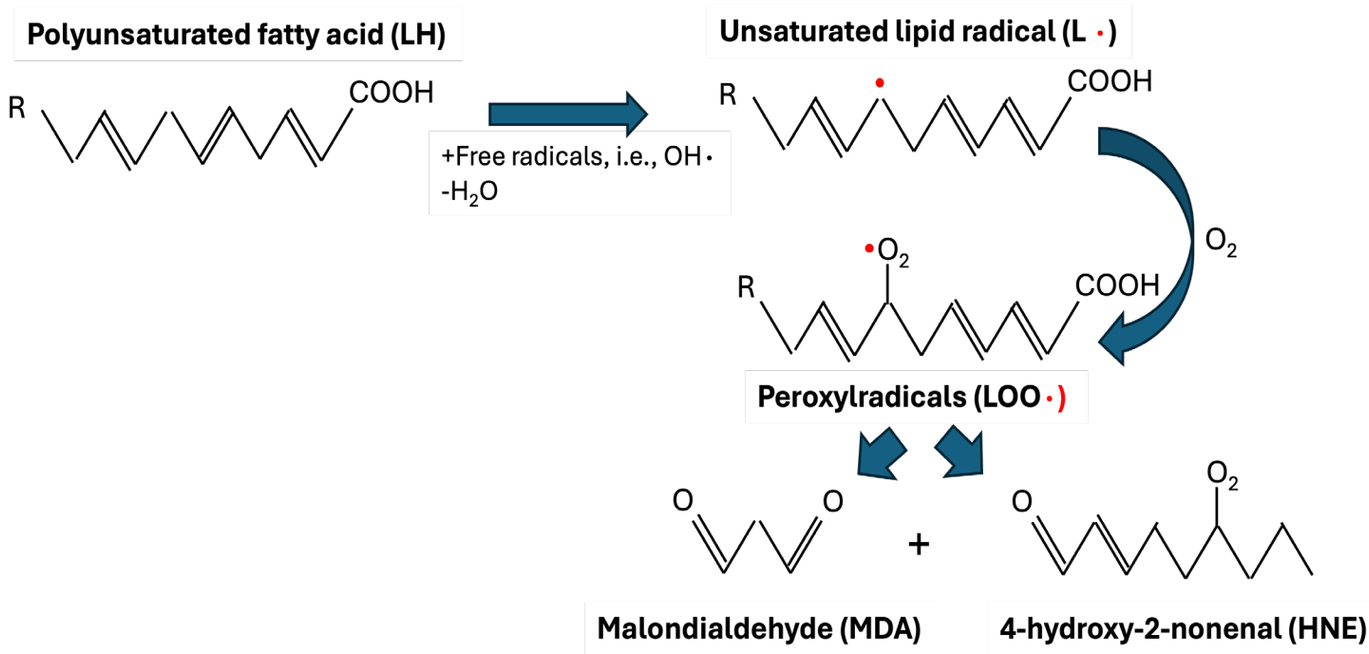

Figure 1 | Process of MDA formation as a byproduct from Lipid peroxidation reaction.

not wholly specific for MDA and may also detect other aldehydes or sugar degradation products. [4,8]

Assay Validation

To evaluate the accuracy of the MDA-based assay for estimating copper exposure, a standard curve was generated by correlating known soil concentrations of $CuSO_4$ with corresponding MDA levels measured in plant tissues. A test sample grown in soil containing 250 ppm $CuSO_4$ was then analyzed, and its MDA concentration was used to interpolate the Copper exposure from the established standard curve. A ±5% deviation threshold was predetermined as the target range for acceptable assay accuracy.

Results

Effects of Copper Sulfate on Root Elongation

The root elongation assay revealed a clear dose-dependent inhibition of growth in both Pisum sativum (pea) and Raphanus sativus (radish) seedlings exposed to increasing concentrations of $CuSO_4$. In control conditions (0 µM $CuSO_4$), both species exhibited healthy, elongated root systems, with average root lengths of 7–10 cm after seven days of growth (**Figure 2A&B**).

Upon exposure to 50 µM $CuSO_4$, a significant reduction in root length was observed, indicating early signs of metal-induced stress. More pronounced inhibition occurred at 100 µM. At 250 µM and above, root growth was significantly impaired (**Figure 2C&D**). At 500 µM $CuSO_4$, radish roots showed marked browning and necrosis at the tips—symptoms often associated with metal. This progressive reduction in root elongation reflects a dose-dependent phytotoxic response to copper exposure.

Quantification of Lipid Peroxidation via MDA Levels

The TBARS assay used to estimate MDA content in radish leaves showed a strong positive correlation between $CuSO_4$ concentration in soil and the degree of lipid peroxidation. In control plants, baseline MDA levels were minimal, indicating low levels of oxidative stress under non-toxic conditions.

With the introduction of 50 ppm $CuSO_4$ into the soil, a measurable increase in MDA content was observed, suggesting the onset of oxidative stress (**Figure 3**). At 100 ppm, MDA levels nearly doubled and continued to rise steadily with each subsequent concentration. The highest MDA concentration was recorded in the 300 ppm treatment group. The MDA concentration at 400 ppm was lower than that observed in 300 ppm, the cause for which could indicate failure of metabolic functions due to very high toxicity from copper.

The results align with those of Baryla *et al*.,[4] who observed similar increases in MDA content in *Brassica napus* exposed to Cu-enriched media. These findings support the hypothesis that copper-induced oxidative stress can be reliably detected by assessing lipid peroxidation in plant tissues.

Linear regression analysis demonstrated a statistically significant correlation (**Figure 3A**, $R^2 > 0.95$) between $CuSO_4$ concentration and MDA levels in plant tissues. The generation of a standard curve using 1,1,3,3-tetraethoxypropane (TEP) allowed for precise quantification of MDA, confirming the assay's sensitivity and reproducibility across a range of copper treatments.

The regression model confirmed the linear behavior of the TBARS assay within the tested concentration range, validating its use as a quantifiable indicator of stress severity.

Assay Validation and Accuracy

To evaluate the accuracy of the TBARS assay in estimating Cu-induced oxidative stress, a validation sample was cultivated in soil amended with 250 ppm $CuSO_4$. A target tolerance of ±5% deviation from the known concentration was established a priori. The assay estimated internal Cu exposure at 264.2 ppm, corresponding to a 5.6% deviation—slightly exceeding the predefined threshold (**Figure 3B**). While this result did not meet the established criterion

for accuracy, the minimal overage suggests the method may approach a practical level of reliability with refinement. These findings support further refinement of the assay protocol and warrant its re-evaluation in future studies aimed at field-applicable soil toxicity screening and bioavailability assessment.[4]

Visual and Physiological Symptoms

Beyond quantitative data, visual inspection of the radish plants **(data not shown)** revealed symptoms that further supported the biochemical findings. As $CuSO_4$ concentration increased, radish leaves exhibited curling, reduced leaf area, and, in severe cases, chlorosis and necrosis. These symptoms corresponded with MDA trends and are consistent with copper's role in disrupting photosynthesis and generating ROS.[1]

Discussion

The findings support the hypothesis that lipid peroxidation serves as a measurable marker of oxidative stress in plants exposed to heavy metal contamination. Despite the need for further refinement, the TBARS assay proved to be a straightforward and reproducible method for quantifying MDA levels.

Root elongation assays complemented the biochemical data by directly correlating copper toxicity with impaired plant health. Studies have consistently reported that copper accumulation significantly inhibits root growth—even at relatively low concentrations—serving as a sensitive indicator of metal-induced outcomes.[9,10] Our root assays confirm this well-established relationship, strengthening the validity of the TBARS results by linking oxidative damage to physiological impairment. Although the validation assay slightly overestimated Cu concentration—yielding a 5.6% deviation from the known value—this result remains near the predefined ±5% margin of acceptability. This minimal discrepancy underscores the assay's potential for practical use in environmental monitoring and preliminary diagnostic applications.

The tentative correlation between $CuSO_4$ concentration and MDA accumulation demonstrates that this method can be used for early and quantitative detection of environmental contamination. The simplicity and cost-effectiveness of the TBARS assay make it a valuable tool for agricultural and ecological applications.

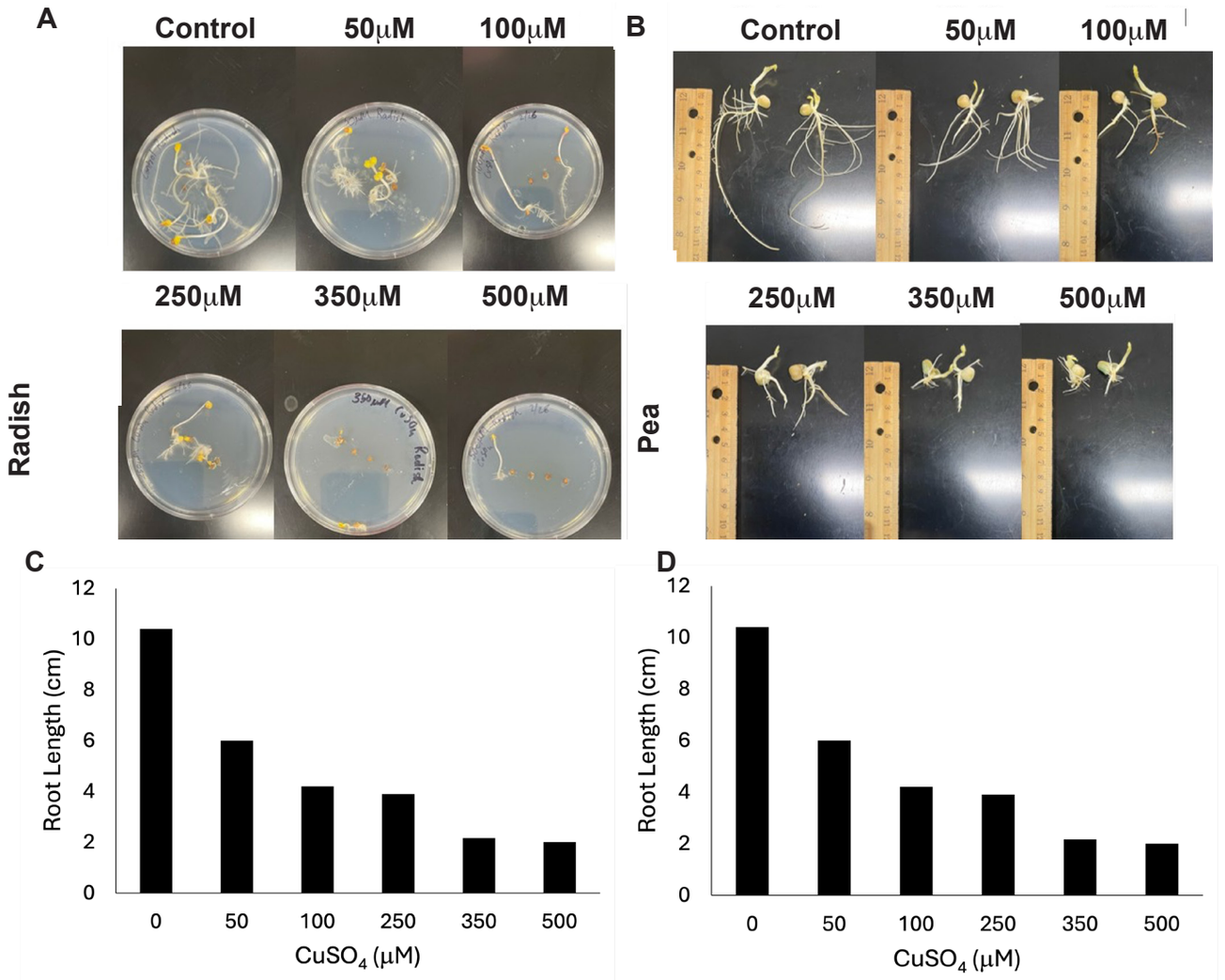

Figure 3 | Root Growth is inversely correlated with concentration of $CuSO_4$ in soil. Root Elongation Tests on *Pisum sativum* (pea) and *Raphanus sativus* (radish). A & B show Radish and Pea roots respectively grown in a petri dish with 1% Agar and $CuSO_4$. C & D show corresponding graphs of the A & B. Readings were taken after 7 days of sowing.

Future Directions

Given that the validation assay marginally exceeded the established accuracy threshold, the current methodology will be reviewed for potential improvements. While this study centered on copper exposure, future research should evaluate the specificity of MDA as a biomarker for other heavy metals, including cadmium, lead, and zinc. Expanding the assay's application to additional plant species and varied stress conditions will further assess its robustness and broaden its environmental relevance.

Acknowledgments

The author would like to thank Terri Woodburn for her expert consulting on the design of this paper.

Author Biography

Soham Kawade is arecent graduate of the Biotechnology program at the University of Kansas. His research focuses on plant stress responses and biomarker development. He plans to pursue a career in industrial biotechnology, developing innovative solutions to improve human and environmental health through applied research and technology development.

Author Contributions

S.K. contributed to the experimental work, design, and writing of this work; B.M., S.T., M.D., and J.F.T contributed to the design and editing of this work.

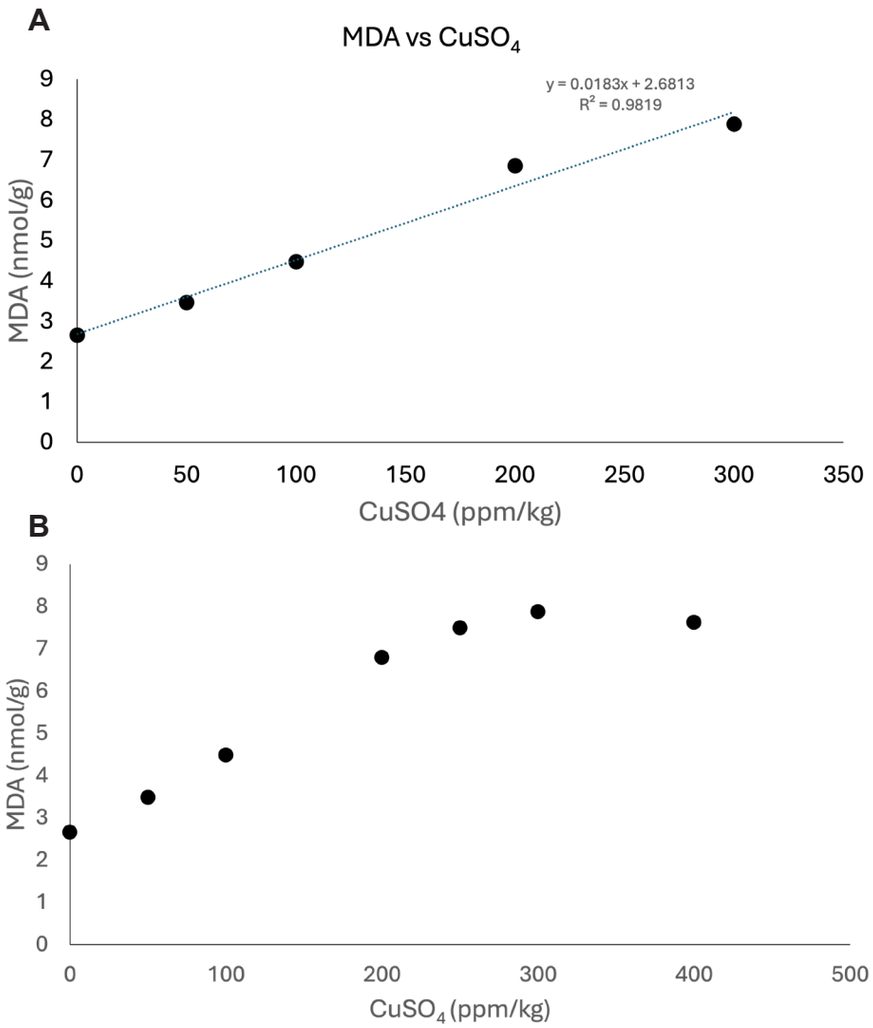

Figure 3 | MDA Calculation as a function of $CuSO_4$ in soil. A Shows a standard curve of MDA readings from plants grown in $CuSO_4$ -infused soil with regression analysis for standard curve generation (R^2 = 0.9819). B shows an 'unknown' plant sample plotted against the standard for assay validation. Samples were collected after 2 weeks of planting.

References

1. Halliwell, B. & Gutteridge, J. M. Oxygen toxicity, oxygen radicals, transition metals and disease. Biochem. J. 219, 1–14 (1984).
2. Janero, D. R. Malondialdehyde and thiobarbituric acid-reactivity as diagnostic indices of lipid peroxidation and peroxidative tissue injury. Free Radic. Biol. Med. 9, 515–540 (1990).
3. Dhindsa, R., Plumb-Dhindsa, P. & Thorpe, T. Leaf senescence and lipid peroxidation. J Exp Bot 32, 93–101 (1981).
4. Baryla, A., Laborde, C., Montillet, J. L., Triantaphylidès, C. & Chagvardieff, P. Evaluation of lipid peroxidation as a toxicity bioassay for plants exposed to copper. Environ. Pollut. Barking Essex 1987 109, 131–135 (2000).
5. D, S. & M, M. Standardizing the Methods for Breaking Seed Dormancy to Enhance Germination of Gloriosa superba Seeds. Expert Opin. Environ. Biol. 04, (2016).
6. Hajiboland, R. An evaluation of the efficiency of cultural plants to remove heavy metals from growing mediu. Plant Soil Environ. 51, (2005).
7. Heath, R. L. & Packer, L. Photoperoxidation in isolated chloroplasts. I. Kinetics and stoichiometry of fatty acid peroxidation. Arch. Biochem. Biophys. 125, 189–198 (1968).
8. Bird, R. P. & Draper, H. H. Comparative studies on different methods of malonaldehyde determination. Methods Enzymol. 105, 299–305 (1984).
9. Rooney, C. P., Zhao, F.-J. & McGrath, S. P. Soil factors controlling the expression of copper toxicity to plants in a wide range of European soils. Environ. Toxicol. Chem. 25, 726–732 (2006).
10. Copper-induced stress in *Solanum nigrum L.* and antioxidant defense system responses - Fidalgo - 2013 - Food and Energy Security - Wiley Online Library. https://onlinelibrary.wiley.com/doi/full/10.1002/fes3.20?utm_source=chatgpt.com.

Targeting Streptococcus salivarius in Peri-Implantitis:

Two Antimicrobial and Antibiofilm Peptides

Samia Chergui*, S. Thomas*, M. Daggett*, B. Mattingly*, and J. F. Treml*†

Peri-implantitis, a persistent complication associated with dental implants, is driven by complex, antibiotic-resistant oral biofilms. Antimicrobial Peptides (AMPs) may represent novel, safe, and effective therapies against Streptococcus salivarius, a key early colonizer in peri-implant biofilms. S. salivarius was isolated and identified by 16S sequencing from human saliva, followed by standardized growth and biofilm assays to establish a physiologically relevant testing model. RR12 is a novel peptide that was rationally designed, synthesized, and characterized for structural integrity for comparison against KR12, a natural LL-37 derivative known to be effective against bacteria. Both peptides demonstrated dose-dependent inhibition of S. salivarius biofilm formation, but KR12 consistently achieved superior antimicrobial and antibiofilm effects with lower cytotoxicity. These findings underscore the necessity of biological validation in peptide development and support the use of AMPs as promising alternatives to traditional antibiotics. AMP-based coatings and gels for dental implants could offer localized, resistance-proof infection control.

The widespread adoption of dental implants has transformed restorative dentistry, offering functional and aesthetic solutions for tooth loss.[1] However, their long-term success is increasingly compromised by peri-implantitis—a chronic inflammatory condition associated with bone loss and implant failure.[2] Central to this disease is the rapid colonization of implant surfaces by oral biofilms, which confer resistance to host defenses and antibiotics.[3,4] Among these biofilm-forming organisms, Streptococcus salivarius plays a pivotal role as an early colonizer, facilitating the adhesion of pathogenic species and contributing to biofilm maturation.[4,5]

The biofilm matrix not only acts as a mechanical barrier but also promotes horizontal gene transfer and antimicrobial resistance.[6] Consequently, standard interventions like debridement or antibiotics often fail to fully eradicate the infection.[7] This has led to growing interest in antimicrobial peptides (AMPs), which possess broad-spectrum activity, low resistance potential, and biofilm-disrupting capabilities.[8,9] AMPs derived from human cathelicidins, particularly LL-37, have inspired the development of synthetic analogs with improved selectivity and reduced cytotoxicity.[5,10]

*University of Kansas, Edwards Campus, Biotechnology

†Corresponding Author jtreml@ku.edu

This study investigates the design and functional characterization of a novel AMP, RR12, as a targeted strategy against S. salivarius. The performance of RR12 was compared to KR12—a validated LL-37 fragment—with emphasis on antimicrobial efficacy, biofilm inhibition, and cytotoxicity. Our findings support the use of engineered AMPs in next-generation dental therapeutics and highlight the translational potential of AMP-based coatings for peri-implantitis control.

Materials and Methods

Bacterial Isolation

Saliva samples were collected from healthy adult volunteers and immediately streaked onto Mitis Salivarius Agar plates (Sigma-Aldrich, Cat. No. 01337-500G-F) to selectively isolate *Streptococcus* species. Plates were incubated at 37°C for 24 hours. To ensure purity, single colonies with distinct morphologies were subcultured onto fresh Mitis Salivarius Agar. Each colony was characterized by Gram staining and catalase testing using standard protocols. For genomic analysis, a single colony from each morphology was inoculated into 5 mL Luria-Bertani (LB) Broth (Fisher BioReagents, Cat. No. BP9723-500) and grown overnight at 37°C with shaking. Genomic DNA was isolated from these cultures using a heat shock method: 1 mL of culture was centrifuged, the pellet was resuspended in 100 µL PBS, heated at 95°C for 10 minutes, and centrifuged again to recover the supernatant containing DNA. PCR amplification of the 16S rRNA gene was performed using universal primers 27F and 1492R, with commercial *S. salivarius* DNA (provided by M. Daggett) as a positive control and a no-template reaction as a negative control. PCR products were separated on a 1% agarose gel (Fisher BioReagents, Cat. No. BP1356-500), excised, and purified using the Monarch DNA Gel Extraction Kit (New England Biolabs, Lot#0051612). Purified PCR products were submitted to Eurofins Genomics for 16S rRNA sequencing to confirm bacterial identity.

AMP Design

Antimicrobial peptide sequences were electronically submitted to the University of Kansas Medical Center Synthetic Chemical Biology Core Facility for synthesis. Physicochemical properties, including net charge, hydrophobicity, and CPP potential, were analyzed using the CellPPD web server. Three-dimensional structural models of the peptides were generated and visualized using UCSF ChimeraX.

pH Tolerance Assay

To assess environmental adaptation, *S. salivarius* was cultured in tryptic soy broth Tryptic Soy Broth (Fisher scientific LOT# 1306492) adjusted to various pH levels using sterile-filtered HCl or NaOH. Media

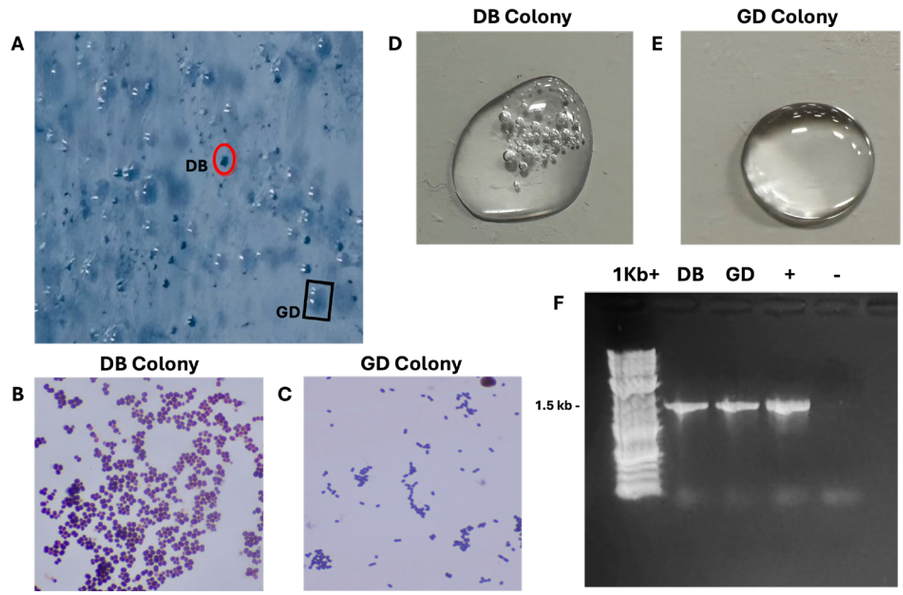

Figure 1 | Phenotypic and molecular identification of oral bacterial colonies isolated from human saliva.
(A) Distinct colony morphologies appear on Mitis Salivarius Agar after overnight incubation. Dark blue colonies (DB) and gumdrop-like colonies (GD) are visually distinguishable and selected for further analysis.
(B&C) Gram staining shows cocci in clusters for DB (**B**), consistent with Staphylococcus spp., and cocci in chains for GD (**C**), characteristic of Streptococcus spp. Both stain purple, indicating Gram-positive cell walls.
(D&E) Catalase testing reveals bubble formation in DB colonies (**D**, Catalase+), while GD colonies show no reaction (**E**, Catalase–), supporting preliminary genus-level classification.
(D) PCR amplification of the 16S rRNA gene yields ~1.5 kb amplicons for both isolates. Sanger sequencing and BLAST analysis identify DB as Staphylococcus haemolyticus and GD as Streptococcus salivarius, confirming phenotypic observations.

were autoclaved post-adjustment. Overnight cultures were inoculated into each pH-adjusted broth and incubated at 37°C for 12-18 hours. Growth was quantified by optical density at 600 nm (OD_{600}) using a spectrophotometer and SpectraMax software.

Growth Monitoring and Bacterial Enumeration

S. salivarius was cultured in tryptic soy broth (TSB) and incubated at 37 °C under aerobic conditions for 36 hours. Bacterial growth was monitored at multiple time points 0, 6, 12, 24, and 36 hours) by measuring optical density at OD_{600} using a spectrophotometer.
Once cultures reached an OD_{600} of approximately 0.9, a series of ten-fold serial dilutions were prepared in sterile PBS. For bacterial enumeration, 100 µL from each dilution was plated onto LB agar plates in triplicate and incubated overnight at 37 °C. Colony-forming units per milliliter (CFU/mL) were calculated by counting visible colonies and accounting for the dilution factor.
To establish a correlation between OD_{600} and bacterial concentration, the CFU values were plotted against the corresponding OD readings from the TSB cultures. This standard curve was used to normalize bacterial input across subsequent experimental assays.

Optical Density Assay

Antimicrobial activity of RR12 and KR12 was evaluated using a 96-well microplate OD assay. Peptides were prepared at various concentrations in TSB. An overnight S. salivarius culture was diluted to OD_{600} = 0.3. For each assay, 100 µL of standardized bacteria and 100 µL peptide solution were added per well (triplicates). Ampicillin powder (Alfa Aesar, Cat. No. J60977.06) served as a positive control; bacteria-only wells served as negative controls. Initial OD_{600} was measured at t=0. Plates were incubated overnight at 37°C with shaking at 200 rpm, and OD_{600} was measured again after 12 hours.

Biofilm Formation Assay

Biofilm formation was quantified using the same 96-well plates post-OD assay. Media and non-adherent bacteria were gently aspirated, and wells were washed twice with 200 µL PBS. The wells were air-dried and stained with 100 µL 0.1% crystal violet (Fisher Scientific, Cat. No. C581-100) for 20 minutes. Excess stain was removed by washing three times with PBS, and plates were air-dried. Crystal violet was solubilized with 150 µL methanol (Fisher Scientific, Cat. No. A452-4) per well for 15 minutes. Absorbance was measured at 595 nm. All assays were performed in triplicates, with ampicillin as a positive control and uninoculated media as a negative control. This assay was not done in triplicates at the time of publication.

Cytotoxicity Assay

KR12 and RR12 cytotoxicity against mammalian cells was assessed using an MTT assay on HCT116 colon carcinoma cells. Cells were maintained in DMEM with 10% FBS and 1% penicillin-streptomycin. HCT116 cells were seeded into 96-well plates and allowed to adhere overnight. Peptides were added at various concentrations and incubated for 24 hours at 37°c. MTT reagent (0.5 mg/mL) was added and incubated 3–4 hours. Formazan crystals were dissolved in 100uL DMSO, and absorbance at 490 nm was measured to determine cell viability.

Results

Isolation and Identification of Streptococcus salivarius

Saliva samples were streaked onto Mitis Salivarius Agar and incubated overnight resulting in two distinct colony morphologies: one gumdrop-like and one dark blue (**Figure 1A**). Gram staining showed that the gumdrop colony consisted of Gram-positive cocci in chains, while the dark blue colony consisted of Gram-positive cocci in clusters (**Figure 1B&C**). The dark blue colony was catalase-positive, and the gumdrop colony was catalase-negative **(Figure 1D&E).**
The PCR amplification of the 16S rRNA gene, yielded ~1.5 kb bands for both colony types (**Figure 1F**) which are consistent

for the predicted size of the gene of interest. PCR amplicons were purified from the gen and sent for Sanger sequencing. BLAST analysis identified the gumdrop colony as *S. salivarius* (Score: 1563, E-value: 0, Accession: MZ824593.1) and the dark blue colony as *Staphylococcus haemolyticus* (Score: 693, E-value: 0, Accession: MH542264.1). These identifications are consistent with the test results above.

pH Tolerance of Streptococcus salivarius

The pH tolerance assay showed that S. salivarius exhibited optimal growth in media adjusted to pH 7–8. The highest optical density values were recorded at these pH levels. Growth was still detectable at more acidic or basic pH values but was markedly reduced compared to neutral and slightly alkaline conditions. **(Figure 2A)**

Growth Kinetics and Standardization of S. salivarius Inoculum

The growth curve (**Figure 2B**) shows that *S. salivarius* enters exponential phase between 6- and 12-hours post-inoculation and reaches stationary phase by 24 hours, indicating this is the optimal window for antimicrobial exposure when cells are most metabolically active. Additionally, a standard curve correlating optical density at 600 nm with colony-forming units per milliliter (CFU/mL) (**Figure 2C**) demonstrates a strong linear relationship. This correlation is used to normalize bacterial input across experiments and ensure consistent starting concentrations for all treatments.

Antimicrobial Peptide Design

KR12, derived from human cathelicidin LL-37, exhibits strong antimicrobial and anti-biofilm activity due to its amphipathic α-helical structure and positive charge.[11] Key features such as amphipathicity, cationic charge, and hydrophobic residues are essential for disrupting bacterial membranes and biofilms.[12] To improve these properties, RR12 was designed by increasing lysine content to enhance charge and salt resistance while preserving the α-helical scaffold critical for membrane interaction. Structural modeling with ChimeraX confirmed that both peptides maintain their α-helical conformations, vital for antimicrobial function (**Figure 3A&B**). These findings align with studies showing that optimizing charge and helical structure improves peptide potency and selectivity.[13]

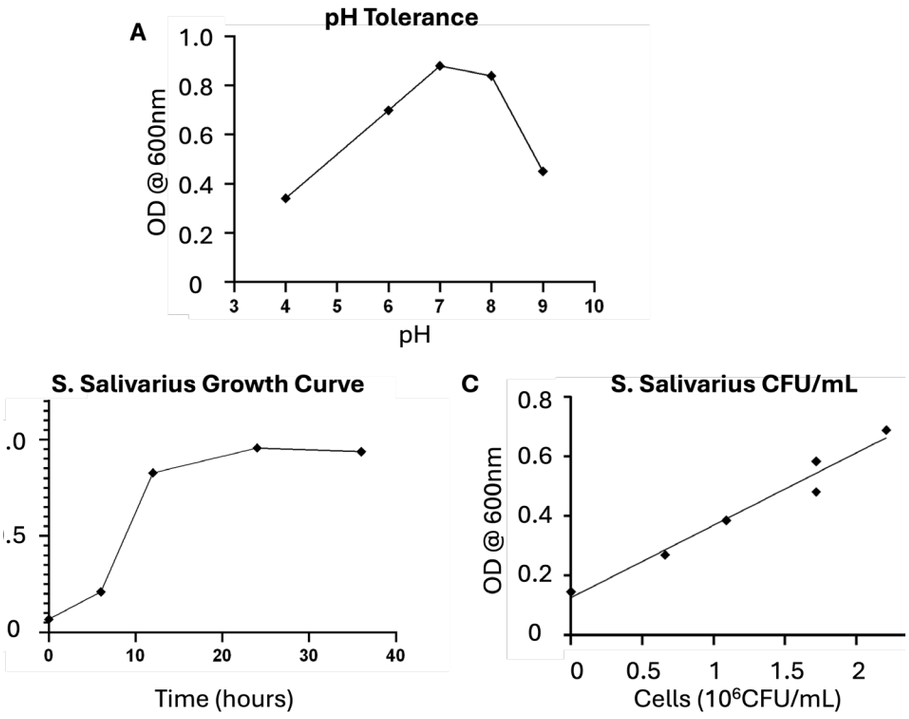

Figure 2 | Physiological characterization of Streptococcus salivarius under simulated oral conditions.

(A) S. salivarius exhibits optimal growth at neutral to slightly alkaline pH, as determined by measuring optical density at 600 nm after 18–24 hours of incubation. Growth decreases significantly at more acidic or basic conditions.

(B) The bacterial growth curve demonstrates that S. salivarius enters exponential phase between 6–12 hours post-inoculation, with stationary phase reached by 24 hours. The 6-12 hour time point is selected for antimicrobial assays to capture peak metabolic activity.

(C) A standard curve establishes a linear correlation between OD_{600} and colony-forming units per milliliter (CFU/mL), allowing accurate standardization of bacterial input in all experimental wells.

Antimicrobial Activity of KR12 and RR12

A dose-dependent inhibition of *S. salivarius* was observed for both KR12 and RR12 peptides (**Figure 4A**). At lower concentrations (10–313 µg/mL), both peptides exhibited minimal inhibition, with percent inhibition values close to zero or slightly negative. As the concentration increased, KR12 showed a marked increase in antimicrobial activity, achieving nearly complete inhibition at concentrations of 625 µg/mL and above. RR12 demonstrated only modest inhibition across all concentrations, with percent inhibition remaining below 40% until the highest dose tested. At 1250 µg/mL and 2500 µg/mL, both peptides resulted in complete growth inhibition.

Inhibition of S. salivarius Biofilm Formation

Biofilm quantification using the crystal violet assay showed that both KR12 and RR12 peptides reduced S. salivariusbiofilm formation in a concentration-dependent manner (**Figure 4B**). At lower concentrations (10–156.5 µg/mL), there was no statistically significant reduction in biofilm biomass for either peptide. At 312.5 µg/mL and above, KR12 showed a marked and statistically significant decrease in biofilm formation compared to RR12. At the highest concentrations tested (1250 and 2500 µg/mL), KR12 virtually eliminated biofilm formation, while RR12-treated wells retained higher OD values, indicating less effective biofilm inhibition. Visual inspection of the stained plates supported these quantitative findings (**Figure 4C**).

Cytotoxicity of RR12 and KR12 on HCT116 Cells

Both peptides exhibited a concentration-dependent reduction in HCT116 human colon carcinoma cells viability (**Figure 5A**). At concentrations up to 375 µg/mL, cell viability remained above 70% for both peptides, with no statistically significant difference. At 750 µg/mL and above, a marked decrease in cell viability was observed, particularly for KR12. At concentrations of 1500 µg/mL and higher, KR12 induced a significantly greater reduction in cell viability compared to RR12, with viability dropping below 30% for both peptides at the highest concentrations tested. Visual inspection of the stained plates supported these quantitative findings (**Figure 5B**).

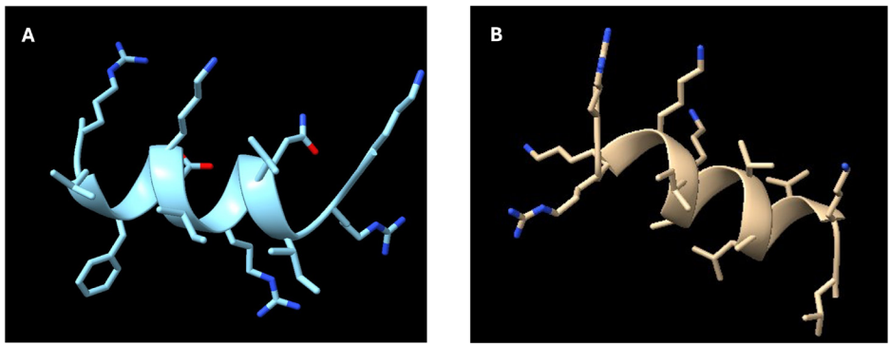

Figure 3 | Structural and physicochemical features of antimicrobial peptides KR12 and RR12. (A) KR12 (KRIVQRIKDFLR) and **(B)** RR12 (RRKKIAKVALVK) are engineered cell-penetrating peptides (CPPs) derived from LL-37. Both peptides form amphipathic helices essential for membrane disruption. KR12 carries a net charge of +4, with moderate hydrophilicity (0.73) and a molecular weight of 1.57 kDa. In contrast, RR12 is more cationic (+6), more hydrophilic (0.87), and slightly smaller (1.41 kDa).

Discussion

This study demonstrates the promise and challenges of using engineered antimicrobial peptides (AMPs) as targeted agents against early oral biofilm colonizers implicated in peri-implantitis. By systematically isolating and confirming *S. salivarius* from human saliva, we established a clinically relevant model for evaluating antibiofilm strategies. The pH tolerance profile of *S. salivarius* confirmed its adaptation to oral conditions and validated the physiological relevance of our in vitro assays.

Both RR12 and KR12 peptides exhibited dose-dependent inhibition of *S. salivarius* planktonic growth and biofilm formation, with KR12 consistently showing superior efficacy. The observed hormesis effect at low concentrations—where sub-inhibitory doses had little or even slightly stimulatory effects—underscores the complexity of AMP-bacteria interactions and the importance of precise dosing.[11] At higher concentrations, KR12 nearly eradicated both planktonic bacteria and biofilms, while

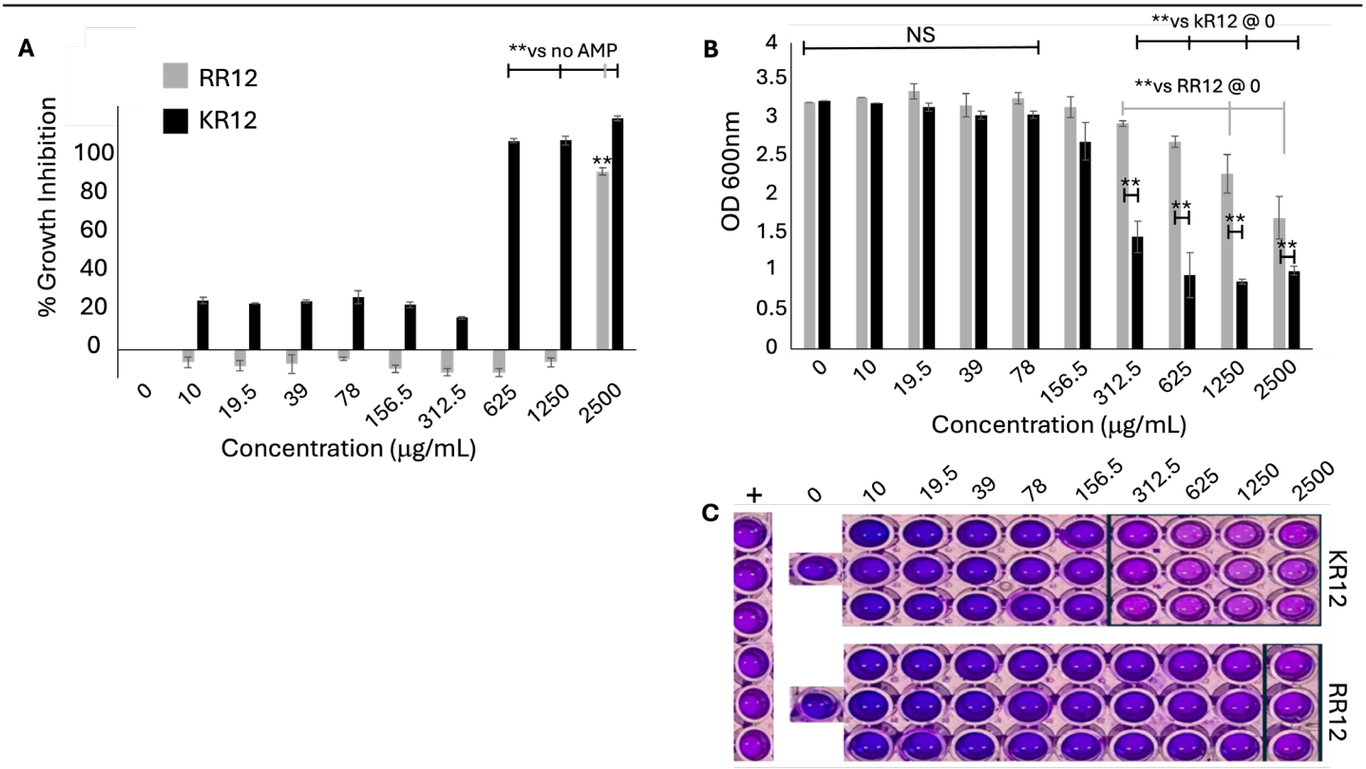

Figure 4 | Antimicrobial and antibiofilm activity of KR12 and RR12 peptides against Streptococcus salivarius. **(A)** Percent inhibition of S. salivarius growth following treatment with increasing concentrations of KR12 and RR12 (10–2500 µg/mL), assessed via OD_{600} after 12 hours. **(B)** Quantification of biofilm biomass using crystal violet staining and absorbance at 600 nm after peptide exposure. **(C)** Representative images of stained 96-well plates show biofilm retention following peptide treatment. Ampicillin (+) and untreated bacteria (–) serve as positive and negative controls, respectively. Data are presented as mean ± standard deviation; statistical significance is indicated.

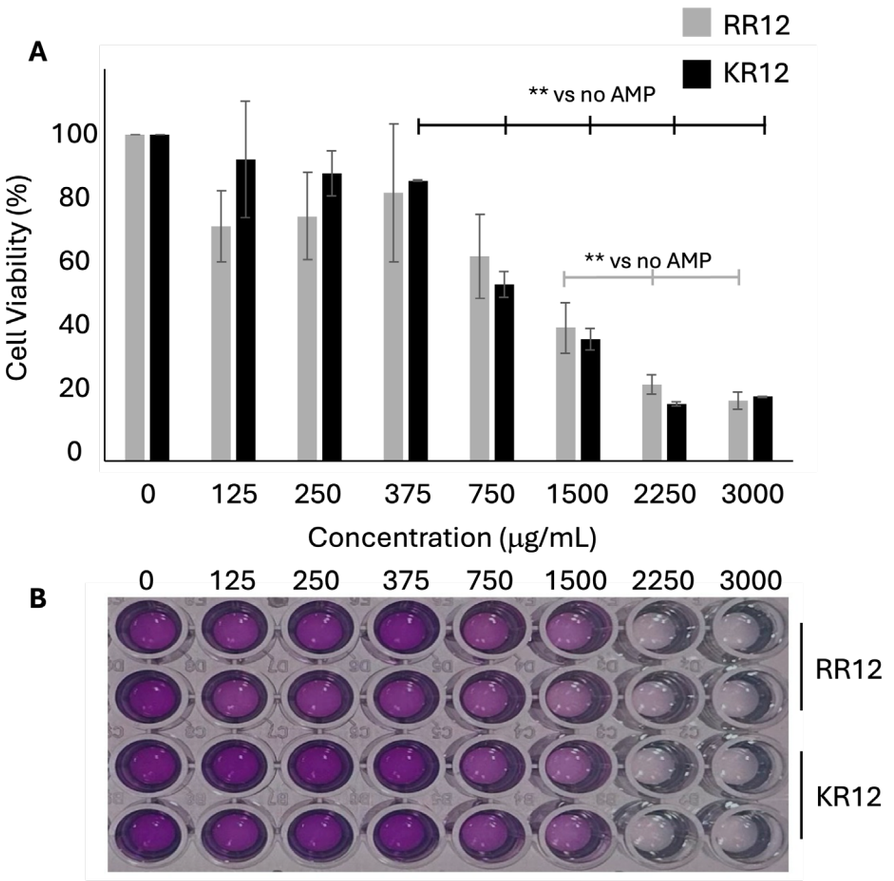

Figure 5 | Cytotoxicity of KR12 and RR12 peptides on HCT116 cells assessed by MTT assay.

(A) Cell viability (%) of HCT116 human colon carcinoma cells treated with increasing concentrations of KR12 and RR12 peptides (0–3000 µg/mL) for 24 hours. Viability is quantified using MTT reduction and expressed relative to untreated controls.

(B) Representative image of 96-well plates post-MTT assay showing the intensity of formazan staining across the concentration range for each peptide.

RR12 achieved only partial inhibition under similar conditions.

Cytotoxicity assays revealed that both peptides were relatively well-tolerated by mammalian cells at concentrations effective against bacteria, but KR12 displayed cytotoxicity at higher doses. This finding highlights the central challenge that even synthetically derived AMPs must balance antimicrobial potency with host cell compatibility to ensure clinical safety.

Taken together, these results support the potential of AMPs—particularly KR12—as promising alternatives or adjuncts to traditional antibiotics for the prevention and treatment of peri-implantitis. Their ability to disrupt early biofilm formation and overcome some limitations of conventional antimicrobials is especially relevant in an era of rising antibiotic resistance. However, the therapeutic window must be carefully optimized to maximize efficacy while minimizing cytotoxicity.

Future Directions

Future work should focus on peptide optimization for improved selectivity, in vivo validation using relevant animal models, and the development of delivery systems such as implant coatings or local gels. As AMPs move closer to clinical translation, their integration into dental practice could offer a new paradigm for biofilm management and implant longevity.

Acknowledgments

I would like to express my sincere gratitude to Dr. Jack Treml for his outstanding mentorship and guidance throughout the course of this research. I am also deeply thankful to Dr. Mattingly, Dr. Thomas, and Dr. Dagget for their support and insightful feedback, which greatly enriched the development of this work.

Special thanks to my classmate Kuljet for generously providing HCT116 human colon carcinoma cells, and to the University of Kansas and JCERT for their institutional support.

This research was funded in part by the KU Edwards Research Grant, with additional generous support from Catalent, Hill's Pet Nutrition and ICON.

Author's Biography

Samia Chergui is a senior in the Biotechnology program at the University of Kansas Edwards Campus. Upon completing her undergraduate degree, she plans to enter the biotechnology industry to gain hands-on research experience before choosing a focus for her Ph.D. studies. Her primary academic interests lie in immunology and genetics.

Author Contributions

S.C. contributed to the experimental work, design, and writing of this work; B.M., S.T., M.D., and J.F.T contributed to the design and editing of this work.

References

1. Berger, D., Rakhamimova, A., Pollack, A. & Loewy, Z. Oral Biofilms: Development, Control, and Analysis. High-Throughput 7, 24 (2018).
2. Körtvélyessy, G., Tarjányi, T., Baráth, Z. L., Minarovits, J. & Tóth, Z. Bioactive coatings for dental implants: A review of alternative strategies to prevent peri-implantitis induced by anaerobic bacteria. Anaerobe 70, 102404 (2021).
3. Roger, P., Delettre, J., Bouix, M. & Béal, C. Characterization of Streptococcus salivarius growth and maintenance in artificial saliva. J. Appl. Microbiol. 111, 631–641 (2011).
4. Patras, K. A. et al. Streptococcus salivarius K12 Limits Group B Streptococcus Vaginal Colonization. Infect. Immun. 83, 3438–3444 (2015).
5. Zhuo, H., Zhang, X., Li, M., Zhang, Q. & Wang, Y. Antibacterial and Anti-Inflammatory Properties of a Novel Antimicrobial Peptide Derived from LL-37. Antibiot. Basel Switz. 11, 754 (2022).
6. Vertillo Aluisio, G. et al. Streptococcus salivarius 24SMBc Genome Analysis Reveals New Biosynthetic Gene Clusters Involved in Antimicrobial Effects on Streptococcus pneumoniae and Streptococcus pyogenes.

Microorganisms 10, 2042 (2022).
7. Wang, Z., Shen, Y. & Haapasalo, M. Antibiofilm peptides against oral biofilms. J. Oral Microbiol. 9, 1327308 (2017).
8. Khurshid, Z. et al. Oral antimicrobial peptides: Types and role in the oral cavity. Saudi Pharm. J. SPJ Off. Publ. Saudi Pharm. Soc. 24, 515–524 (2016).
9. Li, J. et al. Membrane Active Antimicrobial Peptides: Translating Mechanistic Insights to Design. Front. Neurosci. 11, 73 (2017).
10. Calabrese, E. J. & Mattson, M. P. Hormesis provides a generalized quantitative estimate of biological plasticity. J. Cell Commun. Signal. 5, 25–38 (2011).
11. Mahlapuu, M., Håkansson, J., Ringstad, L. & Björn, C. Antimicrobial Peptides: An Emerging Category of Therapeutic Agents. Front. Cell. Infect. Microbiol. 6, 194 (2016).
12. Nguyen, L. T., Haney, E. F. & Vogel, H. J. The expanding scope of antimicrobial peptide structures and their modes of action. Trends Biotechnol. 29, 464–472 (2011).
13. Fjell, C. D., Hiss, J. A., Hancock, R. E. W. & Schneider, G. Designing antimicrobial peptides: form follows function. Nat. Rev. Drug Discov. 11, 37–51 (2011).
14. Castillo-Juárez, I., Blancas-Luciano, B. E., García-Contreras, R. & Fernández-Presas, A. M. Antimicrobial peptides properties beyond growth inhibition and bacterial killing. PeerJ 10, e12667 (2022).

Modeling human phenotypes in the nematode *C. elegans* during an undergraduate developmental biology course

Sireen Aburaide, Suad Ahmed, Mason Chamberlain, Yoskar Deleon, Ahmed Elewa[1,2], Allison Hookom, Evelyn Juen, Divine Katasi, Bobby Lee, Samantha Meyer, Luís Millan, Madeline Shaw, DJ Smith, Anthony Vassallo, Tashi Wangmo, Daniel Wolfson, Pader Xiong, Lian Yaeger

*Authors are listed alphabetically by last name

***Caenorhabditis elegans* is a widely used model organism in biomedical research due to its genetic tractability, short life cycle, and conservation of many developmental processes with humans. In this study, undergraduate students conducted nine independent experiments during a Developmental Biology course to model human phenotypes using *C. elegans*. Each group selected a human phenotype of interest, identified a gene associated with the phenotype, and then determined the orthologous or homologous gene in *C. elegans*. By obtaining mutants and designing phenotypic assays, students investigated the extent to which the worm models could recapitulate aspects of the human condition. This collective work highlights both the potential and limitations of *C. elegans* as a model for human phenotypic variation and disease and demonstrates the value of undergraduate inquiry as a catalyst for scientific engagement and research-based learning.**

Beneath the superficial differences between species lurk the remains of common ancestry. Learning to trace and chase this yarn of evolution provides the student of nature with the skill to weave together disparate facts and compose our epic of descent with modification. Such learning is not attained by memorizing facts but by posing challenging questions, distilling principles, testing hypotheses and feeling the satisfaction of coherence post-confusion.

Therefore, integrating research into undergraduate education has emerged as a transformative approach to fostering scientific inquiry and critical thinking.[1] For instance, investigating the impact of course-based undergraduate research experiences (CUREs) revealed that students participating in full-semester CUREs reported greater gains in experimental design skills, career interests, and intentions to conduct future research compared to those in shorter module-based CUREs or traditional laboratory courses.[2] Similar initiatives collectively underscore a shift from traditional, didactic teaching to active, research-based education, where students are not passive learners but active contributors to scientific knowledge.

Here we report the experimental results of a research-based learning module as part of a 30-lecture course on Developmental Biology. Students independently selected phenotypes from the Human Phenotype Ontology database, selected associated human genes, and identified *C. elegans* orthologs or homologs for study.[3,4] *C. elegans* is widely recognized for its rapid life cycle, abundant experimental resources, and conservation of key developmental processes with humans, making it an ideal species for modeling human phenotypes and for undergraduate research.[5-7] Each group designed experiments using loss-of-function mutant strains to test whether the nematode could recapitulate aspects of the human condition. The results reflect a range of plausible and implausible models, revealing both opportunities and limits of modeling human phenotypes in *C. elegans* in an undergraduate setting.

Department of Biology, Augsburg University, Minneapolis, MN 55454, USA
1. Current address: Department of Biology, Miami University, Oxford, OH 45056, USA
2. Corresponding author: elewaa@miamioh.edu

Materials and Methods

Instruction in C. elegans

A fifteen week lab course was designed to complement thirty lectures in developmental biology (BIO474 Developmental Biology). During the first four weeks, students learned to pick *C. elegans* worms under a dissecting microscope and distinguish its different life stages. Students also learned how to mount worms on an agarose pad and observe fertilization and early embryonic cleavages under a compound microscope. Per worm tradition, students traced their academic mentorship lineage to Sydney Brenner (who initiated the use of *C. elegans* as a model organism). It was a particularly nice surprise to learn later on during the semester that Victor Ambros, a connection in their lineage, was a co-recipient of the 2024 Nobel Prize in Medicine or Physiology. Each student was responsible for their worm colony and maintained it by singling worms onto fresh seeded NGM plates and working with the resulting population the following week. A shared spreadsheet was used to log the overall state of each colony each week. Between weeks 5 and 8, students were grouped in pairs and each pair chose two human phenotypes of interest by

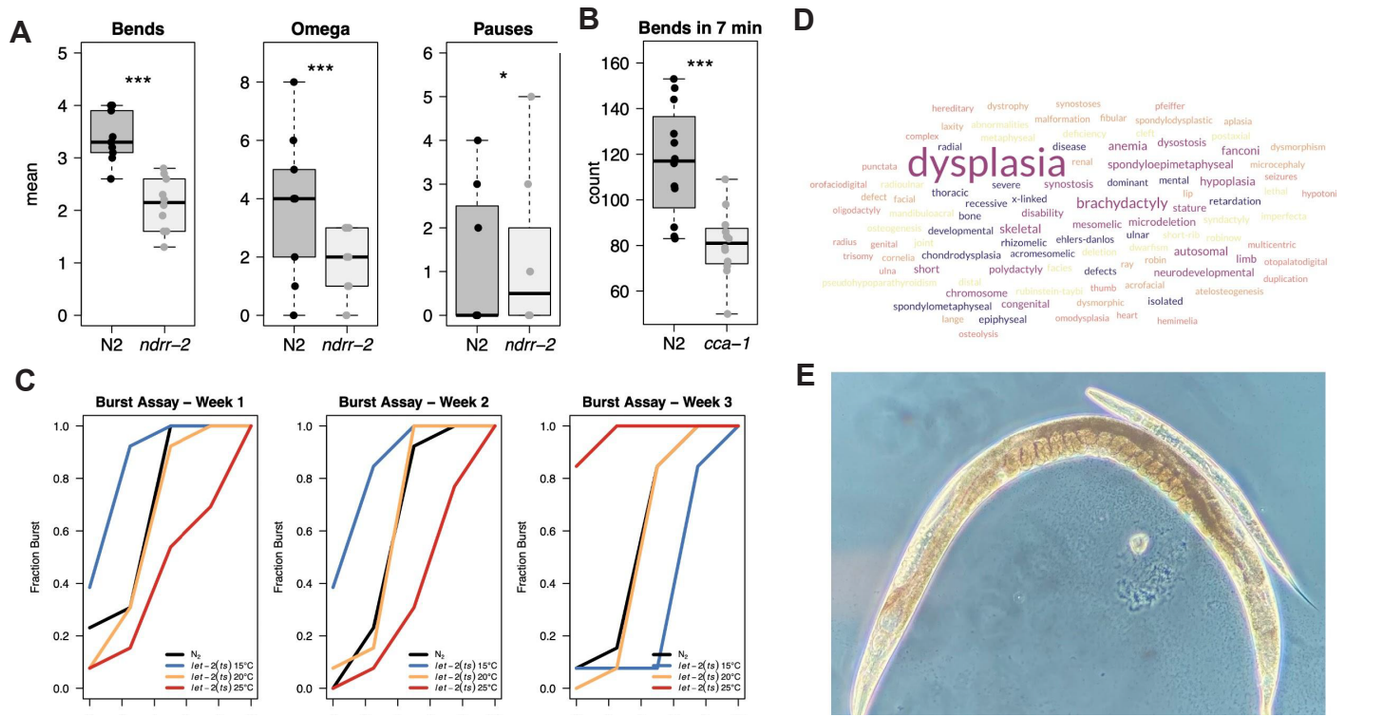

Figure 1 | Modeling areflexia, hip flexor weakness, arterial stiffness and abnormal limb morphology in C. elegans. a) The mean number of tail bends and omega turns in wildtype and ndrr-2(ok1899) worms following ten evenly spaced head taps (n = 10 trials), and the mean number of pauses observed following ten evenly spaced head taps (n = 8 trials). Individual data points are overlaid on boxplots. Student's t-test: $p \leq 0.01$ (*); $p \leq 0.001$ (***). b) The number body bends that wildtype and cca-1(ad1650) worms performed over a period of 7 minutes (n = 12 trials). Individual data points are overlaid on boxplots. Student's t-test: $p \leq 0.001$ (***). c) Burst assay results across three successive weekly trials using wildtype and let-2(ts) worms. In Weeks 1 and 2, worms reared at the permissive temperature (15°C) appeared to rupture more readily, likely due to uncontrolled temperature-dependent effects on cuticle elasticity. In Week 3, incorporation of a room temperature acclimation step demonstrated that let-2(ts) worms raised at the restrictive temperature (25°C) ruptured significantly faster than those raised at 15°C. d) A word cloud of the disease terms associated with Abnormal upper limb bone morphology. e) A wildtype (larger) and let-2(ts) worm 4 days after hatching displaying the stark difference in growth rate. The wildtype worm has reached adulthood as evidenced by the embryos developing in its uterus. The let-2(ts) worm was hatched and reared at permissive temperature (15°C) for 24 hours before being shifted to the restrictive temperature (25°C).

browsing The Human Phenotype Ontology database. The sole criterion for choosing a human phenotype was curiosity. Students then were asked to choose a gene associated with the human phenotype of interest and present their choices to the class. Only afterwards were the students informed that they will now attempt to model the human phenotype via the associated gene in *C. elegans* . Students were encouraged to generate interesting hypotheses and if needed sufficiency abstract the phenotype in question to reach a conserved core developmental process. Finally, students sought *C. elegans* orthologs or homologs of their human gene of interest and identified suitable strains provided through the *Caenorhabditis* Genetics Center. By the end of this process, one of the two phenotypes originally chosen proved more promising and practical to pursue. In parallel to activities of this segment, students were also introduced to a host of *C. elegans* mutants and phenotypes to prepare them for work with non-wildtype strains. Between weeks 9 and 15 and while waiting for strains to arrive, students designed experiments to test the extent to which the *C. elegans* strain of choice could model the human phenotype of interest. This iterative process came hand in hand with consulting course lectures, scientific literature via Pubmed[8] and the databases UniProt,[9] AlphaFold[10,11] and WormBase[4] to learn more about the phenotype of interest, its associated diseases, the function of its associated gene and the documented phenotypes of the *C. elegans* homologs. The swift delivery of worm strains from CGC allowed each student group at least three weeks to troubleshoot and optimize their protocols and obtain data to evaluate their hypotheses.

Strains

The following *C. elegans* strains used in this study were obtained from the Caenorhabditis Genetics Center (University of Minnesota):

N2
CB1 dpy-1(e1) III. (Dpy)
CB1009 unc-54(e1009) I. (Unc - paralyzed)
CB1026 lin-1(e1026) IV. (Muv)
CB1138 him-6(e1104) IV. (Him)
CB1179 unc-22(e1179) IV. (Unc - twitcher)
CB1309 lin-2(e1309) X. (Vul)

CB1393 daf-8(e1393) I. (Daf)
CB1515 mec-10(e1515) X. (Mec)
CB1598 unc-1(e1598) X. (Unc - coiler)
CB91 rol-1(e91) II. (Rol)
RB1565 ZK1073.1(ok1899) X. Not outcrossed.
VC1224 polg-1(ok1548)/mT1 II; +/mT1 [dpy-10(e128)] II. polg-1(ok1548) outcrossed once.
JD21 cca-1(ad1650) X. Outcrossed 7 times.
GG25 let-2(g25) X. Outcrossed status unknown.
MT1079 egl-15(n484) X. Outcrossed once.
RB1091 Y64G10A.7(ok1062) IV. Not outcrossed.
LT121 dbl-1(wk70) V. Outcross status unknown.
KR827 let-363(h502) dpy-5(e61) unc-13(e450) I; sDp2 (I;f). Outcross status unknown.
Additionally, the E. coli strain OP50-GFP was ordered from the *Caenorhabditis* Genetics Center (see Worm Maintenance).

Worm maintenance
Worms were grown on solid agar nematode growth media (NGM) plates with ampicillin at 20°C. Temperature sensitive mutants were maintained at 15°C. Instead of OP50 E. coli, OP50-GFP, a strain of OP50 that contains a GFP plasmid (pFPV25.1) was used since it was resistant to ampicillin and allowed addition of the antibiotic in NGM plates (100 µg/ml). This measure was taken to minimize contamination as students began to learn how to maintain and experiment
with *C. elegans* . As a weekly practice, students picked single worms onto seeded NGM plates and worked with the resulting population the following week.

Orthology and Homology
To assess orthology between a *C. elegans* gene and the human proteome we use the DIOPT search engine https://www.flyrnai.org/cgi-bin/DRSC_orthologs.pl, which aggregates results from 16 different orthology matching programs. Protein homology was quantified by aligning C. elegans and Human proteins using NCBI Protein Blast https://blast.ncbi.nlm.nih.gov/Blast.cgi. For the protein alignment a single sequence was selected when multiple isoforms existed. In these cases, "isoform a" was always selected for *C. elegans* and the "canonical" sequence from UniProt https://www.uniprot.org/ was selected for human (Supplementary File 1). Orthology for the purpose of phenolog statistical analysis was based on a different method (see below).

Phenolog statistical analysis
Human orthologs as well as RNAi and allele phenotypes associated with *C. elegans* genes were retrieved from WormBase https://wormbase.org/tools/mine/simplemine.cgi. Human phenotypes associated with human genes were retrieved from The Human Phenotype Ontology (HPO) project https://hpo.jax.org/data/annotations. Hypergeometric testing was performed in R (see Data and Code Availability).

Tap response assay (areflexia)
Individual wildtype (N2) and ndrr-2(ok1899) (RB1565) worms were placed on unseeded NGM plates and allowed to acclimate for 2 minutes. A sterile eyelash attached to a pipette tip was used to deliv-

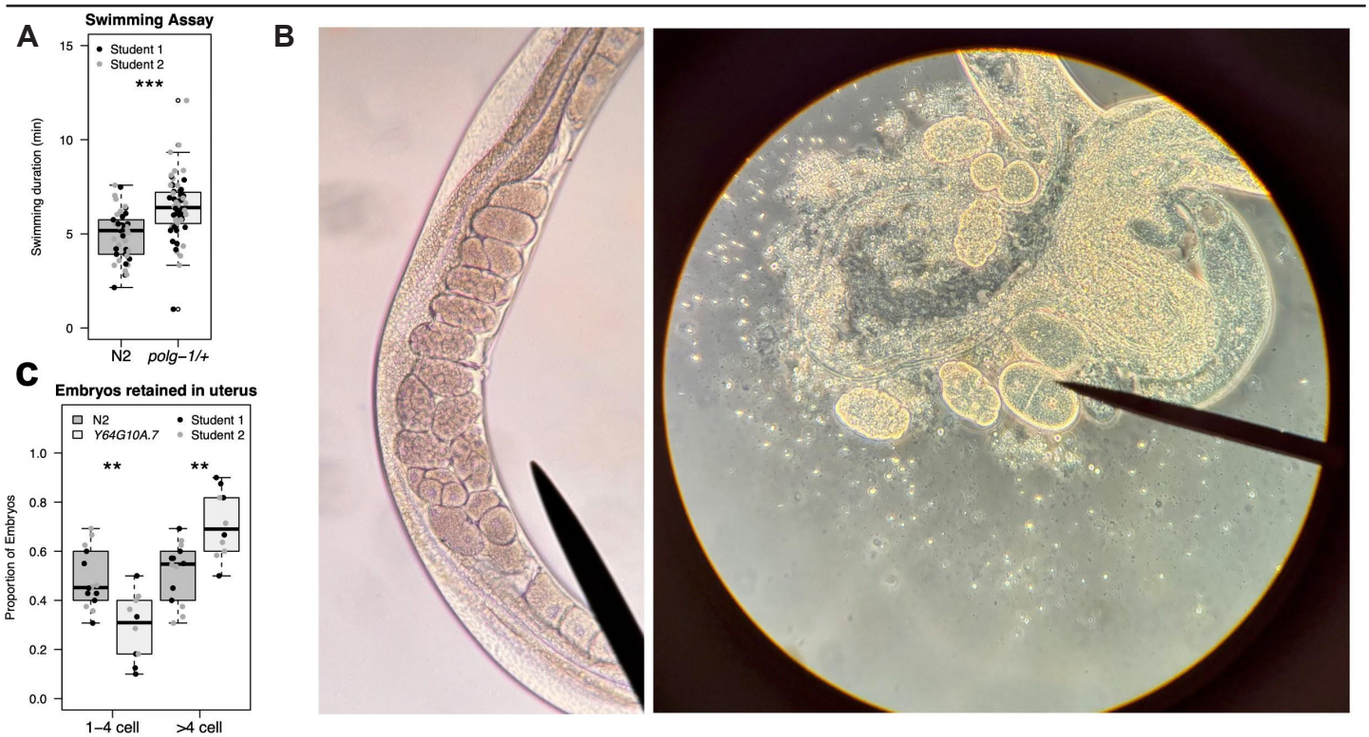

Figure 2 | Modeling abnormal cell morphology and premature birth in C. elegans. a) Swimming durations of wildtype and polg-1(ok1548)/+ heterozygous worms. Boxplots represent 42 wildtype and 60 polg-1 heterozygous individuals. Data points reflect two durations measured by two different researchers, both of which independently confirmed the enhanced swimming phenotype in polg-1 heterozygotes. Statistical significance was assessed using the Wilcoxon rank-sum test: $p \leq 0.001$ (***). b) An example of the setup used to quantify egg retention. Embryonic stages were quantified in utero or ex utero after worm rupture. The needle in the image to the right points to a two-cell stage embryo. c) The proportions of embryos with few (i.e. 1 to 4 cells) versus many (i.e., > 4 cells) in 28 wildtype and 20 Y64G10A.7(ok1062) young adults. Data points reflect values ascertained by two independent researchers. Wilcoxon rank-sum test: $p \leq 0.01$ (**).

er head taps. Each worm received 10 taps, with 15–20 seconds between each tap. The number of tail bends during withdrawal, omega turns and pauses were recorded and used to quantify reflex. ndrr-2(ok1899) (RB1565) was not outcrossed.

Locomotion assay (hip flexor weakness)
Young adult *C. elegans* individuals maintained on seeded NGM plates were transferred to unseeded plates. For each worm, the number of complete body bends (forward or backward) was recorded over a 7-minute period. A two-sample t-test was used to compare body bend frequency between wildtype and cca-1 mutants.

Bursting assay (arterial rupture)
N2 and let-2(ts) larvae were maintained at 15°C, 20°C, or 25°C and then acclimated to room temperature the night before testing. Adult worms (5–7 days old) were transferred to individual wells of a 96-well plate containing 300 µL of distilled water. Worms were monitored under a microscope at 2.5-minute intervals for 10 minutes. Phenotypic categories included mobile, immobile, rod-like, or ruptured. The number of ruptured worms at each time interval was recorded for each condition.

Identifying optimal temperature shift conditions (abnormal upper limb bone morphology)
Eight let-2(ts) worms were individually plated and shifted to 25°C at varying timepoints to determine the optimal temperature shift for survival. Plates shifted after 24 hours produced the highest number of viable adults.

Viability and pharyngeal development (cleft soft palate)
Synchronized populations of wildtype N2 and dbl-1(wk70) worms were transferred to seeded NGM plates and incubated at 25°C. Larvae were counted daily for two days and dead embryos scored. Pharyngeal morphology was examined under a compound microscope (40X magnification). A Welch two sample t-test was used to test the difference between wildtype and dbl-1 since variance between the two samples was assumed to be different.

Swimming Behavior Assay (abnormal cellular phenotype)
Synchronized young adult wildtype and polg-1(ok1548) heterozygous worms were grown on seeded NGM plates. Worms were transferred into droplets of M9 buffer on microscope slides. Swimming durations were recorded for each worm, with swimming defined as thrashing within a 30 sec-

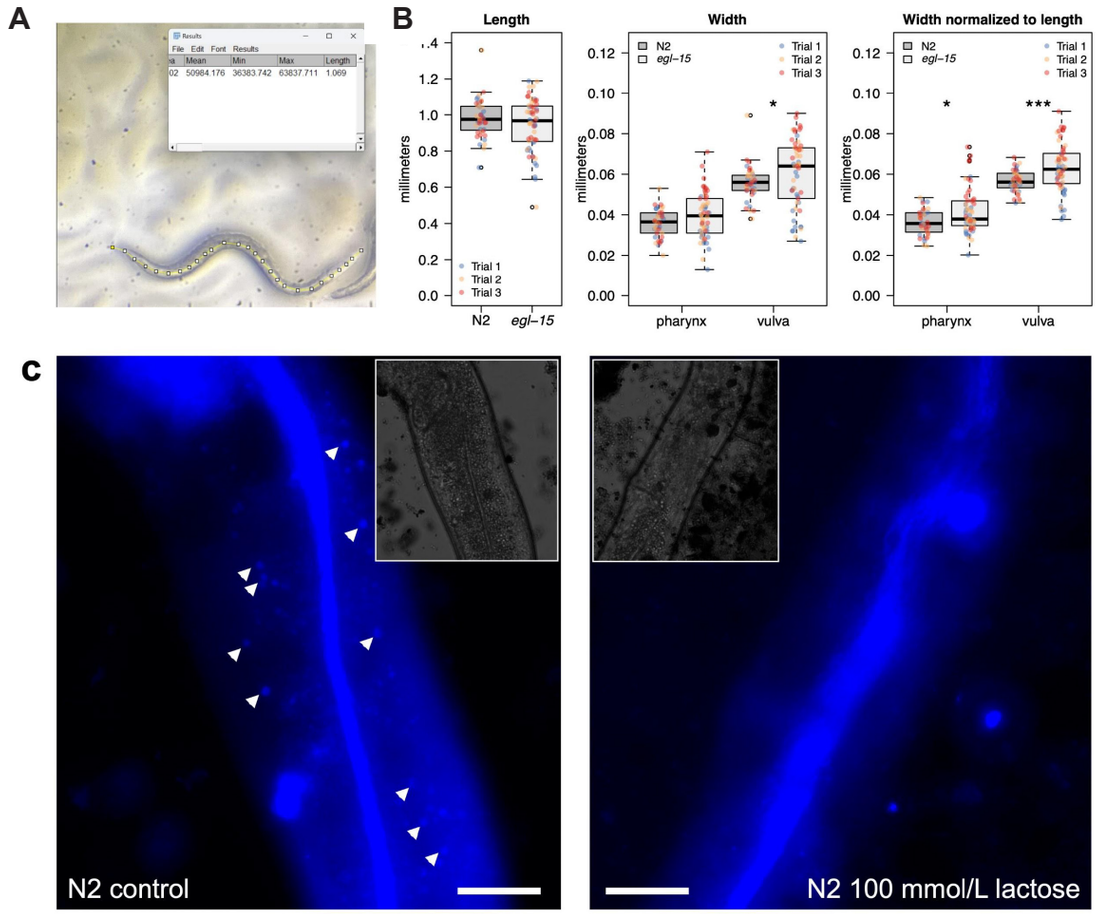

Figure 3 | Modeling lethal short-limb status and lactose intolerance in C. elegans. a) An example of the interface used for in situ quantification of worm morphometrics in Fiji. b) Morphometric data for wildtype and egl-15(n484) animals across three successive weekly trials were collected for total body length and for body widths at pharynx and vulva. Length was measured in 44 wildtype and 59 egl-15 worms; pharynx width in 38 and 58; and vulva width in 40 and 58, respectively. Wilcoxon rank sum test: $p \leq 0.01$ (*); $p \leq 0.001$ (***). c) Representative fluorescence microscopy images of wild-type C. elegans intestine stained with neutral red. Brightfield images shown in insets. Arrowheads indicate visible gut granules.

Table 1 | *C. elegans*/Human gene orthologies based on DRSC - DRSC Integrative Ortholog Prediction Tool

C. elegans	Human	DIOPT Score	Rank	Best Score	Best Score Reverse
Y48G10A.3	*NDRG3*	15	high	Yes	Yes
cca-1	*CACNA1I*	14	high	Yes	Yes
let-2	*COL4A6*	9	high	Yes	Yes
col-104	*COL5A2*	2	high	Yes	Yes
dbl-1	*BMP2*	9	high	Yes	Yes
dbl-1	*BMP5*	9	high	Yes	Yes
polg-1	*POLG*	15	high	Yes	Yes
Y64G10A.7	*MEGF6*	12	high	Yes	Yes
egl-15	*FGFR3*	13	high	Yes	Yes
let-363	*MTOR*	13	high	Yes	Yes

ond time window (i.e., if worms stopped moving for more than 30 seconds it was deemed no longer swimming).

Embryo Staging by Microscopy (premature birth)

Adult worms were transferred to slides with deionized water or M9 buffer and ruptured using coverslip pressure or osmotic stress. Released embryos were categorized by cell stage. In some cases, embryos were counted while still inside the worm. Two worms with 3 embryos in their uteri each were considered outliers and excluded from downstream analysis.

Digestive tract integrity (lactose intolerance)

Worms were washed off plates using M9 buffer and divided into three treatment conditions: control, 50 mmol/L lactose, and 100 mmol/L lactose. Each group was washed three times using centrifugation at 1000 rpm for 3 minutes. After washing, worms were stained with Neutral Red (75 mmol) in 20% acetone and 80% DI water, incubated in the dark for 1 hour, and then washed with DI water. Neutral Red has an excitation peak at approximately 530–540 nm and emits at 640–650 nm. The available fluorescence microscope was equipped with DAPI (excitation 350–370 nm, emission 420–480 nm), GFP (excitation 460–490 nm, emission 510–550 nm), and TXR (excitation 540–580 nm, emission 600–660 nm) filter sets. Although none of these filter sets matched Neutral Red's spectral properties exactly, the TXR filter provided the closest overlap with both its excitation and emission spectra. Thus, the TXR filter was adopted for imaging, enabling qualitative visualization of dye retention in the gut despite suboptimal excitation efficiency. Imaging parameters were standardized for exposure (192.1), gain (4.4), and magnification (40 X)

Morphometric Analysis (lethal short-limb stature)

Wildtype N2 and egl-15(n484) mutant worms were maintained on seeded NGM plates and selected for imaging at the young adult stage. Using a mobile phone, images were taken through a calibrated binocular microscope with a stage micrometer eyepiece (90 units = 2 millimeters). Magnification was set to 5X and the microscope was focused on young adult worms before acquisition. Images were converted to TIFF format and manually analyzed using Fiji (ImageJ) to determine body length and widths at the vulva and pharynx. We chose to measure worms on an NGM plate at 5 X rather than on an agarose pad at 40 Xin order to increase the number of assayed individuals for better statistical analysis.

Results

Weak response to tapping as a model for areflexia

Areflexia (HP:0001284) is the absence of neurologic reflexes such as the knee-jerk reaction.[3] Among the genes with inferred associations, NDRG1 was selected to attempt modeling areflexia in C. elegans. The NDRG family derives its name from "N-myc downstream regulated gene".[12] C. elegans has a different yet orthologous MYC network in which two Max orthologs, MXL-1 (MaX-Like 1) and MXL-3 act as central dimerization partners for the Mad-like ortholog MDL-1 (MAD-Like 1) and a single Mlx ortholog, MXL-2, acts as central dimerization partner for Mondo-like protein MML-1 (Myc and Mondo-Like 1).[13] While a bona fide *C. elegans* ortholog of NDRG1 could not be ascertained since no reciprocal best hits were found, genes Y48G10A.3 and ZK1073.1 are homologs of NDRG1, NDRG2 and NDRG3, with Y48G10A.3 also being an ortholog of NDRG3 (Tables 1 and 2).[14] Furthermore, ZK1073.1 is a target of MDL-1 supporting its identity as an N-myc downstream regulated gene.[15] Since Y48G10A.3 and ZK1073.1 are "NDRG family member related" we named these two genes ndrr-1 and ndrr-2, respectively.

We reasoned that if *C. elegans* could serve as a model for areflexia, then perhaps ndrr-2 loss-of-function would impede the nematode's ability to react to its surroundings. Therefore, we hypothesized that the knockout ndrr-2(ok1899) would show a dampened response in a tap-withdrawal as-

say compared to wildtype animals (Methods). To test this hypothesis we recorded the number of tail bends and omega turns after a series of ten separate head taps with an eyelash (n = 10 trials of ten taps for each strain). Additionally, we counted the number of times a worm paused while withdrawing from the tap, an indication of a dampened response (n = 8 trials of ten taps for each strain). In support of our hypothesis, we found that the mean number of tail bends was significantly reduced in ndrr-2(ok1899) animals (2.1 vs 3.4 tail bends per tap, p-value = 4.1×10^{-12}). Likewise, we observed a significant reduction in total number of omega turns performed by each assayed worm (1.7 vs 3.8 omega turns during 10 taps, p-value = 1.2×10^{-5}). Moreover, ndrr-2(ok1899) animals paused significantly more times during their withdrawal compared to wildtype worms (1.25 vs 1.13 pauses during 10 taps, p-value = 0.01) (Figure 1a). Taken together, these findings suggest that ndrr-2 loss-of-function can recapitulate aspects of areflexia, providing a functional model for investigating motor and sensory neuropathy associated with NDRG1 mutations in humans.[16]

Impaired sinusoidal movement as model for hip flexor weakness

Hip flexor weakness (HP:0012515) is the reduced ability to flex the femur, that is, to pull the knee upward [3]. Among the genes with inferred associations, SCN4A (Sodium Voltage-Gated Channel Alpha Subunit 4) was selected to model hip flexor weakness in *C. elegans* . SCN4A encodes a voltage-gated sodium channel and is responsible for sodium ion conductance in muscle cells [12]. Unbeknownst to us when selecting SCN4A, the *C. elegans* genome does not encode any voltage-gated sodium channels.[17] Instead, voltage-gated calcium channels serve an equivalent role in translating electrical signals into muscle contractions. Therefore, to model hip flexor weakness as a result of cation channel loss-of-function the *C. elegans* voltage-gated calcium channel cca-1 (Calcium Channel, Alpha subunit) was adopted (Tables 1 and 2).[18]

We drew an analogy between impaired gait in humans due to hip flexor weakness and impaired locomotion in nematodes due to reduced muscle activity. Consequently, we hypothesized that the number of sinusoidal wave motions will be reduced in cca-1 mutants. To test this hypothesis we recorded the number of body bends that wildtype and cca-1(ad1650) worms perform over a period of 7 minutes (n = 12 trials each) and found that the mean number of bends was significantly reduced in cca-1(ad1650) (81 vs. 117 bends, p-value = 5.4×10^{-15}) (**Figure 1B** and Methods). This finding supports the hypothesized importance of cca-1 in locomotion and suggests that its disruption can model neuromuscular phenotypes such as hip flexor weakness.

Worm bursting as a model for arterial rupture

Arterial rupture (HP:0025019) is the sudden breakage of an artery leading to leakage of blood from the circulation.[3] Among the genes with inferred associations, COL5A2 (Collagen Type V Alpha 2 Chain) was selected to model arterial rupture in C. elegans. COL5A2 encodes a collagen alpha-2(V) chain and contributes to extracellular matrix structure and stability.[12] In *C. elegans* , let-2 (LEThal 2) encodes a structural collagen involved in maintaining cuticle integrity [19]. While not an ortholog of COL5A2, we chose let-2 to model arterial rupture due to compromised collagen function (**Tables 1 and 2**).

We reasoned that reduced cuticle integrity in nematodes could lead to breakage reminiscent of arterial rupture in humans. Consequently, we hypothesized that the internal pressure resulting from placing let-2(ts) worms in a hypotonic solution after rearing them at the restrictive temperature would lead to cuticle breakage and worm bursting. Initial trials yielded inconsistent results, likely due to uncontrolled effects of temperature on tissue elasticity (Figure 1c). Therefore, we incorporated an acclimation step at room temperature before each trial (Methods). The revised assay revealed that let-2(ts) worms raised at the restrictive temperature (25°C) ruptured significantly faster than those raised at the permissive temperature (15°C), as indicated by a log-rank test ($\chi^2(1) = 23.7$, $p = 1 \times 10^{-6}$) (**Figure 1C**).

Table 2 | *C. elegans*/Human protein homologies

C. elegans	Human	DIOPT Score	Rank	Best Score	Best Score Reverse
Y48G10A.3	*NDRG3*	15	high	Yes	Yes
cca-1	*CACNA1I*	14	high	Yes	Yes
let-2	*COL4A6*	9	high	Yes	Yes
col-104	*COL5A2*	2	high	Yes	Yes
dbl-1	*BMP2*	9	high	Yes	Yes
dbl-1	*BMP5*	9	high	Yes	Yes
polg-1	*POLG*	15	high	Yes	Yes
Y64G10A.7	*MEGF6*	12	high	Yes	Yes
egl-15	*FGFR3*	13	high	Yes	Yes
let-363	*MTOR*	13	high	Yes	Yes

This finding indicates that let-2(ts) worms exhibit temperature-dependent sensitivity to osmotic pressure, consistent with defects in structural integrity and supports the use of let-2(ts) as a model for exploring arterial rupture due to compromised collagen function.

Worm body size as a model for abnormal limb bone morphology

Abnormal upper limb bone morphology (HP:0040070) refers to the atypical shape or structure of the bones that make up the arm, which could impact function of the arm or hand.[3] According to The Human Phenotype Ontology (HPO) website, this phenotype is associated with over 800 human diseases. A word cloud of the disease terms highlights a common theme of dysplasia, a usually neoplastic transformation of the cell, associated with altered architectural tissue patterns (Figure 1d). From among the genes associated with abnormal upper limb bone morphology, COL10A1 (Collagen Type X Alpha 1 Chain) was selected for further study. The protein encoded by COL10A1 is 680 amino acids long alpha-1 chain of type X collagen that affects cartilage and endochondral osteogenesis.[12,20]

Although nematodes do not develop limbs, we surmised that abnormal upper limb morphology could nevertheless be modeled in C. elegans. We reasoned that since abnormal limb bone morphology could represent an misexpression of the COL10A1 gene during osteogenesis then misexpression of collagen in the worm could lead to an analogous phenotype during cuticle formation. The C. elegans ortholog of COL10A1 is col-104 (COLlagen 104), however we adopted the homolog let-2 to investigate the effects of collagen misexpression to take advantage of a temperature sensitive mutant (**Tables 1 and 2**).[19] We hypothesized that let-2 mutants would display atypical shapes or structures in the cuticle when grown at a restrictive temperature.

We shifted a temperature sensitive let-2 mutant to restrictive temperatures at different developmental stages to determine conditions that allowed survival to adulthood (Methods). let-2(ts) worms shifted from 15°C to 25°C 24 hours after fertilization showed reduced lethality and were used to score for abrupt angulations in the worm body. We noted that one-day-old let-2(ts) larvae shifted to, and maintained at, restrictive temperature until adulthood were significantly shorter in body length compared to wildtype controls (Figure 1e). Due to time constraints, this phenotype was not thoroughly quantified. However, the observation of short let-2 worms led us to explore performing a phenolog analysis.[21] We asked if a significant number of orthologs associated with abnormal upper limb bone morphology in humans were also associated with the short phenotype in C. elegans. Hypergeometric testing revealed that indeed the overlap in orthologs associated with these two phenotypes was statistically significant (N = 16,329, n = 375, m = 145, c = 22, p-value = 2.1 X 10^{-12}). Together, these results
suggest that reduced body length in let-2 mutants can serve as a proxy for modeling limb morphologies associated with collagen defects in humans.

Modeling cleft soft palate via pharyngeal development in *C. elegans*

Cleft soft palate (HP:0000185) is a result of a developmental defect that leads to malformation of soft tissue structures in the oral cavity.[3] Among the genes with inferred associations, TGFB3 (Transforming Growth Factor Beta 3) was selected to model cleft soft palate in *C. elegans* . Although dbl-1 (DPP/BMP-Like 1) is not a bona fide ortholog of TGFB3 it is the best alignment match and shares functional similarity as ligands in TGF-β signaling pathway (**Tables 1 and 2**).[12,14]

We hypothesized that dbl-1 mutants would display defective pharyngeal development and morphology reminiscent of a cleft soft palate. To test this hypothesis, the offspring of individual N2 and dbl-1(wk70) animals were scored for embryonic lethality (N = 3 parents for each genotype). The mean number of offspring from dbl-1(wk70) moms was significantly lower than wildtype (41±31.2 vs. 161±11.4 animals, t = 5.9312, df = 2.4631, p-value = 0.016). However, no embryonic lethality nor signs suggestive of pharyngeal maldevelopment in larvae were observed at 25°C (Methods). Consistent with published findings, dbl-1(wk70) animals were reduced in size underscoring the importance of this gene for growth and development.[22] Although a pharynx-specific phenotype was not detected, the reduced growth observed in dbl-1(wk70) encourages further investigation into whether this gene can be used to model aspects of soft tissue developmental defects associated with TGFB3 dysfunction.

Modeling mitochondrial dysfunction through impaired motility in C. elegans

Abnormal cellular phenotype (HP:0025354) ecompasses a wide range of anomalies of cellular morphology or physiology.[3] Among the hundreds of genes associated with this phenotype we chose to study POLG (DNA Polymerase Gamma, Catalytic Subunit), which encodes the mitochondrial DNA polymerase.[12] In *C. elegans* , the ortholog polg-1 (mitochondrial DNA POLymerase Gamma 1), was adopted for modeling abnormal cellular physiology caused by mitochondrial dysfunction (**Table 1**)].[23]

We reasoned that polg-1 mutants would suffer from energy deficits due to disrupted mitochondrial function. Indeed, worms homozygous for a polg-1(ok1548) mutation are sterile and have shortened lifespan.[24] Therefore, we hypothesized that polg-1 heterozygous animals
would have impaired mitochondrial activity leading to reduced physical fitness in the worm. To test this hypothesis, we conducted assays to measure how long worms could swim (Methods). Surprisingly, polg-1(ok1548) heterozygotes swam for significantly longer periods than wildtype worms! Worms with one copy of mutated polg-1 swam on average for 6.4 minutes compared to 4.9 minutes swam by N2 individuals (**Figure 2A**). A Wilcoxon rank-sum test indicated that the observed difference was significant (Wilcoxon rank-sum test, W = 564, p-value = 2.3 X 10^{-6}). Importantly, this result was confirmed independently by two students (Wilcoxon rank-sum test, W = 147, p = 0.019 and W = 133, p = 0.00032) thereby adding credence to the counterintuitive enhanced swimming fitness in polg-1 heterozygotes. These results rule out the hypothesized consequence of polg-1 loss-of-function and is interpreted as a form of systemic overcompensation for mitochondrial deficiency.

Egg retention dynamics as a model for premature birth

Premature birth (HP:0001622) is the birth that occurs before 37 weeks of gestational age.[3] Among the genes with inferred associations, LTBP3 (Latent Transforming Growth Factor Beta Binding Protein 3) was chosen to attempt and model human premature birth in *C. elegans* . LTBP3 encodes a protein rich in EGF-like domains and a

β-sheet core and is a regulator of TGF-beta signalling.[12] LTBP3 does not have any orthologs in *C. elegans* .[14] However, the top match is the uncharacterized Y64G10A.7, which in turn is a bona fide ortholog of the human gene MEGF6 (Multiple EGF Like Domains 6) (**Tables 1 and 2**).[14]

Despite the fact that *C. elegans* is an oviparous species that lays its embryos rather than retain and nourish them in utero, we wondered if egg retention versus premature egg laying could be an analogous phenotype to premature birth in humans. We hypothesized that Y64G10A.7 loss-of-function would lead to premature egg-laying, detectable by an increased number of early-stage embryos retained in the uterus. To test this, gravid worms from both wildtype N2 and the knockout strain Y64G10A.7(ok1062) were ruptured between an agarose pad and coverslip and the developmental stages of released embryos were categorized based on cell number (Methods and **Figure 2B**). Contrary to our hypothesis, wildtype *C. elegans* retained a significantly higher proportion of early-stage embryos (1-cell to 4-cell stage) compared to the Y64G10A.7(ok1062) mutant (Wilcoxon rank-sum test, W = 120.5, p = 0.003; Figure 2c). This finding suggests that loss of Y64G10A.7 function may promote retention of later-stage embryos, potentially acting as a negative regulator of egg-laying. Consequently, this result questions whether the inferred association between human LTBP3 and premature birth reflects a positive

or negative association and encourages further exploration of TGF-β signaling in developmental timing.

Modeling lethal short-limbed short stature C. elegans morphometrics

Lethal short-limbed short stature (HP:0008909) is also known as lethal micromelic dwarfism.[3] The only gene hitherto associated with this phenotype is FGFR3 (Fibroblast Growth Factor Receptor 3), which encodes a transmembrane tyrosine kinase receptor that plays a critical role in chondrocyte proliferation and skeletal development.[3,12] The C. elegans ortholog of FGFR3 is egl-15 (EGg Laying defective 15), which also encodes a fibroblast growth factor receptor critical for development and cell migration (Table 1).[25] Therefore, we aimed to model lethal micromelic dwarfism in C. elegans by studying the consequences of egl-15 loss-of-function. We hypothesized that egl-15(n484) would result in reduced body length and altered body shape, recapitulating aspects of short-limbed dwarfism. To test this, young adult worms were imaged using a calibrated stereo microscope (Methods and **Figure 3A**). Morphometric data were collected for total body length and for body widths at two anatomical landmarks: the pharynx and the vulva . We found no significant difference between the mean lengths of wildtype and mutant animals (0.98±0.11 vs 0.94±0.15 mm, p-value = 0.39, Wilcoxon rank sum test) or between the width at the pharynx (35.9±7 vs 39.6±11 microns, p-value = 0.13), although a modestly significant difference in body width at the vulva was detected (55.7±9 vs 60.4±17 microns, p-value = 0.043). However, when width at pharynx or vulva were normalized to the length of an individual a more compelling difference was detected in both cases (pharynx: 35.3±6 vs 41.7±11 microns, p-value = 0.022 and vulva: 56.4±5 vs 63.2±12 microns, p-value = 0.0008958) (Figure 3b). Therefore, while there was no significant difference in absolute body length, overall shape was different between wildtype and mutants with egl-15(n484) being relatively broader.

These findings are consistent with the known role of FGFR3 in regulating tissue elongation and skeletal growth and highlights the potential of C. elegans to capture key aspects of growth impairment and body proportion changes associated with skeletal dysplasias.

Gut integrity as model for lactose intolerance

Lactose intolerance is a human metabolic phenotype (HP:0004789) characterized by the inability to digest lactose.[3] Among the genes with inferred associations, mTOR (Mammalian/Mechanistic Target Of Rapamycin Kinase) was selected to model lactose intolerance in *C. elegans* . The ortholog of mTOR in *C. elegans* is let-363 (LEThal 363) and similar to mTOR, the encoded protein is a member of the PI3/PI4K kinase family and shares a similar domain architecture, supporting functional conservation and justifying its selection to model lactose intolerance in *C. elegans* (Tables 1).[26]

We hypothesized that loss of let-363 function would reduce gut integrity in *C. elegans* in response to a lactose rich diet. To test this, we first adapted protocols to treat both wildtype and let-363 mutant worms with lactose and then asses gut integrity by staining with neutral red, a vital dye that accumulates in lysosome-rich gut cells and serves as a marker of tissue viability.[27] Using the developed protocol we could detect a difference in the number of fluorescent gut granules when comparing untreated N2 worms to worms treated with 100 mmol/L lactose (Methods and **Figure 3C**). Due to time constraints, we could not quantify the difference in observed gut granules, determine the contribution of autofluorescence or compare with a let-363(h502) mutant. Nevertheless, the developed protocol provides a starting point for future students to pursue this experiment and determine the plausibility of using let-363 as a model for lactose intolerance resulting from mTOR loss-of-function.

Discussion

This study presents the scientific output of a research-based undergraduate learning module. Through nine independent experiments, students explored the conservation of molecular and phenotypic traits and gained hands-on experience in experimental design and data interpretation. A key significance of this work lies in empowering undergraduates to engage as active contributors to scientific inquiry and to share their contributions with the broader scientific community.

The use of *C. elegans* proved highly effective for undergraduate education due to its genetic accessibility and well-documented developmental biology. The challenge of modeling aspects of complex human development in a nematode prompted students to trace the common ancestry of seemingly distant phenotypes. Such “homology chasing” offered opportunities to see beyond visible phenotypes and deeper into layers of conserved and interconnected genetic effects. Additionally, developing and troubleshooting protocols within the allotted time period required students to cooperate, multitask and practice prudent time management. Weekly evaluation of worm colonies in a transparent manner using a common spreadsheet aimed to instill an

openness with regards to success and failure (e.g., starved worms) and a willingness to mitigate shortcomings (e.g., better worm maintenance). Engagement with Worm-

Base, AlphaFold, Uniprot and the Human Phenotype Ontology database further equipped students to navigate and use increasingly important resources. Invariably, each group experienced the satisfaction of overcoming an obstacle or the surprise of an unexpected experimental outcome. Such a sense of satisfaction and associating it with methodical and open scientific inquiry is one of the key goals this educational module aimed to achieve.

By compiling these experiments into a publishable manuscript, this work challenges the traditional ephemerality of undergraduate research outputs and positions students as emerging scientists whose work merits global dissemination. This approach not only validates their contributions but also integrates undergraduate research into the broader scientific endeavor. The rapid delivery of strains from the *Caenorhabditis* Genetics Center and guidance from WormBase on gene nomenclature were critical to the project's success, highlighting the importance of community resources in supporting both research and education.

Limitations, such as time constraints and suboptimal assay conditions (*e.g.*, neutral red imaging using Texas Red filter), underscore areas for future refinement. Nevertheless, these challenges provided valuable lessons in resourcefulness and adaptability. This work advocates for a model of undergraduate science education where students are active contributors driven by curiosity and empowered to share their findings with the world. By demonstrating the feasibility and impact of such an approach, this study lays the foundation for future curricula that inspire and equip the next generation of scientists.

Data and Code Availability

Data and the R script used for statistical analysis and figure generation is available at https://github.com/elewahub/homo_elegans

Acknowledgements

We thank Matthew Beckman and Chris Palahniuk for support throughout the semester. The Caenorhabditis Genetics Center offered strains in a timely manner thereby enabling the success of this educational module. WormBase (Tim Schedl and Stavros Diamantakis) guided the process of naming ZK1073.1 and Y48G10A.3 and provided an intuitive platform for students to learn about their genes of interest. David Greenstein (University of Minnesota) recommended using twist ties for worm picking which proved to be a suitable and economical alternative to platinum wire picks.

Author Contributions

AE taught the developmental biology course and instructed students on how to work with *C. elegans* . EJ and LM investigated weak response to tapping as a model for areflexia. DK and YD investigated worm bursting as a model for arterial rupture. LY investigated impaired sinusoidal movement as a model for hip flexor weakness. Sireen Aburaide, AH and SM investigated abnormal worm body size as a model for human limb malformation and AE performed the phenolog statistical analysis. MC investigated modeling cleft soft palate via pharyngeal development in *C. elegans* Suad Ahmed and TW investigated modeling mitochondrial dysfunction through impaired motility in *C. elegans* . AV and PX investigated egg retention dynamics as a model for premature birth. BL and DS investigated modeling lethal short-limbed short stature via morphometrics in *C. elegans* . MS and DW investigated modeling lactose intolerance. All authors participated in writing the manuscript together with AE.

References

1. Brownell, Sara E, Hekmat-Scafe, Daria S, Singla, Veena, Chandler Seawell, Patricia, Conklin Imam, Jamie F, Eddy, Sarah L, et al. (2015). A high-enrollment course-based undergraduate research experience improves student conceptions of scientific thinking and ability to interpret data. CBE life sciences education 14, 14:ar21. https://doi.org/10.1187/cbe.14-05-0092 PMID: 26033869
2. Malotky, Michele K H, Mayes, Kayla M, Price, Kailyn M, Smith, Gustavo, Mann, Sherese N, Guinyard, Mesha W, et al. (2020). Fostering Inclusion through an Interinstitutional, Community-Engaged, Course-Based Undergraduate Research Experience. Journal of microbiology & biology education 21. https://doi.org/10.1128/jmbe.v21i1.1939 PMID: 32431766
3. Gargano, Michael A, Matentzoglu, Nicolas, Coleman, Ben, Addo-Lartey, Eunice B, Anagnostopoulos, Anna V, Anderton, Joel, et al. (2024). The Human Phenotype Ontology in 2024: phenotypes around the world. Nucleic acids research 52, D1333-D1346. https://doi.org/10.1093/nar/gkad1005 PMID: 37953324
4. Sternberg, Paul W, Van Auken, Kimberly, Wang, Qinghua, Wright, Adam, Yook, Karen, Zarowiecki, Magdalena, et al. (2024). WormBase 2024: status and transitioning to Alliance infrastructure. Genetics 227. https://doi.org/10.1093/genetics/iyae050 PMID: 38573366
5. Markaki M, Tavernarakis N. Caenorhabditis elegans as a model system for human diseases (2020). Curr Opin Biotechnol 63:118-125. https://doi.org/10.1016/j.copbio.2019.12.011 PMID: 31951916.
6. Loges LN, Walstrom KM. Modeling human glucose-6-phosphate dehydrogenase mutations using C. elegans GSPD-1 (2021). microPublication Biology. https://doi.org/10.17912/micropub.biology.000451 PMID: 34532700.
7. Duan Y, Li L, Panzade GP, Piton A, Zinovyeva A, Ambros V. Modeling neurodevelopmental disorder-associated human AGO1 mutations in Caenorhabditis elegans Argonaute alg-1 (2024). Proceedings of the National Academy of Sciences of the United States of America 5;121(10):e2308255121. https://doi.org/10.1073/pnas.2308255121 PMID: 38412125.
8. Sayers, Eric W, Bolton, Evan E, Brister, J Rodney, Canese, Kathi, Chan, Jessica, Comeau, Donald C, et al. (2022). Database resources of the national center for biotechnology information. Nucleic acids research 50, D20-D26. https://doi.org/10.1093/nar/gkab1112 PMID: 34850941
9. UniProt Consortium (2025). UniProt: the Universal Protein Knowledgebase in 2025. Nucleic acids research 53, D609-D617. https://doi.org/10.1093/nar/gkae1010 PMID: 39552041
10. Jumper, John, Evans, Richard, Pritzel, Alexander, Green, Tim, Figurnov, Michael, Ronneberger, Olaf, et al. (2021). Highly accurate protein structure prediction with AlphaFold. Nature 596, 583-589. https://doi.org/10.1038/s41586-021-03819-2 PMID: 34265844
11. Varadi, Mihaly, Bertoni, Damian, Magana, Paulyna, Paramval, Urmila, Pidruchna, Ivanna, Radhakrishnan, Malarvizhi, et al. (2024). AlphaFold Protein Structure Database in 2024: providing structure coverage for over 214 million protein sequences. Nucleic acids research 52, D368-D375. https://doi.org/10.1093/nar/gkad1011 PMID: 37933859
12. Stelzer, Gil, Rosen, Naomi, Plaschkes, Inbar, Zimmerman, Shahar, Twik, Michal, Fishilevich, Simon, et al. (2016). The GeneCards Suite: From Gene Data Mining to Disease Genome Sequence Analyses. Current protocols in bioinformatics 54, 1.30.1-1.30.33. https://doi.org/10.1002/cpbi.5 PMID: 27322403
13. McFerrin, Lisa G, Atchley, William R (2011). Evolution of the Max and Mlx networks in animals. Genome biology and evolution 3, 915-37. https://doi.org/10.1093/gbe/evr082 PMID: 21859806
14. Hu, Yanhui, Flockhart, Ian, Vinayagam, Arunachalam, Bergwitz, Clemens, Berger, Bonnie, Perrimon, Norbert, et al. (2011). An integrative approach to ortholog prediction for disease-focused and other functional studies. BMC bioinformatics 12, 357.

https://doi.org/10.1186/1471-2105-12-357 PMID: 21880147
15. Johnson, David W, Llop, Jesse R, Farrell, Sara F, Yuan, Jie, Stolzenburg, Lindsay R, Samuelson, Andrew V (2014). The Caenorhabditis elegans Myc-Mondo/Mad complexes integrate diverse longevity signals. PLoS genetics 10, e1004278. https://doi.org/10.1371/journal.pgen.1004278 PMID: 24699255
16. Dacković, J, Keckarević-Marković, M, Komazec, Z, Rakocević-Stojanović, V, Lavrnić, D, Stević, Z, et al. (2008). Hereditary motor and sensory neuropathy Lom type in a Serbian family. Acta myologica 27, 59-62. PMID: 19364063
17. Goodman, M B, Hall, D H, Avery, L, Lockery, S R (1998). Active currents regulate sensitivity and dynamic range in C. elegans neurons. Neuron 20, 763-72. https://doi.org/10.1016/s0896-6273(00)81014-4 PMID: 9581767
18. Steger, Katherine A, Shtonda, Boris B, Thacker, Colin, Snutch, Terrance P, Avery, Leon (2005). The C. elegans T-type calcium channel CCA-1 boosts neuromuscular transmission. The Journal of experimental biology 208, 2191-203. https://doi.org/10.1242/jeb.01616 PMID: 15914662
19. Sibley, M H, Graham, P L, von Mende, N, Kramer, J M (1994). Mutations in the alpha 2(IV) basement membrane collagen gene of Caenorhabditis elegans produce phenotypes of differing severities. The EMBO journal 13, 3278-85. https://doi.org/10.1002/j.1460-2075.1994.tb06629.x PMID: 8045258
20. Shen, G (2005). The role of type X collagen in facilitating and regulating endochondral ossification of articular cartilage. Orthodontics & craniofacial research 8, 11-7. https://doi.org/10.1111/j.1601-6343.2004.00308.x PMID: 15667640
21. McGary, Kriston L, Park, Tae Joo, Woods, John O, Cha, Hye Ji, Wallingford, John B, Marcotte, Edward M (2010). Systematic discovery of nonobvious human disease models through orthologous phenotypes. Proceedings of the National Academy of Sciences of the United States of America 107, 6544-9. https://doi.org/10.1073/pnas.0910200107 PMID: 20308572
22. Suzuki, Y, Yandell, M D, Roy, P J, Krishna, S, Savage-Dunn, C, Ross, R M, et al. (1999). A BMP homolog acts as a dose-dependent regulator of body size and male tail patterning in Caenorhabditis elegans. Development 126, 241-50. https://doi.org/10.1242/dev.126.2.241 PMID: 9847238
23. Addo, Matthew Glover, Cossard, Raynald, Pichard, Damien, Obiri-Danso, Kwasi, Rötig, Agnès, Delahodde, Agnès (2010). Caenorhabditis elegans, a pluricellular model organism to screen new genes involved in mitochondrial genome maintenance. Biochimica et biophysica acta 1802, 765-73. https://doi.org/10.1016/j.bbadis.2010.05.007 PMID: 20580819
24. Bratic, Ivana, Hench, Jürgen, Henriksson, Johan, Antebi, Adam, Bürglin, Thomas R, Trifunovic, Aleksandra (2009). Mitochondrial DNA level, but not active replicase, is essential for Caenorhabditis elegans development. Nucleic acids research 37, 1817-28. https://doi.org/10.1093/nar/gkp018 PMID: 19181702
25. DeVore, D L, Horvitz, H R, Stern, M J (1995). An FGF receptor signaling pathway is required for the normal cell migrations of the sex myoblasts in C. elegans hermaphrodites. Cell 83, 611-20. https://doi.org/10.1016/0092-8674(95)90101-9 PMID: 7585964
26. Jia, Kailiang, Chen, Di, Riddle, Donald L (2004). The TOR pathway interacts with the insulin signaling pathway to regulate C. elegans larval development, metabolism and life span. Development 131, 3897-906. https://doi.org/10.1242/dev.01255 PMID: 15253933
27. Zhu, Huanhu, Shen, Huali, Sewell, Aileen K, Kniazeva, Marina, Han, Min (2013). A novel sphingolipid-TORC1 pathway critically promotes postembryonic development in Caenorhabditis elegans. eLife 2, e00429. https://doi.org/10.7554/eLife.00429 PMID: 23705068

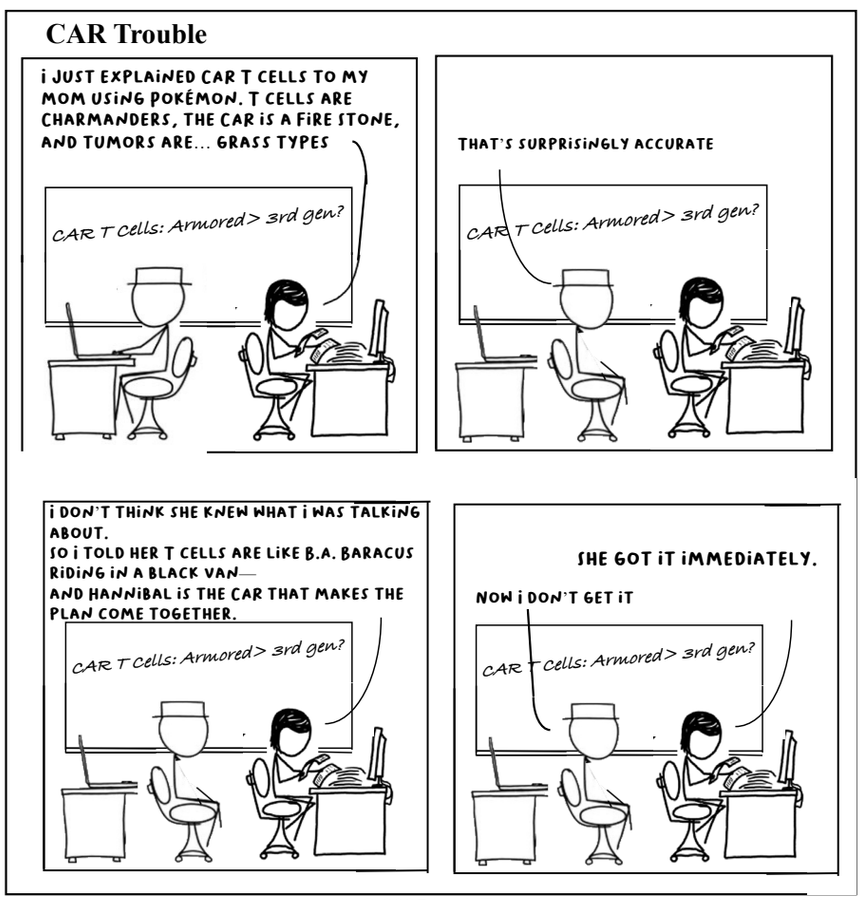

The Pro-Apoptotic Effects of Curcumin on HCT116 Colorectal Cancer Cells

Kuljeet Kaur*, Thomas, S.*, Daggett, M.*, Mattingly, B.*, and JF. Treml*†

Colorectal cancer (CRC) is a leading cause of cancer-related deaths worldwide, often originating from benign polyps in the colon and rectum that may become malignant if left untreated. While current treatments such as surgery, chemotherapy, and radiation are effective, they often come with severe side effects that impact patient quality of life. This has spurred interest in natural compounds like curcumin, which may offer therapeutic benefits with fewer adverse effects. Curcumin, the main active compound in turmeric, has demonstrated anti-inflammatory, antioxidant, and anticancer properties in various studies, suggesting its potential as an adjunct therapy for CRC. This study investigates the effects of curcumin and 5-Fluorouracil (5-FU), a chemotherapy drug commonly used to treat CRC, on HCT116 colorectal cancer cells. 5-FU works by DNA integration requiring extensive repair, ultimately leading to cell death in cells lacking effective DNA-damage sensing and repair. Cells were treated with varying concentrations of curcumin and 5-FU, followed by viability and apoptotic assays using the eBioscience™ Annexin V Apoptosis Detection Kit, the SYTOX™ viability assay, and by observing morphological changes under the microscope. The primary goal is to determine the LD_{50} concentration of curcumin and observe morphological changes at that concentration. This research aims to provide insights into curcumin's potential as a safe adjunct or alternative to current CRC therapies. By identifying effective concentrations and comparing their effects to those of 5-FU, the study seeks to contribute to more informed treatment strategies for CRC.

Colorectal cancer (CRC) is a form of cancer that affects the colon or rectum, part of the large intestine. It is the third most diagnosed cancer in the United States with 141,902 new cases reported in 2022.[1] Globally, CRC accounted for 16.5 million cases in 2015, and this number is projected to rise to over 2.2 million by 2030.[2] While CRC is most prevalent in Northern and Western Europe and the United States, it is less common in regions such as Africa, Asia, and India.[3] One of the significant challenges in CRC treatment is the lack of clear symptoms at the time of diagnosis (often by routine screening), which leads to delayed detection at advanced stages. Later-stage diagnosis limits treatment effectiveness and significantly reduces survival rates.[3]

The development of colorectal cancer is complex and multifactorial, influenced by factors within the tumor microenvironment. Disruptions in the gut microbial profile, along with a compromised intestinal barrier, can lead to inflammation in the intestines, which plays a key role in the initiation and progression of CRC.[4] Most cases of colorectal cancer begin as neoplastic polyps, benign growth in the mucus-secreting epithelial cells of the colon. While the exact cause of these polyps is unclear, genetic and environmental factors, such as diet and lifestyle, are believed to play a key role in their development.[5]

One critical genetic factor in the pathogenesis of CRC is the mutation of the adenomatous polyposis coli (APC) gene. This tumor suppressor gene plays an essential role in early colorectal tumor development. The mutation and inactivation of this gene represent significant early events specifically linked to the development of colorectal tumors.[6] Mutations that inactivate the APC gene are present in approximately 80% of human colon tumors. Heterozygosity of these mutations leads to autosomal dominant predispositions to colon cancer in humans.[7]

Risk factors associated with the development of CRC include smoking, a diet high in red meats, obesity, alcohol consumption, physical inactivity, and a low intake of dietary fiber.[8] Current treatment options for CRC consist of chemotherapy (regimens such as FOLFOX and FOLFIRI), radiotherapy, and surgical interventions. These treatments are often accompanied by severe side effects, low long-term survival rates, and high rates of cancer recurrence.1 Given these limitations, there is a growing interest in exploring safer modifications to medications and dietary interventions.

Turmeric is a spice known for its diverse health benefits, including antioxidant, antimutagenic, antimicrobial, anticancer, and anti-inflammatory effects.[9] These benefits appear to come from a polyphenolic compound called curcumin. Due to its conjugated double bonds, curcumin acts as an effective electron donor and has been shown to improve systemic markers of oxidative stress by scavenging free radicals, such as reactive oxygen and nitrogen species.[10] This antioxidant activity is critical in preventing DNA damage and lipid peroxidation, which are precursors to oncogenesis.[11]

Studies have observed curcumin's anticancer properties in the context of CRC. In vitro studies on human colon cancer cell lines have shown curcumin's ability to inhibit cell proliferation by inducing cell cycle arrest at the G1 and G2/M phases.[12] Additionally, curcumin promotes apoptosis by targeting multiple molecular pathways in cancer progression.[12] For example, one

*University of Kansas, Applied Biological Sciences

†Corresponding author: jtreml@ku.edu

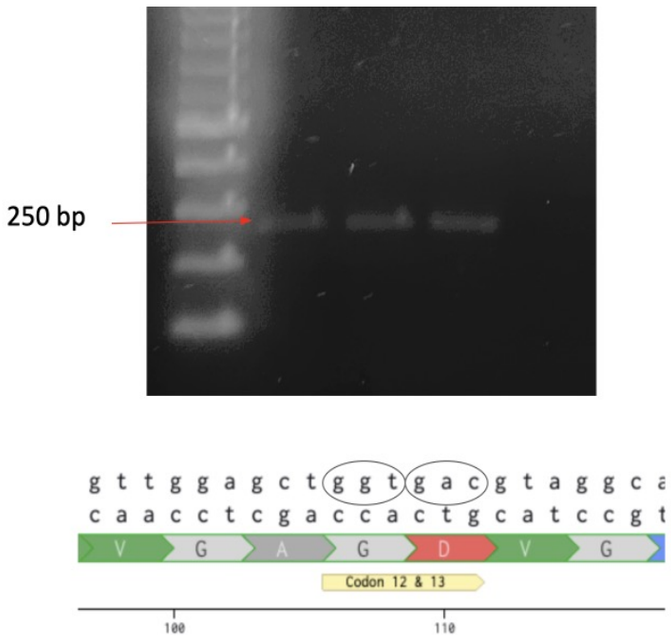

Figure 1 | Gel electrophoresis showing PCR amplification of the KRAS gene from HCT116 colorectal cancer cells. A band at approximately 250 base pairs confirms the successful amplification of the region containing the G13D mutation.

in vitro study on HCT-116 colon cancer cells demonstrates that curcumin induces the production of reactive oxygen species, leading to the downregulation of E2F4, a transcription factor involved in cell growth. This disruption in the cell cycle ultimately leads to apoptosis in HCT-116 cells.[13]

Additionally, an in vivo study was conducted on a mouse model, where the mice were fed diets containing curcumin concentrations of 0.1%, 0.2%, and 0.5% over 15 weeks. The results indicated that the 0.1% concentration did not have significant effects, while the 0.2% and 0.5% concentrations led to a 39% and 40% decrease, respectively, in the number of tumors compared to untreated mice. Additionally, this study suggests that curcumin may be a valuable chemo-preventive agent for human intestinal malignancies associated with APC gene mutations.[14]

Despite curcumin's potential as an anticancer agent, there are challenges related to its solubility and bioavailability in the gastrointestinal tract, limiting its clinical effectiveness.[11] Through the development of nano curcumin, the bioavailability and anticancer activity has been enhanced compared to curcumin, making nano curcumin a more effective option for clinical use.[11]

In addition to its direct anti-cancer properties, curcumin has the potential to alleviate chemotherapy-related side effects. Chemotherapy for CRC is often accompanied by nausea, diarrhea, constipation, neutropenia, and weight loss.[15] Studies have shown that curcumin can protect mitochondria by preventing mitochondrial damage, enhancing the activity of mitochondrial complex enzymes, and reducing oxidative stress. As a result, curcumin can help mitigate some of the side effects of chemotherapy.

Altogether, the potential of curcumin mediating significant anti-cancer properties by inducing apoptosis, reducing tumor growth, and alleviating chemotherapy-related side effects in colorectal cancer make it an attractive drug candidate.

Materials and Methods:

Cell Culture of HCT116 Cells

HCT116 colorectal cancer cells (obtained previous lab member, Allayah Stillwell)[16] were cultured in Dulbecco's Modified Eagle Medium (DMEM) supplemented with 10% fetal bovine serum (FBS) and 100 units/mL penicillin and 100 µg/mL streptomycin. The cells were maintained at 37°C in a humidified 5% CO_2 incubator. Cells were subcultured every 2–3 days when they reached 70–80% confluence. For passaging, cells were detached using 0.25% trypsin EDTA (1X). The cells were initially at passage #4, and some were cryopreserved at passage #7 in 95% complete media and 5% DMSO, with a final concentration of 1.6×10^6 cells per vial for later use.

Cell Imaging

Cell imaging was performed using an Invitrogen™ EVOS™ XL Core Configured Cell Imager with a mechanical stage. Images were acquired using the appropriate objective lens and analyzed using the built-in software provided by the EVOS™ system.

Cell Counting

Cell counting was performed after trypsinization and prior to cell passage. HCT116 colorectal cancer cells were resuspended in complete growth medium (DMEM supplemented with 10% fetal bovine serum and 1% penicillin-streptomycin). A 1:1 dilution was prepared by mixing 100 µL of the cell suspension with 100 µL of 0.4% Trypan Blue solution (Gibco; Lot #2517874) and incubated at room temperature for 3 minutes. The mixture was loaded onto a hemocytometer, and viable (unstained) and non-viable (blue-stained) cells were counted manually in the four corner quadrants under a light microscope using a 10× objective. The total cell concentration was calculated using the following formula:

Cell concentration (cells/mL) = average cell count per quadrant × 10^4 × dilution factor.

% Viability = (number of viable cells / total number of cells) × 100.

These values were used to determine the appropriate seeding density for further experiments.

Reagents For Treatments

Curcumin (Fisher Scientific; Cat. No. NBP2262435G) was initially dissolved in dimethyl sulfoxide (DMSO) to prepare a 10 mM stock solution. The solution was aliquoted and stored at –4°C, protected from light. For cell treatment, the stock solution was diluted in complete culture medium to achieve final concentrations ranging from 0 µM to 100 µM.

5-Fluorouracil (5-FU; Thermo Scientific; Lot: L18E028) was dissolved in DMSO to create a fresh stock solution immediately prior to each treatment. This stock was subsequently diluted in culture media to reach the desired final concentration for each experimental condition.

DMSO (ChemCruz; Lot: G0816) was used as the vehicle control for both curcumin and 5-FU treatments and for preparation of their respective stock solutions. To account for potential cytotoxic effects of

DMSO, the final DMSO concentration was standardized and kept consistent across all treatment groups, including vehicle controls.

MTT Assay for Cell Viability

Cell viability was assessed using the MTT assay (Biosynth; CAS 298-93-1). The MTT reagent (3-[4,5-dimethylthiazol-2-yl]-2,5-diphenyltetrazolium bromide) was prepared as a 5 mg/mL stock solution in sterile phosphate-buffered saline (PBS), protected from light, and stored at 4°C for up to 1–2 weeks before use.

HCT116 cells were seeded into 96-well plates at a density of 10,000 cells per well and incubated for 24 hours at 37°C in an incubator with 5% CO_2 to allow for adherence. After 24 hours, the culture medium was aspirated, and the cells were treated with the desired compounds for 24 hours or the designated treatment duration.

Following treatment, the medium was removed, and 100 µL of MTT working solution (0.5 mg/mL in DMEM, freshly prepared from the stock) was added to each well. Plates were incubated for 4 hours at 37°C to allow viable cells to reduce the MTT reagent to insoluble formazan crystals. After incubation, the MTT solution was aspirated, and 100 µL of dimethyl sulfoxide (DMSO) was added to each well to dissolve the formazan crystals. Plates were gently agitated for 10 minutes to ensure complete solubilization.

Absorbance was measured at 490 nm using a microplate spectrophotometer. Wells containing media without cells were used as negative controls to account for background absorbance. The absorbance values were directly proportional to the number of viable cells, with higher absorbance indicating greater cell viability.

Flow Cytometry for Apoptosis Detection

Apoptosis was evaluated using the Invitrogen™ eBioscience™ Annexin V Apoptosis Detection Kit (Lot #2904486), which contains Annexin V and 7-aminoactinomycin D (7-AAD) for the discrimination of viable, apoptotic, and necrotic cells.

Following treatment, HCT116 cells were harvested by trypsinization and washed twice with phosphate-buffered saline (PBS) to remove residual media. Cells were resuspended in 1X Binding Buffer (provided in the kit) at a density of approximately 1 × 10^6 cells per 100 µL. Staining was performed by adding 5 µL of Annexin V-FITC and 5 µL of 7-AAD to the cell suspension, followed by incubation for 10–15 minutes at room temperature in the dark.

After staining, 200 µL of 1X Binding Buffer was added to each sample to stop the reaction. Samples were immediately ana-

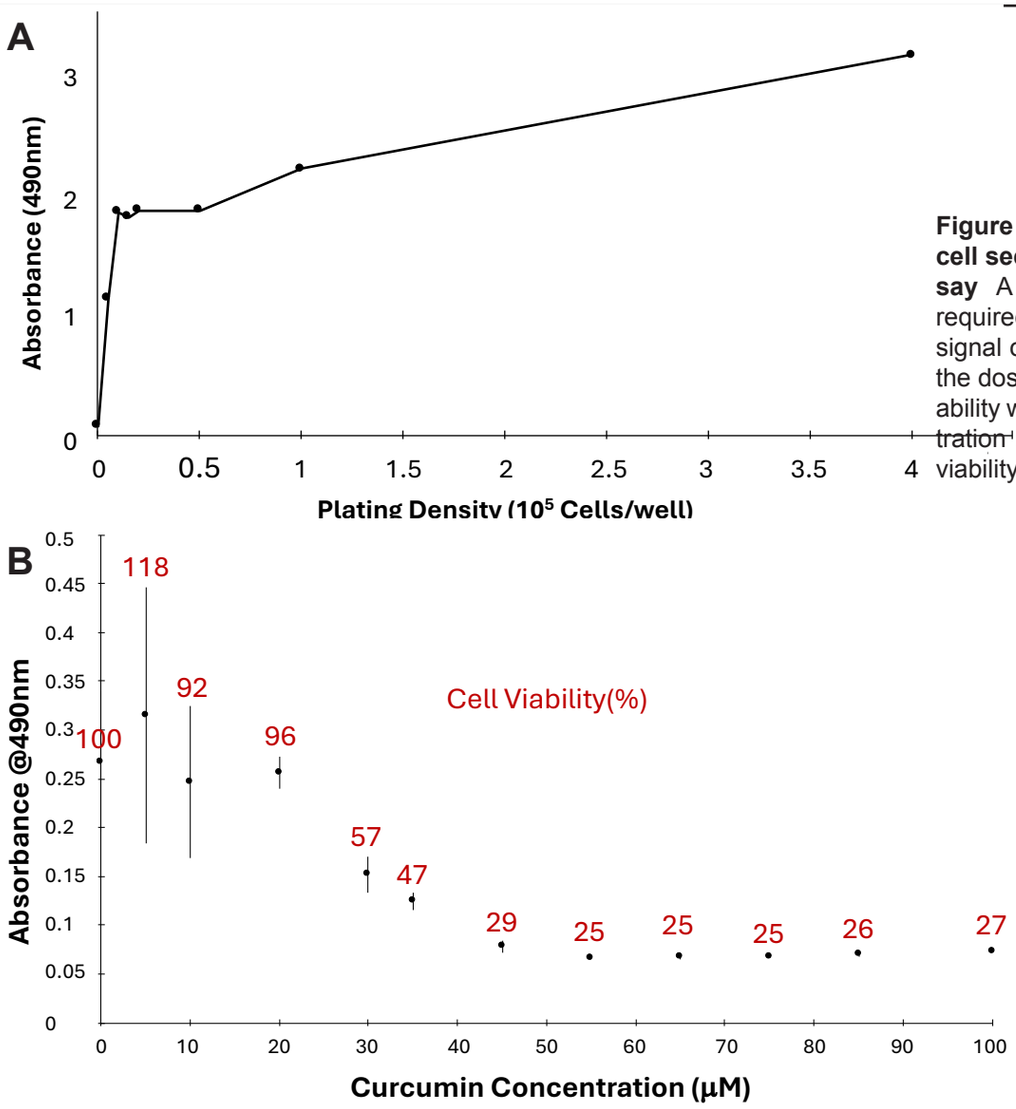

Figure 2 | Optimization of HCT116 cell seeding density and the MTT assay A demonstrates the cell densities required to obtain a strong and reliable signal over the assay time. B illustrates the dose-dependent decrease in cell viability with increasing curcumin concentration (x axis in black) with calculated viability overlaid in red.

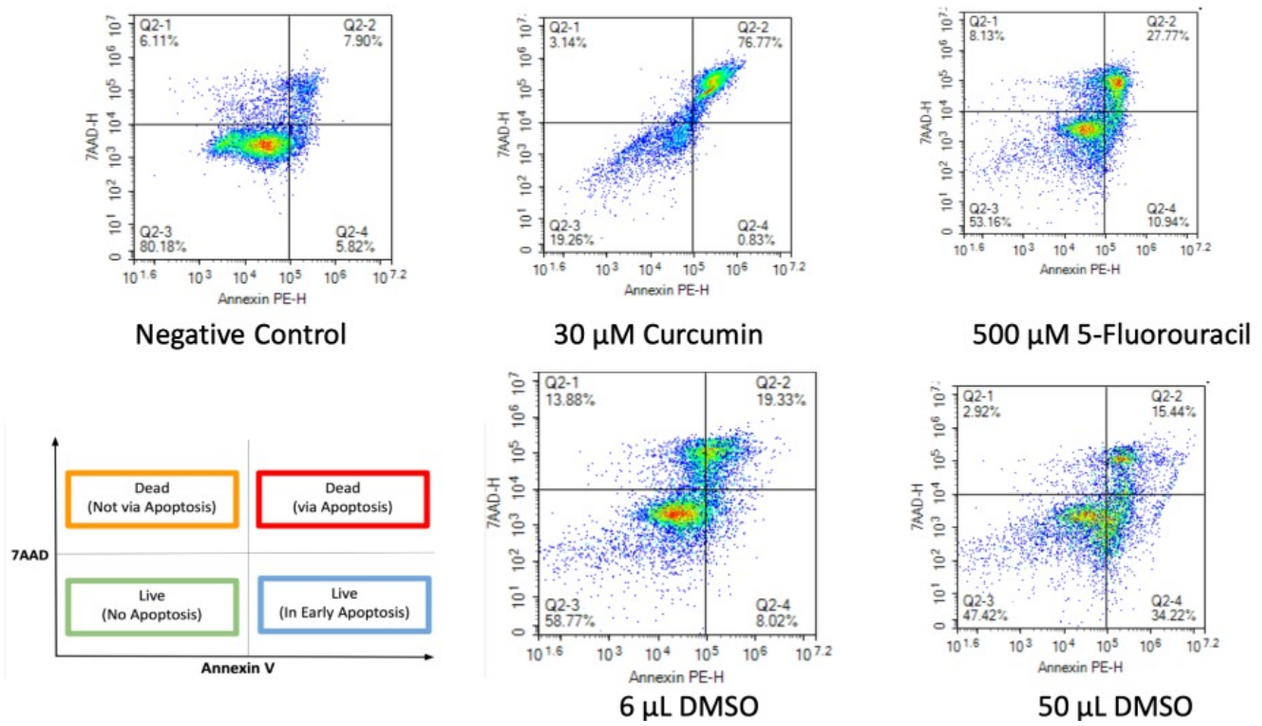

Figure 3 | Detection of apoptosis in HCT116 cells by Annexin V/7-AAD staining following treatment with curcumin and 5-fluorouracil (5-FU). HCT116 cells were treated for 48 hours with either 30 µM curcumin, 500 µM 5-FU, or DMSO controls. Apoptotic and necrotic populations were assessed using flow cytometry, with gates as follows: Q1: dead cells (not via apoptosis), Q2: dead cells via apoptosis, Q3: viable cells, and Q4: early apoptotic cells. Both curcumin and 5-FU treatments increased the proportion of apoptotic cells compared to untreated and DMSO control groups, with curcumin showing a greater extent of apoptosis induction.

lyzed by flow cytometry using a NovoCyte Flow Cytometer (Agilent Technologies). Fluorescence intensities were used to determine the percentage of cells in the following categories:
viable (Annexin V- / 7-AAD-),
early apoptotic (Annexin V+ / 7-AAD-),
late apoptotic (Annexin V+ / 7-AAD+),
and necrotic (Annexin V- / 7-AAD+).

Negative controls (media only) and vehicle controls (DMSO, at volumes equivalent to those used in curcumin and 5-FU treatments) were included to account for background fluorescence and potential solvent effects on apoptosis. Data acquisition and quadrant-based analysis were conducted using NovoExpress software (Agilent Technologies), and results were reported as scatterplots indicating the percentage of cells in each category.

Results

The identity of the HCT116 cell line was confirmed through PCR of a portion of the KRAS gene and electrophoresis on a 2% agarose gel (**Figure 1A**). The resulting single, 250bp band was extracted from the gel and sent for Sanger sequencing, which revealed the characteristic G13D mutation at codon 13, consistent with published HCT116 genomic profiles (**Figure 1B**). This confirmation ensured experimental validity for all subsequent treatments.

Optimization of Viability Assay Conditions

Preliminary optimization of the MTT assay determined that a seeding density of 10,000 cells per well yielded reproducible absorbance readings within the linear range of detection (See **Figure 2A**), avoiding the signal saturation observed at higher densities (≥20,000 cells/well).

Effects of Curcumin on Cell Viability

Treatment of HCT116 cells with increasing concentrations of curcumin (0–100 µM) for 23 hours produced a clear dose-dependent decrease in metabolic activity as measured by the MTT assay See Figure 2B). The calculated LD_{50} was approximately 30 µM. At concentrations ≥50 µM, viability dropped below 20% of the untreated control. DMSO vehicle controls maintained >90% viability at concentrations equivalent to those used for curcumin delivery, although mild cytotoxicity (<10% reduction in viability) was observed at the highest DMSO volume used (**Figure 2C&D**).

Morphological Observations

Phase-contrast imaging supported the cytometric findings. Curcumin-treated cells displayed hallmark apoptotic morphology, including cell rounding, shrinkage, membrane blebbing, and detachment from the substrate. 5-FU-treated cells exhibited apoptotic bodies but retained partial adherence to the plate surface, suggesting slower or less extensive detachment. Untreated negative controls maintained normal epithelial-like morphology, while DMSO controls appeared morphologically comparable to untreated cells, with minor rounding at the highest DMSO levels, but few apoptotic bodies evident (See **Figure 3**).

Comparison of Curcumin and 5-FU Cytotoxicity

Flow cytometry following 48-hour treatments revealed differential patterns of cell death. **Figure 4** illustrates how curcumin at 30 µM induced pronounced apoptosis, with

approximately 45–55% of cells in the late apoptotic (Annexin V+/7-AAD+) quadrant and a smaller fraction (~10–15%) in early apoptosis (Annexin V+/7-AAD-). In contrast, 5-FU at 100 µM produced a moderate apoptotic response, with ~25–30% late apoptotic cells and a similar proportion in early apoptosis. Necrotic cell percentages remained low (<5%) in both treatments, indicating that cell death was primarily apoptotic rather than necrotic.

Overall, curcumin exerted stronger and more rapid pro-apoptotic effects on HCT116 cells than 5-FU under the tested conditions, with both agents acting primarily through apoptotic rather than necrotic pathways.

Discussion

This study provides evidence that curcumin induces significant cytotoxic effects in HCT116 colorectal cancer cells, primarily through apoptosis. Flow cytometric analysis using Annexin V/7-AAD staining revealed that 48-hour curcumin treatment led to a substantial increase in late apoptotic cell populations compared to both the vehicle control and 5-fluorouracil (5-FU), a clinically used chemotherapeutic agent. The pro-apoptotic activity of curcumin was further supported by morphological changes observed under microscopy, including cell rounding, shrinkage, detachment, and the presence of apoptotic bodies—all characteristic of programmed cell death. In contrast, 5-FU treatment resulted in fewer cells undergoing apoptosis at this timepoint, with many remaining adherent and intact, indicating a less robust apoptotic response under the tested conditions.

The dose-response curve from the MTT assay demonstrated that curcumin's cytotoxicity is dose-dependent, with a plateau observed after 50 µM, suggesting saturation of its effect. The calculated LD_{50} of approximately 30 µM is consistent with previously reported values in literature for HCT116 cells, further validating the sensitivity of this cell line to curcumin. Notably, the vehicle control (DMSO) induced early apoptosis at higher concentrations, emphasizing the importance of minimizing solvent concentrations in future experimental designs.

Taken together, these findings reinforce curcumin's potential as an anti-cancer agent capable of inducing apoptosis more effectively than 5-FU in vitro.

However, the differential response also highlights the need for further mechanistic studies to elucidate curcumin's molecular targets and assess its therapeutic synergy or resistance mechanisms when combined with conventional chemotherapy.

Future Direction

There are several directions this project could take in future studies. One important area for investigation is the comparison of curcumin and 5-FU treatments on colorectal cancer cells (HCT116) versus normal colon epithelial cells. By testing these treatments on normal cells, we can determine if they selectively target cancer cells or have similar effects on healthy cells. This would be valuable in understanding whether curcumin and 5-FU could be used in a way that minimizes damage to normal tissue (*i.e.*, results in a favorable therapeutic window), which is a major consideration in cancer therapy.

Another area to explore is the effect of longer treatment periods on cell viability. In this study, curcumin and 5-FU treatments were tested for 24 hours and 48 hours. However, it would be useful to extend the treatment times to 60 or 72 hours to see if a longer exposure period increases the cytotoxic effects on cancer cells. This could help determine the optimal length of treatment for achieving the best results in terms of cell viability and apoptosis.

Finally, a promising area for future research is testing combination treatments. Combining curcumin with 5-FU or other chemotherapy drugs could potentially lead to synergistic effects, where the combination is more effective than either treatment alone. This could improve the overall effectiveness of the treatment and reduce the required doses of each drug, minimizing side effects for patients.

Investigating combination therapies could lead to new strategies for enhancing the efficacy of current cancer treatments.

In conclusion, future research should focus on testing the selectivity of curcumin and 5-FU on normal versus cancer cells, exploring the effects of longer treatment times, and evaluating the potential benefits of combination therapies. These studies could provide important information for improving colorectal cancer treatment.

Acknowledgements

I am grateful for the mentorship and guidance of Dr. Treml, Dr. Thomas, and Dr. Mattingly. I also thank Allayah Stillwell for providing the HCT116 colorectal cancer cells. This project was supported by the KU Edwards Research Small Grants Program, which funded the purchase of the eBioscience Annexin V Apoptosis Detection Kit.

Author's Biography

Kuljeet Kaur is a senior in Applied Biological Sciences at KU Edwards. Through her research and clinical experiences, she has gained valuable skills and a deeper understanding of how biology translates to real-world applications. She is eager to apply her knowledge to contribute to healthcare, research, and community-driven initiatives.

References

1. U.S. Cancer Statistics Colorectal Cancer Stat Bite | U.S. Cancer Statistics | CDC.
2. Ismail, N. I., Othman, I., Abas, F., H. Lajis, N. & Naidu, R. Mechanism of Apoptosis Induced by Curcumin in Colorectal Cancer. Int. J. Mol. Sci. 20, 2454 (2019).
3. Colorectal Cancer: An Overview - Gastrointestinal Cancers - NCBI Bookshelf.
4. Weng, W. & Goel, A. Curcumin and colorectal cancer: An update and current perspective on this natural medicine. Semin. Cancer Biol. 80, 73–86 (2022).
5. Shussman, N. & Wexner, S. D. Colorectal polyps and polyposis syndromes. Gastroenterol. Rep.
2, 1–15 (2014).
6. Multiple Roles of APC and its Therapeutic Implications in Colorectal Cancer - PMC.
7. APC and its modifiers in colon cancer - PMC.
8. Colon Cancer - StatPearls - NCBI Bookshelf.
9. Curcumin A Review of Its' Effects on Human Health - PMC.
10. Effect of curcuminoids on oxidative stress A systematic review and meta-analysis of randomized cont.
11. Anticancer Properties of Curcumin Against Colorectal Cancer A Review - PMC.
12. Pricci, M. et al. Curcumin and Colorectal Cancer: From Basic to Clinical Evidences. Int. J. Mol. Sci.21, 2364 (2020).
13. Kim, K.-C. & Lee, C. Curcumin Induces Downregulation of E2F4 Expression and Apoptotic Cell Death in HCT116 Human Colon Cancer Cells; Involvement of Reactive Oxygen Species. Korean
J. Physiol. Pharmacol. 14, 391 (2010).
14. Perkins S, Verschoyle RD, Hill K, Parveen I, Threadgill MD, Sharma RA, Williams ML, Steward WP, Gescher AJ. Chemopreventive efficacy and pharmacokinetics of curcumin in the min/+ mouse, a model of familial adenomatous polyposis. Cancer Epidemiol Biomarkers Prev. 2002 Jun;11(6):535-40. PMID: 12050094.

15. Layos L, Martínez-Balibrea E, Ruiz de Porras V. Curcumin: A Novel Way to Improve Quality of Life for Colorectal Cancer Patients? Int J Mol Sci. 2022 Nov 14;23(22):14058. doi: 10.3390/ijms232214058. PMID: 36430537; PMCID: PMC9695864.
16. Stillwell, A., Treml, J., & Logan, R. (2022). Analysis of the Anticancer Potential of Green Tea's EGCG Component to Inhibit Immortal Cells. Midwestern Journal of Undergraduate Sciences, 1(1), 23-26. https://doi.org/10.17161/mjusc.v1i1.18563

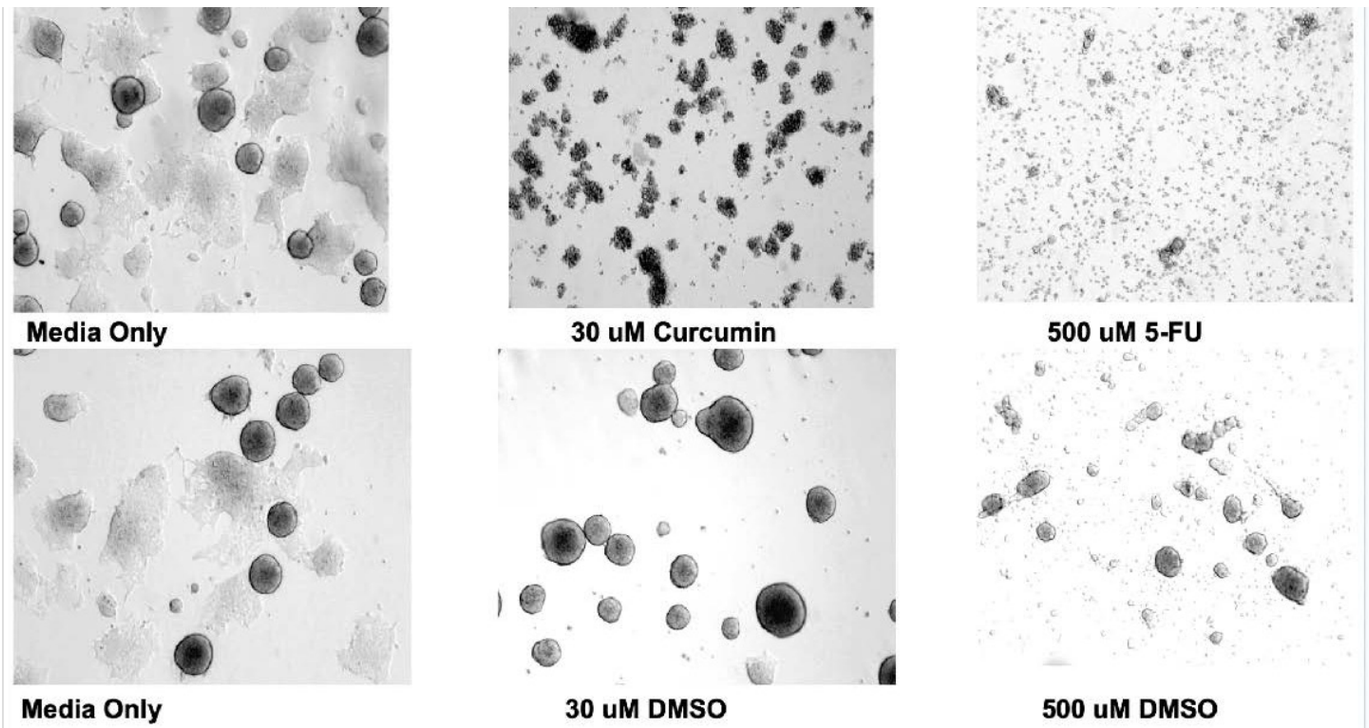

Figure 4 | Morphological changes in HCT116 cells following treatment with curcumin and 5-fluorouracil (5-FU). Cells were treated for 48 hours with 30 μM curcumin or 500 μM 5-FU. DMSO controls (6 μL and 50 μL) were included to match the solvent volumes used in the curcumin and 5-FU treatments, respectively. Curcumin-treated cells appeared smaller and more rounded compared to untreated controls, with frequent aggregation into clusters and the presence of floating cells, indicating detachment. In 5-FU-treated cells, extensive morphological changes were observed, including a pronounced reduction in cell size, fragmentation into apoptotic bodies, and a dramatic loss of confluence, more severe than that seen with curcumin treatment.

The Synthesis of Environmental Health Impacts on Mental & Physical Wellness in Olathe, KS

Robb M. Morris* and S. Schulte*†

The aim of this assessment is to bridge the gap between mental and environmental health conditions in Olathe, Kansas. It does so by synthesizing existing environmental and human health data to form a narrative about the most important threats, potential mitigation strategies, and their expected impacts on the community. The work being done to bring these two areas of research together is of growing importance as we continue to see a rise in climate-related health outcomes and mental health awareness and advocacy reach a wider public audience.

This community health assessment bridges the gap between mental and environmental health in Olathe, KS, for the purpose of enhancing the local understanding of the connection between the health of their environment and their own quality of life. This assessment builds upon a community resilience assessment by students and faculty at the University of Kansas Edwards Campus (KUEC) in Overland Park, with additional research and data from the Johnson County Department of Health and Environment (JCDHE), Johnson County Mental Health Clinic (JCMHC), the US Census Bureau, the Mid-America Regional Council (MARC), the Johnson County Parks & Recreation District (JCPRD), the Kansas Health Institute (KHI), the U.S. EPA's recently discontinued Environmental Justice Screening Tool (EJScreen),[1] and data collected from the author's capstone project.

Olathe Community Characteristics

Olathe, Kansas is the seat of Johnson County and the home of approximately 151,000 people, making it the fourth largest city in Kansas.[2] It serves as a crossroads of a variety of socioeconomic groups living in Kansas, making it an ideal case study location for determining the human health impacts of existing environmental conditions in a community. Vulnerable populations in Olathe include the Hispanic and Black population, the Deaf community, and the Low-Income population (Personal communication, Dubey,E., JCDHE 2025). A variety of environmental health conditions renders these populations especially vulnerable to threats posed to the entire community. The KUEC community resilience assessment for 2024 lists the top three threats to Olathe as: 1) extreme heat, 2) pollution, and 3) economic recession. Olathe is particularly susceptible to these threats due to a lack of tree-canopy coverage and greenspace, high-percentile rankings for air pollution and proximity to Superfund and other contaminated sites, and a very high cost of living (mostly associated with high housing costs).[3] The following data illustrates the significant environmental health conditions impacting physical and mental wellness in the Olathe community. **Figure 1** illustrates the distribution of low-income residents in Johnson County.

As we can see from the distribution in this Figure, Olathe has the highest concentration of residents living at or below 200% of the Federal Poverty Level (FPL) in Johnson County, where 35% of residents are considered low-income, or living on approximately $53,000 per year or less (EJScreen, 2024, no longer available), including 5.59% of the population in Olathe which is 'impoverished'.[2] The Federal Poverty Level (FPL) for a household of three (2.7 average for Olathe) in this region (the lower 48 states) is $26,650 annual salary.[4] Income disparity within Olathe is extreme, where "median income ranges per household from a low of $24,297 to a high of $250,001 in some neighborhoods. Higher income areas are typically found in the southeast parts of the city, and lower income areas are in the central areas,"[5] including Downtown Olathe. This indicates a financial vulnerability for many residents, which leaves them at greater risk of suffering the most severe and disproportionate impacts of extreme heat and recession as discussed below. This also speaks to the necessity of addressing uniquely local vulnerabilities.

These financial vulnerabilities are compounded for low-income residents living in Olathe by the remarkably high housing costs and costs of living in Johnson County. Researchers in the Johnson County Department of Health and Environment in 2024 developed a community health assessment which in its analysis noted the cost of living for "…a single parent with two children living in our community [Johnson County] in 2024 needs to earn $95,177 per year to maintain an adequate standard of living - nearly $14,000 more per year than they did two years ago."[6] This is significantly higher than what low-income residents are earning in Olathe. As seen from the distribution in Figure 1, neighborhoods in Downtown Olathe range from 51% to 100% of individuals living in these neighborhoods that are low-income residents. As stated previously for this region, that indicates a salary lower than about $53,000 per year.[4]

High housing costs are the main source of financial pressure for people living in Johnson County, leaving some neighborhoods with up to "79% of homeowners being housing-burdened [those who spend 30% or more of their income on housing costs]" and housing costs which "have jumped between 20-24% for renters, homeowners with a mortgage and homeowners without a mortgage.[7] After rent and mortgage costs, energy burden stands to be the next among the top housing financial pressures in Johnson County in the face of extreme heat threats, with heating and cooling units as the cause of an "increased energy demand of 8-19%", compounded by the number of days in a given year which exceed 105 degrees Fahrenheit increasing from 0.7 to

*University of Kansas, Environmental Studies

†Corresponding author: s211s202@ku.edu

This community health assessment bridges the gap between mental and environmental health in Olathe, KS, for the purpose of enhancin also speaks to the necessity of addressing uniquely local vulnerabilities.

These financial vulnerabilities are compounded for of Downtown Olathe. Prolonged exposure to extreme heat without sufficient resources (financial) to off-set these temperatures leaves vulnerable populations more at-risk of developing physical and mental health complications, such as "... heat exhaustion, hyperthermia, compromised internal temperature regulation, and in extreme cases, heatstroke leading to multi-organ failure."[3]

Neighborhoods most at risk from emerging heat patterns are those with extensive heat-absorbing, impervious surfaces and minimal tree-canopy coverage—a condition driven by the Urban Heat Island (UHI) effect. Downtown Olathe is particularly vulnerable to this phenomenon.[8] The lack of tree cover and green space, which are critical for sequestering carbon and absorbing heat, combined with an abundance of impervious surfaces, intensifies the UHI effect. As a result, an increase in heat-related health complications and illnesses is highly likely in Downtown Olathe. Olathe can also expect to see heightened pressure on its water systems, and degraded air quality (an area which is already of high concern as noted by the Olathe Resilience Assessment Summary of 2024 conducted by KUEC researchers). Extended periods of rain-free days can quickly turn into droughts, and droughts associated with high temperatures and little tree canopy are the most at-risk for adverse health effects because of extreme heat, poor air quality, and degraded water quality. Over the past 25 years, Olathe, KS has experienced drought of some level in 55% of weeks.[10] These previously mentioned effects include but are not limited to heatstroke, hyperthermia, dehydration, and aggravated or increased asthma symptoms (currently Johnson County experiences a rate of 9.7% of adult asthma).[3,11,12]

Figure 3 presents a map of tree-canopy coverage in Downtown Olathe today.

Among some of the more concerning negative mental health impacts of extreme heat is an observable increased rate of violent crime. In a study published in 2024 by the International Journal of Biometeorology, higher outside temperatures and the onset of Urban Heat Island (UHI) effects were positively correlated with increased rates of violent crime, citing that "violent crime is generally higher in summer and increases with temperature" and that "urban heat island (UHI) effect... the additional heat in the built-up environment from hard surfaces, which absorb, store and radiate heat" is poised to aggravate those symptoms in urban environments (such as Downtown Olathe), and increase over time as the temperatures increase as a result of climate change.[13] This is backed up by MARC, citing that "Increased heat will lead to a 5.3% increase in violent crime" in addition to a "decreased labor productivity of 2.3%" and an "increased energy demand of 8-19%."[8]

A decrease in labor productivity of 2.3% is likely to be indicative of a proportionate decrease in income, a financial shock which many (at least 5.59% in Downtown Olathe, but likely more) can ill-afford. Less income should be interpreted as less resiliency to threats (including greater energy demand to off-set extreme heat), and economic recession which will place even greater pressure on residents struggling to afford housing costs such as rent, mortgage payments, or home repair and weatherization.

Residents in the Downtown Olathe area are also especially vulnerable to mental and environmental health complications because of the city's proximity to multiple hazardous emissions and contaminated sites, and significant air pollution. Contaminated sites include one active National Priorities List (NPL) Superfund site at Chemical Commodities, Inc. (CCI) on South Keeler Street. The CCI site "...occupies approximately 1.5 acres in central Olathe, a suburban community of Kansas City with a population of approximately 60,000...Land use in the area is primarily commercial and residential."[14] Four additional non-NPL active Superfund sites in Olathe are shown in

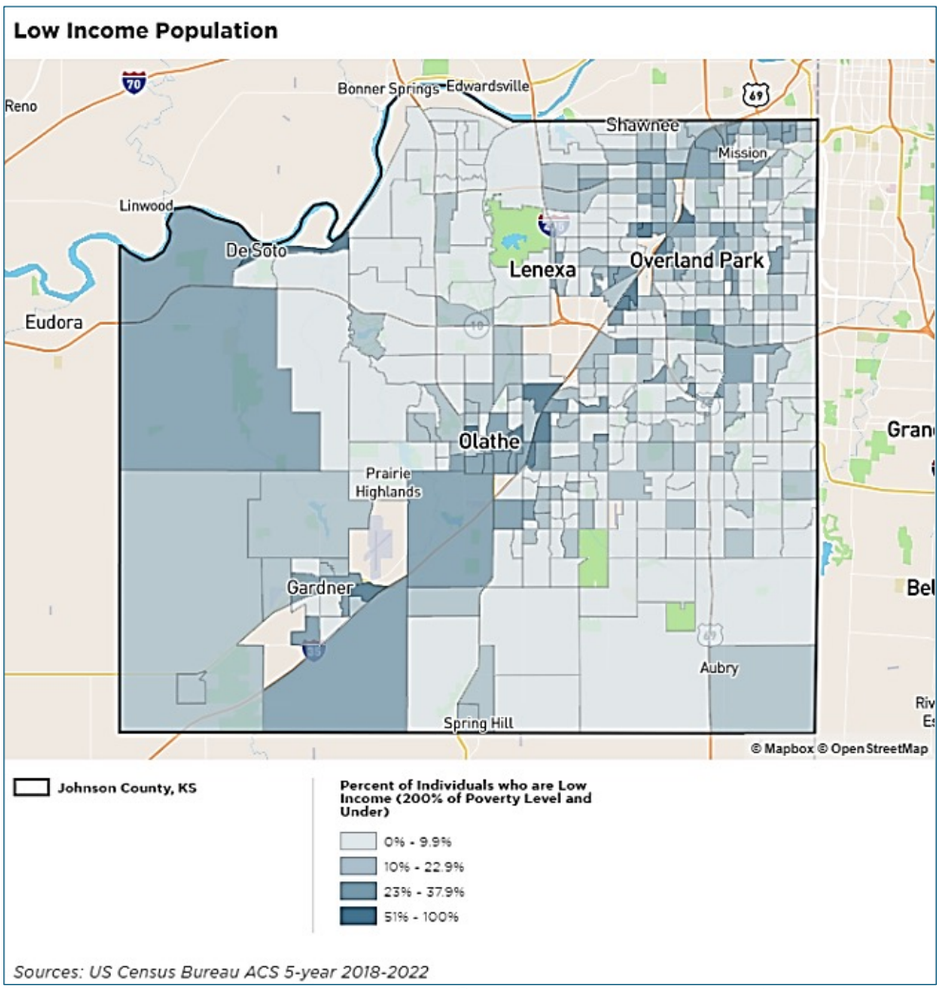

Figure 1 | Income disparity between Olathe and other cities within Johnson County (US Census Bureau 2018-2022). The highest concentration (51-100%) of low-income residents (those living 200% or more below the poverty level) is found in Olathe.

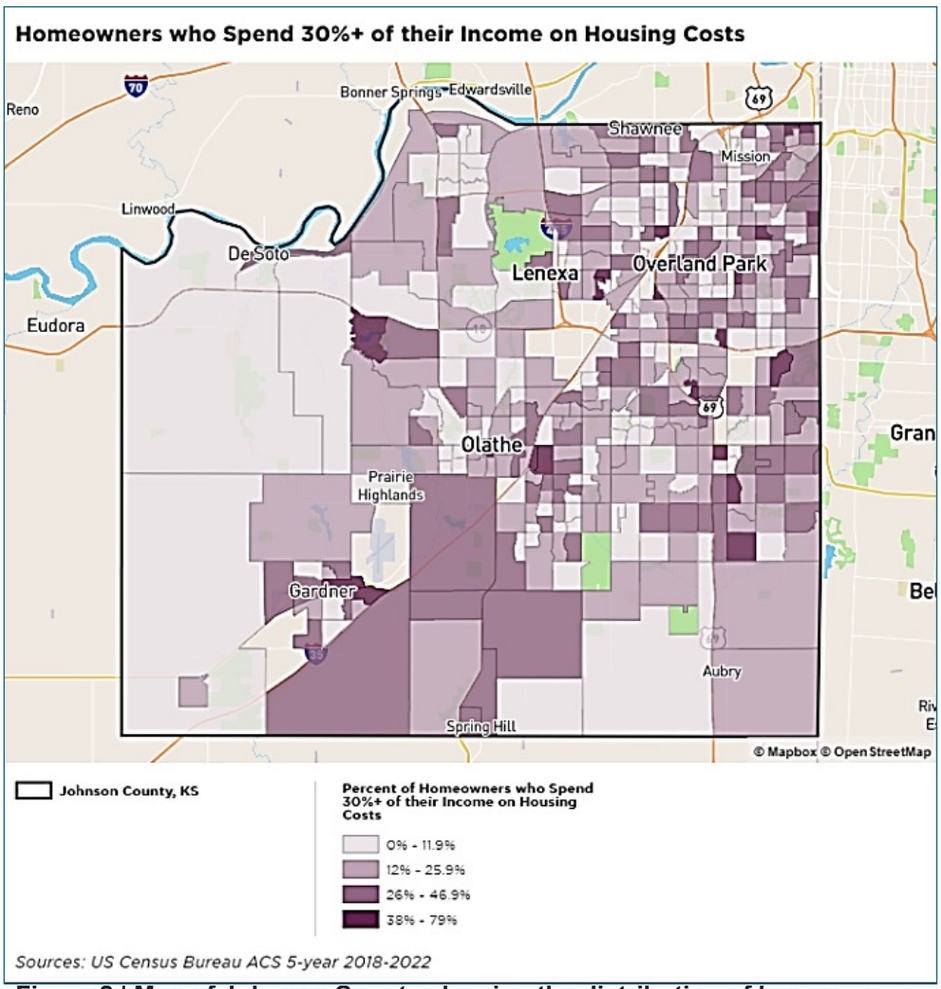

Figure 2 | Map of Johnson County showing the distribution of homeowners who spend more than 30% of their income on housing costs (housing burdened). Source: US Census Bureau, 2018-2022.

the land-use mp of **Figure 4**.

The abundance and proximity of industrial land use areas to single-family residential areas is of high concern. Olathe rated 96th in the national percentile ranking for proximity to Superfund sites in the Olathe Resilience Assessment conducted by KU Edwards researchers in 2024. Olathe also ranked in the 91st-percentile for toxic air emissions, 90th percentile for diesel particulate matter, the 77th-percentile for hazardous waste proximity, and the 63rd-percentile for lead paint prominence in pre-1960s housing. Extreme heat will exacerbate air pollution by means of greater frequency and intensity of wildfires, which release harmful particulate matter into the air, and certain pollutants from vehicle and industrial emissions which feed on higher temperatures (heat waves) and manifest themselves in the form of ground-level ozone, often resulting in a harmful tropospheric haze.[15] Health complications which are closely associated with this phenomenon include pulmonary inflammation, increased risk of heart attack and stroke, Chronic Obstructive Pulmonary Disorder (COPD), and mental health complications as well, including learning disabilities and neurological disease.[15] A summary of Olathe's percentile rankings can be found in the 2024 Olathe Resilience Assessment in **Figure 5**.[3]

Fortunately, a variety of effective mitigation measures for off-setting extreme heat, air and water pollution, and exposure to extremely dangerous neurotoxins such as lead are all within Olathe's reach, both within the city and county, and will now be discussed in further detail. Through a series of strategic governmental and community partnerships, Olathe can begin to see greater resilience to emerging climate patterns and healthier residents, both mentally and physically, as described below.

Mitigation Strategies

Based off data which has been collected and synthesized from previous researchers and case studies at the University of Kansas Edwards Campus (KUEC), the Johnson County Department of Health and Environment (JCDHE), the Mid-America Regional Council (MARC), the Johnson County Parks and Recreation District (JCPRD), and the Johnson County Mental Health Clinic (JCMHC). The recommendation of this assessment is for the City of Olathe to form three strategic partnerships between governmental and community organizations, and to maintain long-term monitoring of the results of these three partnerships. A more detailed description of proposed solutions is included in the full capstone project report. This section will review the recommended strategic partnerships in Olathe as well as examine the expected results of each partnership.

The first partnership should be between the Johnson County Parks & Recreation District (JCPRD), the Olathe Parks & Recreation Department, and the Johnson County Department of Health & Environment (JCDHE). This would be a complementary initiative to expand urban greenspace in Olathe via Superfund (or other contaminated site) remediation projects, followed by a process of turning these remediated sites into parks, and further expanding trails (to include on-street trails) and accessible greenways throughout Olathe (and ideally throughout Johnson County). As a result of such measures Olathe should expect to see an immediate reduction in its percentile ranking for proximity to Superfund sites, as well as reductions in hazardous waste proximity to residential areas, both cited as areas of concern in the 2024 Olathe Resilience Assessment Summary conducted by KUEC researchers. Anticipated health benefits from these measures include a reduction in the prevalence of asthma-related or other respiratory illnesses, a reduction of exposures to hazardous waste and materials, cleaner air, and cleaner groundwater as a result of groundwater filtration and enhanced carbon sequestration into the newly created greenspaces (in addition to further mitigating the Urban Heat Island effect in Downtown Olathe). Quantitative data showing these results in Olathe should be derived from ongoing monitoring.

The second partnership should be between Olathe Public Works and the Heartland Tree Alliance, and possibly JCPRD to initiate tree and native vegetation planting projects along city streets, county greenways, and

on private property. The 2018 Green Heart Louisville Project could be a template for creating natural buffers between industrial sites and residential areas. The Green Heart Louisville Project was launched in Louisville, Kentucky in 2018 to examine the linkages between neighborhood greening and human health and was the first study of its kind to quantify how greening initiatives impact human health and wellbeing. The results of this study concluded that extensive with tree planting and enhanced urban green spaces, we can expect to see "up to a third of particulate matter" filtered out of the air within 300 yards of even a single tree and a significant reduction in rates of cardiovascular disease, strokes, and asthma as a result of improved air quality. We can also expect to see city streets that are about 2-4% cooler than average, reducing high energy demand and energy cost burdens in this low-income community.[16,17] Trees also help reduce stormwater runoff and mitigate urban flooding and simultaneously improve water quality via groundwater filtration.

The third partnership should be between the Olathe Housing Authority (OHA), Olathe Housing Rehabilitation Services, and Hope Builders KC and other non-profit home maintenance organizations to expand their existing home repair and accessibility modification assistance to include home weatherization and lead paint removal. This will help reduce the impacts of and vulnerability to increasing levels of extreme heat (especially for aging residents during the summer months), further reducing the energy burden and expenditures by low-income and housing burdened populations year-round. Doing so also helps maintain sufficient safe and affordable housing stock, an important community priority. Removal of lead paint in older houses also prevents future lead exposure to children living in these neighborhoods, preventing lifelong cognitive injury.

Conclusion

Olathe's significant vulnerabilities to extreme heat, pollution, and economic recession are catalysts for mental and physical health complications including but not limited to respiratory illnesses (including asthma and COPD), heatstroke, multi-organ failure, depression, anxiety, and panic disorders. An economic recession would prove to be devastating to Olathe's sizeable low-income population, leaving many unable to afford adequate housing, utilities (impacting heating and cooling), medical care, or higher education (a pathway for many to attain higher incomes to better provide for their families), creating a feedback loop of vulnerability to negative mental and physical health consequences of extreme heat and pollution.

As described in the mitigation strategies section, however, there is hope. Effective strategies for curbing the onset of extreme heat and pollution such as coordinated strategic partnerships (such as between JCDHE, JCPRD, the Olathe Parks & Rec-

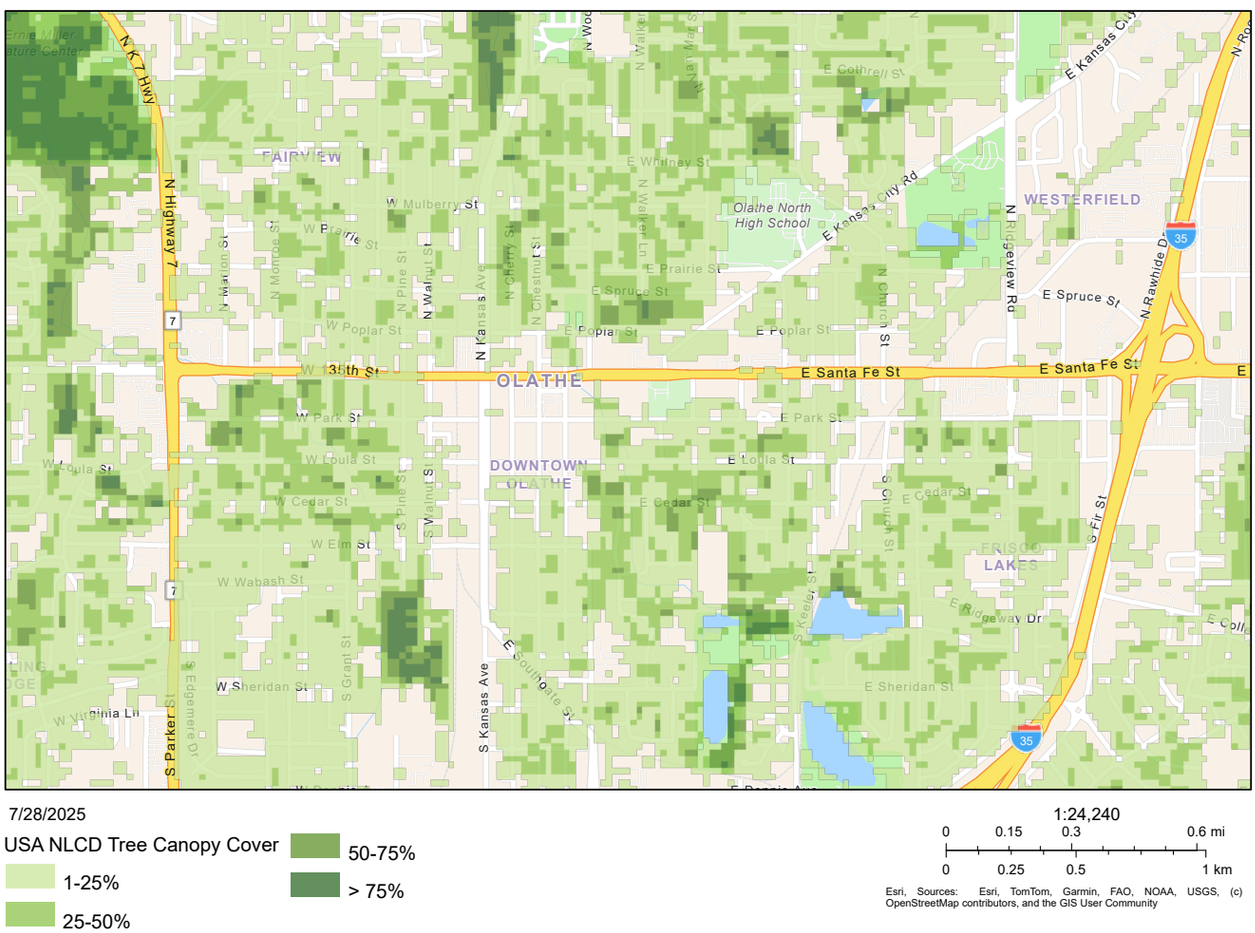

Figure 3 | Map of tree-canopy coverage for Olathe (n.d.). Note the patch of grey area centered on Olathe (Downtown), extending to the south and to the east. University of Kansas Edwards Campus et al., 2024.

reation Department, and community organizations) to expand urban greenspace, tree-canopy coverage, the remediation of contaminated sites found throughout Olathe, and the extension of trail networks, all result in improved health outcomes including but not limited to decreased rates of asthma and other respiratory illnesses (a result of improved air and water quality), cooler temperatures in urban areas (which can potentially decrease the rate of violent crime during the summer months), and a reduction in the energy demand already placing disproportionate amounts of financial stress on low-income communities. Because many of these cited benefits are not yet fully quantified, it is also in the best interest of Olathe and participating organizations to collect and synthesize data on the outcomes of these strategies and strategic partnerships, with the purpose of further quantifying mental health outcomes and prioritizing efforts to address various environmental health threats and conditions in Olathe and beyond.

Author Biography

Robb Morris is a recent graduate of the University of Kansas with a Bachelor of Arts degree in Environmental Studies. During his final semester, he completed a capstone project which had the intended purpose of synthesizing existing human and environmental health data together to form a narrative about the linkages between mental and environmental health, an area of research previously not extensively quantified or studied. The following is a condensed version of his findings. Robb is currently pursuing work in ecological restoration in the Kansas City area.

References

1. EDGI_Team. EPA Removes EJScreen from Its Website. Environmental Data and Governance Initiative https://envirodatagov.org/epa-removes-ejscreen-from-its-website/ (2025).
2. Current World Population: 8,005,176,000. World Population Review https://worldpopulationreview.com/.
3. Schulte, S., Fannin-Hughes, I. & Byers, H. Building Community Resilience: A Proactive, Measurable, Scalable, and Comprehensive Resilience Planning and Forecasting Model. (2021).
4. Federal Poverty Guidelines / Levels for 2025 & Their Relevance to Medicaid Eligibility. https://www.medicaidplanningassistance.org/federal-poverty-guidelines/.
5. The Highest and Lowest Income Areas in Olathe, KS | BestNeighborhood.org. https://bestneighborhood.org/household-income-olathe-ks/.

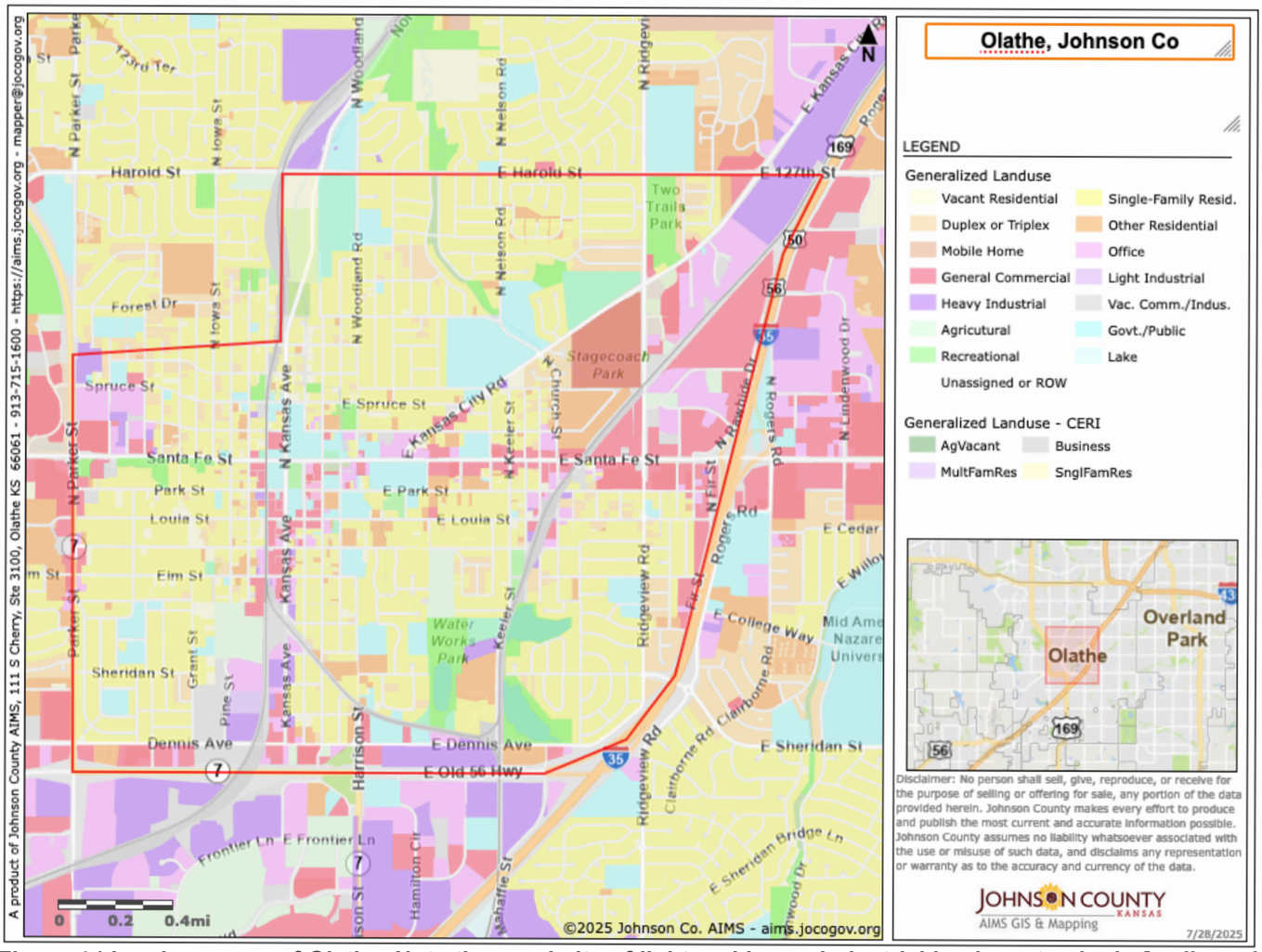

Figure 4 | Land-use map of Olathe. Note the proximity of light and heavy industrial land use to single-family residential parcels (especially along Dennis Avenue & Kansas Avenue). Source: Johnson County, n.d. University of Kansas Edwards Campus et al, 2024.

SELECTED VARIABLES	VALUE	STATE AVERAGE	PERCENTILE IN STATE	USA AVERAGE	PERCENTILE IN USA
ENVIRONMENTAL BURDEN INDICATORS					
Particulate Matter 2.5 ($\mu g/m^3$)	8.36	8.03	61	8.45	57
Ozone (ppb)	55.6	56.8	23	61.8	25
Nitrogen Dioxide (NO_2) (ppbv)	9	7	78	7.8	64
Diesel Particulate Matter ($\mu g/m^3$)	0.21	0.131	90	0.191	67
Toxic Releases to Air (toxicity-weighted concentration)	8,200	13,000	71	4,600	91
Traffic Proximity (daily traffic count/distance to road)	820,000	590,000	69	1,700,000	50
Lead Paint (% Pre-1960 Housing)	0.35	0.36	50	0.3	63
Superfund Proximity (site count/km distance)	2.1	0.24	98	0.39	96
RMP Facility Proximity (facility count/km distance)	2	0.78	94	0.57	94
Hazardous Waste Proximity (facility count/km distance)	4.6	2.4	76	3.5	77
Underground Storage Tanks (count/km^2)	6.2	3.4	80	3.6	82
Wastewater Discharge (toxicity-weighted concentration/m distance)	51	4400	44	700000	50
Drinking Water Non-Compliance (points)	0	1.3	0	2.2	0
SOCIOECONOMIC INDICATORS					
Demographic Index USA	1.45	N/A	N/A	1.34	62
Supplemental Demographic Index USA	1.91	N/A	N/A	1.64	70
Demographic Index State	1.75	1.31	74	N/A	N/A
Supplemental Demographic Index State	1.75	1.32	77	N/A	N/A
People of Color	40%	26%	78	40%	57
Low Income	35%	30%	64	30%	64
Unemployment Rate	7%	4%	81	6%	71
Limited English Speaking Households	7%	2%	87	5%	79
Less Than High School Education	15%	9%	81	11%	74
Under Age 5	6%	6%	59	5%	63
Over Age 64	12%	17%	32	18%	32

Figure 5 | Olathe environmental burdens and socioeconomic indicators. University of Kansas Edwards Campus et al., 2024.

6. https://www.jocogov.org/sites/default/files/files/2025-03/2023-24%20Community%20Health%20Assessment%20DHE%20%281%29.pdf. https://www.jocogov.org/sites/default/files/files/2025-03/2023-24%20Community%20Health%20Assessment%20DHE%20%281%29.pdf.
7. U.S. Census Bureau QuickFacts. https://www.census.gov/quickfacts/fact/table/johnsoncountykansas/PST045224.
8. https://www.marc.org/sites/default/files/2022-05/Climate-Risk-and-Vulnerability-Assessment.pdf. https://www.marc.org/sites/default/files/2022-05/Climate-Risk-and-Vulnerability-Assessment.pdf.
9. TreeCanopy.US. https://treecanopy.us/.
10. Olathe, Kansas Climate Change Risks and Hazards: Heat, Precipitation. ClimateCheck https://climatecheck.com.
11. CDC. Most Recent Asthma Data. Asthma Data https://www.cdc.gov/asthma-data/about/most-recent-asthma-data.html (2024).
12. State Maps for Asthma Prevalence by Six-Level Urban-Rural Classification, 2019–2021 | Asthma | CDC. https://www.cdc.gov/asthma/national-surveillance-data/asthma-prevalence-state-classification.htm.
13. Stevens, H. R., Graham, P. L., Beggs, P. J. & Ossola, A. Associations between violent crime inside and outside, air temperature, urban heat island magnitude and urban green space. Int. J. Biometeorol. 68, 661–673 (2024).
14. https://semspub.epa.gov/work/07/30296151.pdf. https://semspub.epa.gov/work/07/30296151.pdf.
15. Cardenas, B., Akhtar, S. & Elliott, B. What Happens When Extreme Heat and Air Pollution Collide. (2024).
16. Mcdonald, R. et al. Current inequality and future potential of US urban tree cover for reducing heat-related health impacts. Npj Urban Sustain. 4, (2024).
17. Cooling Cities: Harnessing Natural Areas to Combat Urban Heat. Natural Areas Conservancy https://naturalareasnyc.org/research-publications/cooling-cities-harnessing-natural-areas-to-combat-urban-heat/.

RuralMed: Bringing Medical Opportunities to Rural Students

by Arisha Safiq

As a student interested in a future in medicine, living in a rural town of 9,000 residents an hour and a half outside of Kansas City, I've come to recognize an opportunity gap I had never heard anyone talk about before. When I first began thinking about medical school, I didn't even know where to start. In rural areas like mine, this is true for many students. No matter how smart you are or how big your dreams may be, the resources to explore interests in fields like medicine or research simply aren't here.

That's how RuralMed began.

RuralMed helps bridge the gap between students in communities like mine and the medical exposure that schools look for. In my own experience, I had to drive several hours just to complete shadowing or volunteering hours in a hospital—time that came at the expense of schoolwork, extracurriculars, and even other volunteering opportunities. RuralMed changes that by bringing resources directly to students, wherever they are. We offer virtual Q&As with healthcare professionals, accessible shadowing experiences, and volunteering opportunities that can be done remotely. My goal isn't just to help students explore medicine—it's to help them succeed as future medical professionals.

This isn't just a project to me—it's personal. I know what it's like to spend hours searching online for answers that could have been given in minutes by a mentor. I remember wondering if someone from a small, rural community could ever wear a white coat. Rural communities don't just need more doctors—they need doctors who understand them, doctors who come from the very communities they serve. And that starts by helping students connect with opportunities that are otherwise out of reach, and by showing them that they belong in medicine too.

If you, or someone you know, would benefit from RuralMed, please see our flyer in the *Resources for Students* section on the next page.

The Municipal Farm

From Contamination to Conservation: A Plan for the Future

Katelyn Baska

The Municipal Farm is a 441-acre site owned by the City of Kansas City, Missouri, located in the heart of the Eastwood Hills neighborhood. Surrounded by important neighborhoods and regional assets, the former municipal jail and working farm property site holds great potential for the community. It is both a historic and environmental asset in Kansas City.

Over the years, a range of factors—including accumulated city and industrial uses, and the presence or potential presence of hazardous substances in some areas, known as brownfield sites—have contributed to the site being underutilized. Today, Municipal Farm features a rich mix of natural elements such as waterways, wetlands, wooded areas, striking terrain, and pockets of development.

The Municipal Farm site in Kansas City represents a unique opportunity to revitalize a historically significant and environmentally rich area by addressing past contamination concerns and transforming it into a sustainable, community-driven asset that blends ecological restoration, urban development, and public engagement.

A story-map for this site has been compiled at:
https://storymaps.arcgis.com/stories/b28ed87ee40f4d39b0bd4a1fc4c2b134

This story-map additionally includes the documentary:

Land Freed: Municipal Farm Documentary (2025)
by Kathryn Garey

This documentary complements the story of this Kansas City site
and can be found within the article above or independently viewed at:
https://youtu.be/U95PHG427g8

Resources for Students

KU SCHOOL OF PROFESSIONAL STUDIES

January 30

AT
KU EDWARDS CAMPUS
12600 QUIVIRA RD
OVERLAND PARK, KS

BIOTECH DAY 2026

BRINGING SCIENCE TO LIFE

Get your invitation at jtreml@ku.edu
(Please note that at this time, this is an in-person event only)

BECOME AN R&D SCIENTIST!

Kansas City Biotech companies are hiring well-trained biologists with lab experience. To meet this demand, KU offers an intense, hands-on **Bachelor's Degree in Biotechnology** at the KU Edwards Campus!

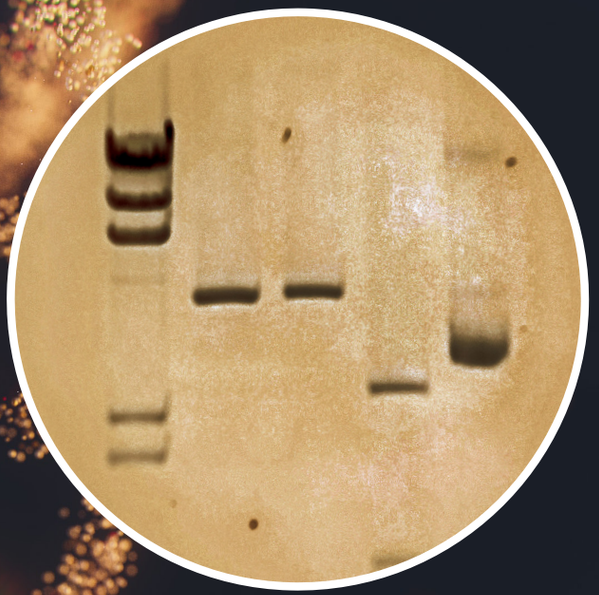

In this unique program, you will focus on applying your scientific knowledge to solve complex biological probelms. You will identify problems, design and execute experiments, analyze results and make conclusions. You will learn by doing biological research.

Already Started College?

No problem!
Apply during your freshman or sophomore year.

Where Can I Start?

Complete your freshman and sophomore coursework then transfer to KU's Biotech Program to complete your Biotechnology Degree.

KU

Meet with an advisor today!
(913) 897 - 8539